

Type II superconductivity

Studied by the Ginzburg–Landau equation

Tommy Sonne Larsen

Master Thesis
Department of Mathematics
Technical University of Denmark

Supervisors:
Mads Peter Sørensen, Niels Falsig Pedersen and Søren Madsen

Contents

1	Ginzburg–Landau Theory	4
1.1	Thermodynamics in superconductors	4
1.2	The Gibbs function	6
1.3	Derivation of Ginzburg–Landau equations	8
1.4	Characteristic lengths	12
1.4.1	London penetration depth	12
1.4.2	Ginzburg–Landau coherence length	14
1.5	Critical magnetic fields	15
1.5.1	The thermodynamic critical field	16
1.5.2	The upper critical field	17
1.5.3	The lower critical field	21
2	Numerical formulation	23
2.1	Normalisation	23
2.1.1	Normalisation with $\mathbf{r} \rightarrow \xi_{GL}\mathbf{r}'$	23
2.1.2	Normalisation with $\mathbf{r} \rightarrow \lambda_L\mathbf{r}'$	25
2.1.3	Choosing normalisation	26
2.2	Gauge transformation	27
2.3	FEMLAB	28
2.3.1	The Finite Element Method	28
2.3.2	Modelling	32
2.3.3	Formulation with $\mathbf{r} \rightarrow \xi_{GL}\mathbf{r}'$	32
2.3.4	Formulation with $\mathbf{r} \rightarrow \lambda_L\mathbf{r}'$	35
3	Numerical results	36
4	Time–Dependent Ginzburg–Landau Theory	44
4.1	Normalisation	45
4.2	Gauge invariance	47
4.3	Correspondence with stationary equations	48
4.4	FEMLAB formulation	49
5	Time–dependent results	52
A	Ginzburg–Landau in cgs	62
A.1	Stationary equations	62
A.2	Time-dependent equations	63

B Gauge invariance	66
B.1 Proof for stationary equations	66
B.2 Proof for time-dependent equations	68
C MATLAB Code	69
C.1 GLE.m	70
C.2 glestart.m	72
C.3 TDGL.m	74
C.4 tdglstart.m	76
C.5 plotter.m	78
D CD content	81

Preface

This Master Thesis is submitted as a part of the Master Programme at the Technical University of Denmark. On this account I would like to express my personal gratitude to my supervisors, whom have all played their separate parts, in order to make this project possible. I would also like to thank my dear friends, Thomas Kittelmann and Jesper Levinsen, both ph.d students in physics, for proof reading the manuscript and providing ideas and feedback on how to improve it.

-Tommy Sonne Larsen

Abstract

In this Master Thesis type I and II superconductors will be studied numerically. The numerical simulations are made using both the stationary and time-dependent Ginzburg–Landau equations. It turns out that it is hard to make simulations having more than one vortex using the stationary equations. This is due to the difficulty of providing an initial guess which is close enough to the solution. For this reason the time-dependent equations are used to create multi-vortex systems.

During the simulations made with the stationary equations, it becomes clear that the assumptions made to derive the London Penetration depth and Ginzburg–Landau coherence length are valid. It will be shown that the numerical simulations act as predicted.

In the time-dependent simulations, vortex dynamics are investigated. It will be seen how the vortices enter the superconductor, and how they approach the steady state solution. It also becomes clear that hysteresis exists in a superconductor. The equations are also solved for defect geometries, and it turns out that these defects have a large impact, on how the vortices enter the superconductor. Finally it will be suggested that based on the numerical solutions, the time-dependent equations converge towards solutions of the stationary Ginzburg–Landau equations.

Resumé

I dette eksamensprojekt, bliver type I og II superledere studeret ved hjælp af numeriske simuleringer. Både de stationære og tids-afhængige ligninger vil blive løst. Det viser sig, at de stationære ligninger er svære at løse for mere end et vortex. Dette er på grund af, at det er vanskeligt at give et godt startsgæt, for systemer som indeholder mere end et vortex. Af denne årsag benyttes de tids-afhængige ligninger til at beregne løsninger, som indeholder mere end et vortex.

I løbet af simuleringerne af de stationære ligninger, bliver det klart, at de forudsætninger der blev stillet under udledningen af London indtrængnings dybden og Ginzburg-Landau kohærent længden er gyldige. De numeriske simuleringer udviser den opførsel, som blev forudset ved hjælp af disse udledninger.

I de tidsafhængige simuleringer bliver dynamikken mellem flere vortex undersøgt. Det vil blive vist hvorledes de trænger ind i superlederen, og hvorledes de går imod en stationær løsning. Det bliver også vist, at der findes hysteresi i systemet. Ligningerne vil også blive løst for geometrier som indeholder defekter, og det viser sig at disse defekter har en stor indflydelse på, hvor og hvorledes et vortex trænger ind i superlederen. Sidst bliver det antydnet, baseret på de numeriske beregninger, at de tidsafhængige ligninger går imod løsninger, som også er løsninger til de stationære ligninger.

Introduction

In 1908, the Dutch physicist Heike Kamerlingh Onnes of Leiden laboratory was able to liquefy Helium. Helium was the last remaining noble gas to be liquefied and has a boiling point at 4.55K. This achievement enabled Onnes to investigate physical properties near absolute zero. At that time, the understanding of electrical conductivity was very incomplete, however it was known that electrical resistance of many metals falls linearly with temperature near room temperature. With liquid helium Onnes began to investigate the electrical properties of metals near absolute zero. In 1911 he discovered superconductivity using Mercury and in his own words [1]

“the experiment left no doubt that, as far as accuracy of measurement went, the resistance disappeared. At the same time, however, something unexpected occurred. The disappearance did not take place gradually, but abruptly. From 1/500 the resistance at 4.2°K drops to a millionth part. At the lowest temperature, 1.5°K, it could be established that the resistance had become less than a thousand-millionth part of that at normal temperature.

Thus the mercury at 4.2°K has entered a new state, which, owing to its particular electric properties, can be called the state of superconductivity.”

With these words Onnes declared the existence of the superconducting state. A superconductor also has a *normal state* in which the superconductor behaves like a normal conductor with resistance. The temperature where the sample switches from normal state into superconducting state is called the transition temperature denoted T_c .

Onnes was not able to conclude that the resistance vanished, but only that it was lowered significantly by measuring an upper limit. Experiments conducted later on suggest that the superconducting state is ideal, that is the electrical resistance completely vanishes. Collins completed an experiment in 1957, where the current flowed within a superconducting ring and even after two and a half years there was no measurable change in the current [2]. Onnes won the Nobel prize in physics in 1913 for his remarkable work and the discovery of superconductors [3].

In 1933 W. Meissner and R. Ochsenfeld discovered an interesting physical property of superconductors by investigating superconductors in magnetic fields [4]. They found that in normal state there was a finite magnetic field inside the sample, but the moment the temperature reached T_c the magnetic field was expelled from the sample (this is in essence ideal diamagnetism). This phe-

nomena was called the Meissner effect, and when the magnetic field is expelled from the superconducting sample it is said to be in the *Meissner phase*.

Besides a critical temperature, a superconductor also has a critical magnetic field value denoted B_c . If the external field is strong enough it will destroy the superconducting phase and force the superconducting sample into normal phase. Whether a material is in the superconducting phase depends on the external magnetic field as well as the temperature.

It turns out that there are two types of superconductors. Type I superconductors can either be in normal phase or Meissner phase, but type II superconductors have a third phase called the *mixed phase* or *vortex phase*. In this third phase the superconducting sample is in the superconducting state. The vortex phase appears as follows; suppose we have a type II superconducting sample with an applied magnetic field strong enough to force the sample to be in the normal phase. The temperature in this setup is below the critical temperature, so if the magnetic field was any weaker the sample would be in a superconducting state. Now the magnetic field is made weaker and what happens is that the sample will first enter the vortex phase, and lowering the magnetic field further will make the sample enter the Meissner phase. In this way a type II superconductor has two critical magnetic field values. In the vortex phase the superconducting sample is partly in Meissner phase and normal phase, such that the external magnetic field penetrates the sample in some areas where vortices appears.

The discovery made by Onnes caused theoretical physicist difficulties for nearly half a decade. A lot a theories trying to describe the phenomena was developed of which three are still in use and will be discussed here briefly. The first theory appeared in 1935 was a phenomenological theory proposed by the London brothers and is now known as London theory [5]. Among other things the theory describes the magnetic properties of Type I superconductors and how the applied magnetic field has a penetration depth into the superconducting sample.

15 years later in 1950, V. L. Ginzburg and L. D. Landau extended the London theory and proposed a phenomenological theory, which is able to describe a superconductor in a strong magnetic field. The Ginzburg–Landau theory enables study of type II superconductors¹.

In 1957 the theoretical breakthrough finally appeared, when J. Bardeen, L. N. Cooper and J. R. Schrieffer laid forth a microscopic theory "Theory of Superconductivity" which later became known as BCS theory [6]. In BCS theory *Cooper* pairs are introduced which are the superconducting electrons. A Cooper pair consist of two electrons which are bound together. The BCS theory explains the superconducting phenomena below a temperature of 30-40K. Above this temperature BCS theory is no longer a valid theory for superconductors. The theory earned a Nobel prize in 1972.

With the theoretical foundation in place, physicist were able to explain the superconducting phenomina and the cause of the Meissner phase. It turns out, that the superconductor creates a current on the surface, which generates a shielding magnetic field opposite of the external magnetic field. This effect also

¹Ginzburg jointly won the Nobel prize in 2003 with A. A. Abrikosov and A. J. Leggett for their work on superconductors and superfluids. Landau also won the Nobel prize, but it was in 1962 "for his pioneering theories for condensed matter, especially liquid helium".

enables a theoretical suggestion that resistance of superconductors are truly zero.

For 29 years the theory of superconductors was thought to be complete, but J. G. Bednorz and K. A. Müller presented a discovery that made another challenge for theoretical physicist. In the IBM Laboratory in Switzerland they discovered a ceramic sample (La-Ba-Cu-O) with a critical temperature at 40K, and thus high temperature superconductors were discovered [7]. High temperature superconductors is beyond the scope of BCS Theory, which fails when the temperature becomes higher than 30-40K. At the moment, high temperature superconductors have several competing theories and it is still being discussed how they work. Bendnorz and Müller received the Nobel prize in 1987 for their discovery.

A curious fact about the discovery made by Bednorz and Müller is that ceramic samples which are insulators at room temperature can become superconductors, and on the contrary good conductors such as copper has no superconducting phase at all.

According to the website superconductors.org, the current record-holder for the highest T_c superconductor is the cuprate $(\text{Hg}_{0.8}\text{T}_{10.2})\text{Ba}_2\text{Ca}_2\text{Cu}_3\text{O}_{8.33}$ whose T_c is 138K.

For more information about the historical development of superconductors refer to the books [2, 1, 8].

Chapter 1

Ginzburg–Landau Theory

The Ginzburg–Landau theory originated in 1950 is a theory based on Landau’s theory on second order phase transitions [9]. In such a transition the molecules of the material in question are continuously being more and more *ordered* as the temperature is lowered (opposed to first order phase transitions as the transition from water to ice where the ordering all happens at one specific temperature). By ordered we mean that in a material in solid state, the molecules are more ordered compared to the fluid state. The Ginzburg–Landau theory treats the transition from normal state to superconducting state as a second order phase transition. On this account an order parameter is defined, that rises in the new phase (here the superconductor phase) which is zero at the temperature $T = T_c$ and one at $T = 0\text{K}$. The order parameter is denoted as $\Psi(\mathbf{r})$ where $|\Psi(\mathbf{r})|^2$ can be interpreted as the density of superconducting charge carriers. The order parameter is normalised such that $|\Psi(\mathbf{r})|^2 \leq 1$. At this point in time the BCS theory was yet to be developed and therefore it was not yet known what the “superconducting charge carriers” actually was. The Ginzburg–Landau theory was not really appreciated until 1959, when Gor’kov proved that Ginzburg–Landau theory can be derived from the microscopic BCS theory near the critical temperature T_c [10]. With the established correspondence between BCS and Ginzburg–Landau theory it became clear that the order parameter squared represents the density of Cooper pairs.

1.1 Thermodynamics in superconductors

The starting point of the time-independent Ginzburg–Landau theory is thermodynamical arguments involving Gibbs free energy. This text will discuss these arguments very briefly where a deeper treatment can be found in the book by W. Buckel and R. Kleiner [8].

To explain why the sample in question changes from a normal state to a superconducting state a Gibbs function with a special behaviour is constructed. A Gibbs function has dimension [energy] so it can be seen as a potential. The sought Gibbs function must fulfil two requirements:

- When the temperature is above T_c it must be energy-wise favourable to be in the normal conducting state. In this case the Gibbs function must have a minima at $\Psi = 0$ since there exists no Cooper pairs in the sample.

- When the temperature is below T_c it must be energy-wise favourable to be in the superconducting state. This means that the Gibbs function must have at least one minima where $\Psi \neq 0$ and the Gibbs function may not have minima at $\Psi = 0$.

This behaviour is exhibited by the Gibbs function shown in figure 1.1. This Gibbs function is constructed as follows; assuming that the Cooper pair density approaches zero sufficiently smoothly as the temperature approaches T_c , the Gibbs function can be expanded in a Taylor series of $|\Psi|^2$ around T_c ¹:

$$g_s = g_n + \alpha|\Psi|^2 + \frac{\beta}{2}|\Psi|^4 + \mathcal{O}(|\Psi|^6) \quad (1.1)$$

where g_n is the Gibbs function of the normal conducting state and g_s is the Gibbs function of the superconducting state. Note that g_s equals g_n when the material is in the normal conducting state (that is when $|\Psi|^2 = 0$). Sufficiently close to T_c a fourth order expansion is a satisfactory approximation so the terms after $|\Psi|^4$ are neglected. Since g_s is of dimension [energy/volume] and the dimension of $|\Psi|^2$ is [1/volume], the dimension of α needs to be [energy] and the dimension of β needs to be [energy · volume].

The signs of α and β can be determined by some physical observations; the equilibrium state of the system will be where g_s is minimal. Furthermore, below the transition temperature it is required that g_s is smaller than g_n otherwise the material will stay in the normal conducting state. With these observations in mind the following can be concluded

- β must be positive, otherwise the minima of g_s is found when $|\Psi| \rightarrow \infty$.
- Since β is positive α must be negative to ensure that $g_s < g_n$ for $T < T_c$.
- For $T > T_c$ the minima of g_s should be at $|\Psi| = 0$ (the normal conducting state). To meet this requirement α must be positive when $T > T_c$.

The values of α can be reversed by changing the sign of α in the Gibbs function, thus a new Gibbs function can be defined as

$$g_s = g_n - \alpha|\Psi|^2 + \frac{\beta}{2}|\Psi|^4 \quad (1.2)$$

where both α and β are positive when $T < T_c$ and α is negative when $T > T_c$. To meet the requirements for α we define $\alpha(T)$ as

$$\alpha(T) = \alpha(0) \left(1 - \frac{T}{T_c}\right) \quad (1.3)$$

Having $\alpha(0)$ as positive we see that $\alpha(T)$ behaves as required. The variable β is positive, so we can roughly set $\beta(T) \approx \beta(0)$. The Gibbs function (1.2) is the function illustrated in figure 1.1.

¹Note that the given Gibbs function is expressed as the energy density. The energy density is the energy per unit volume.

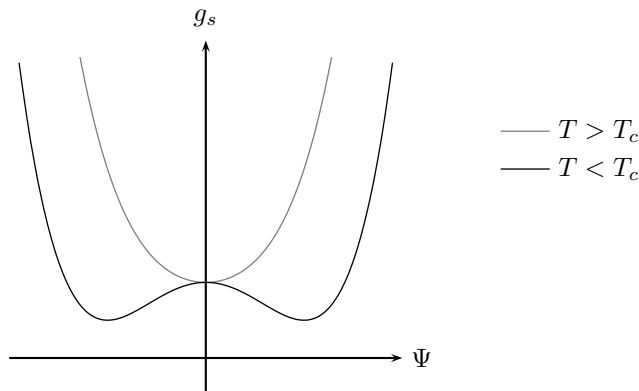


Figure 1.1: The Gibbs function g_s for the normal (gray) and superconducting (black) state.

1.2 The Gibbs function

To get a complete description of the superconducting state some additional terms must be added to the Gibbs function. In the Ginzburg–Landau theory one uses the ansatz

$$g_s = g_n + \frac{1}{2m} \left| \left(\frac{\hbar}{i} \nabla - q\mathbf{A} \right) \Psi \right|^2 - \alpha |\Psi|^2 + \frac{\beta}{2} |\Psi|^4 + \frac{1}{2\mu_0} |\mathbf{B}_a - \mathbf{B}_i|^2 \quad (1.4)$$

Note that SI units are used. Conversion of the Ginzburg–Landau equations from cgs to SI units is described in appendix A.

Two additional terms appear in the Gibbs function and their physical significance will be discussed briefly. To begin with the last term is discussed. It was mentioned in the introduction that the applied magnetic field was expelled from a superconductor in the superconducting phase. To achieve this effect a superconducting current appears in the superconductor. This current induces a magnetic field which expels the applied magnetic field. If \mathbf{B}_i is defined as the magnetic field inside the superconductor and \mathbf{B}_a as the applied magnetic field, then the absolute value of the induced magnetic field must be $|\mathbf{B}_a - \mathbf{B}_i|$. The energy density of the induced magnetic field denoted u_B then is [11]

$$u_B = \frac{1}{2\mu_0} |\mathbf{B}_a - \mathbf{B}_i|^2 \quad (1.5)$$

where μ_0 is the permeability of free space. Furthermore the following relation is found from electromagnetism

$$\mathbf{B}_i = \nabla \times \mathbf{A} \quad (1.6)$$

where \mathbf{A} is a vector potential. Thus the last term of the introduced Gibbs function represents the energy required to expel the applied magnetic field \mathbf{B}_a .

To analyse the first term quantum mechanics needs to be revisited. The classical Hamiltonian² for a charged particle in a magnetic field is [12]

$$H_{classic} = \frac{1}{2m} (\mathbf{p} - q\mathbf{A})^2 + q\phi \quad (1.7)$$

where $m = 2m_e$ and $|q| = 2e$ is the mass and charge of the Cooper pairs. Furthermore \mathbf{p} is the momentum and ϕ is the electric scalar potential. In the expression for $H_{classic}$ the first term refers to the kinetic energy and the last term refers to the potential energy. The quantum mechanical Hamiltonian is now obtained by inserting the momentum operator defined as

$$\hat{\mathbf{p}} = \frac{\hbar}{i} \nabla \quad (1.8)$$

and the resulting quantum mechanical Hamiltonian becomes

$$\hat{H} = \frac{1}{2m} \left(\frac{\hbar}{i} \nabla - q\mathbf{A} \right)^2 + q\phi \quad (1.9)$$

To calculate the energy of a particle with the wavefunction ψ we can use that

$$E = \int_{-\infty}^{\infty} \psi^* \hat{H} \psi d^3\mathbf{r} \quad (1.10)$$

If only the kinetic energy is calculated we get

$$E = \frac{1}{2m} \int_{-\infty}^{\infty} \psi^* \left(\frac{\hbar}{i} \nabla - q\mathbf{A} \right) \left(\frac{\hbar}{i} \nabla - q\mathbf{A} \right) \psi d^3\mathbf{r} \quad (1.11)$$

By using integration by parts³ we obtain

$$E = \frac{1}{2m} \int_{-\infty}^{\infty} \left(-\frac{\hbar}{i} \nabla - q\mathbf{A} \right) \psi^* \left(\frac{\hbar}{i} \nabla - q\mathbf{A} \right) \psi d^3\mathbf{r} \quad (1.12)$$

where it is used that the surface integral vanishes. We see that the integrand equals the second term of \mathcal{L} in equation (1.4). By this fact we can assume that the second term is related to the kinetic energy of the Cooper pairs.

In order to get the Gibbs energy of the entire superconducting sample the Gibbs function needs to be intergrated over the entire sample since the Gibbs function is written as an energy density. Before doing so the difference between the normal state and superconducting state is defined as $\mathcal{L} = g_s - g_n$. The motivation behind this is that g_n merely adds as a constant to g_s and therefore it is really the difference that is interesting. Writing \mathcal{L} in full gives

$$\mathcal{L} = \frac{1}{2m} \left| \left(\frac{\hbar}{i} \nabla - q\mathbf{A} \right) \Psi \right|^2 - \alpha |\Psi|^2 + \frac{\beta}{2} |\Psi|^4 + \frac{1}{2\mu_0} |\mathbf{B}_a - \mathbf{B}_i|^2 \quad (1.13)$$

²The Hamiltonian in general is the sum of kinetic and potential energy. The kinetic energy is usually denoted T and the potential energy V .

³Integration by parts is calculated as $\int_{\Omega} f \nabla g d\Omega = - \int_{\Omega} (\nabla f) g d\Omega + \int_{\partial\Omega} \mathbf{n} f g dS$, which is derived using Gauss' theorem.

And the total energy for the superconducting sample is

$$\begin{aligned} \mathcal{H}(\Psi(\mathbf{r}), \Psi^*(\mathbf{r}), \mathbf{A}(\mathbf{r})) = \int_{\Omega} d^3\mathbf{r} \left(g_n + \frac{1}{2m} \left| \left(\frac{\hbar}{i} \nabla - q\mathbf{A} \right) \Psi \right|^2 \right. \\ \left. - \alpha |\Psi|^2 + \frac{\beta}{2} |\Psi|^4 + \frac{1}{2\mu_0} |\mathbf{B}_a - \mathbf{B}_i|^2 \right) \end{aligned} \quad (1.14)$$

where Ω is the volume of the superconducting sample.

1.3 Derivation of Ginzburg–Landau equations

Since the equilibrium states are determined by the extrema of the Gibbs function, the Gibbs function has to be minimized. To find the minima, variation with respect to the order parameter and vector potential is performed. The resulting equations are the Ginzburg–Landau equations.

Following the rules of calculus of variations the following functions are defined when variation of the Gibbs function is performed

$$\begin{aligned} \Psi^*(\mathbf{r}, \varepsilon) = \Psi_0^*(\mathbf{r}) + \varepsilon \zeta_1(\mathbf{r}) = \Psi_0^* + \delta\Psi^* &\Rightarrow \frac{\partial \Psi^*}{\partial \varepsilon} \varepsilon = \delta\Psi^* \\ \Psi(\mathbf{r}, \varepsilon) = \Psi_0(\mathbf{r}) + \varepsilon \zeta_2(\mathbf{r}) = \Psi_0 + \delta\Psi &\Rightarrow \frac{\partial \Psi}{\partial \varepsilon} \varepsilon = \delta\Psi \\ \mathbf{A}(\mathbf{r}, \varepsilon) = \mathbf{A}_0(\mathbf{r}) + \varepsilon \zeta_3(\mathbf{r}) = \mathbf{A}_0 + \delta\mathbf{A} &\Rightarrow \frac{\partial \mathbf{A}}{\partial \varepsilon} \varepsilon = \delta\mathbf{A} \\ \mathcal{H}(\mathbf{r}, \varepsilon) = \mathcal{H}_0(\mathbf{r}) + \varepsilon \zeta_4(\mathbf{r}) = \mathcal{H}_0 + \delta\mathcal{H} &\Rightarrow \frac{\partial \mathcal{H}}{\partial \varepsilon} \varepsilon = \delta\mathcal{H} \end{aligned} \quad (1.15)$$

These new functions are inserted into (1.14) such that \mathcal{H} now depends on ε too.

The first variation that is calculated is variation of \mathcal{H} with respect to Ψ^* . This means that ζ_2 and ζ_3 are set to zero. Now the only functions in (1.14) that depends on ε are \mathcal{H} , Ψ^* and $\nabla\Psi^*$. To begin with the integrand of (1.14) is written out

$$\begin{aligned} \mathcal{L} = \frac{1}{2m} \left(-\frac{\hbar^2}{i^2} \nabla\Psi \nabla\Psi^* + q^2 \mathbf{A} \cdot \mathbf{A} |\Psi|^2 + \frac{\hbar}{i} q \mathbf{A} \cdot (\Psi \nabla\Psi^* - \Psi^* \nabla\Psi) \right) \\ - \alpha |\Psi|^2 + \frac{\beta}{2} |\Psi|^4 + \frac{1}{2\mu} |\mathbf{B}_a - \nabla \times \mathbf{A}|^2 \end{aligned} \quad (1.16)$$

Note that $|\Psi|^2$ can also be written as $\Psi\Psi^*$. The relevant variables in \mathcal{L} with respect to the variation of Ψ^* is

$$\mathcal{L} = \mathcal{L}(\Psi^*, \Psi_{,x}^*, \Psi_{,y}^*, \Psi_{,z}^*, x, y, z, \dots) = \mathcal{L}(\Psi^*, \nabla\Psi^*, \mathbf{r}, \dots) \quad (1.17)$$

The last rewriting can be done because of the structure of \mathcal{L} . Using the modified functions introduced in (1.15), differentiation of equation (1.14) with respect to ε and multiplication with ε yields⁴

$$\frac{\partial \mathcal{H}}{\partial \varepsilon} \varepsilon = \int_{\Omega} d^3\mathbf{r} \frac{d\mathcal{L}}{d\varepsilon} \varepsilon = \int_{\Omega} d^3\mathbf{r} \left(\frac{\partial \mathcal{L}}{\partial \Psi^*} \frac{\partial \Psi^*}{\partial \varepsilon} \varepsilon + \frac{\partial \mathcal{L}}{\partial (\nabla\Psi^*)} \cdot \frac{\partial (\nabla\Psi^*)}{\partial \varepsilon} \varepsilon \right) \quad (1.18)$$

⁴The notation $\frac{\partial}{\partial \mathbf{V}}$ where \mathbf{V} is a vector means $\frac{\partial}{\partial \mathbf{V}} = \left(\frac{\partial}{\partial V_x}, \frac{\partial}{\partial V_y}, \frac{\partial}{\partial V_z} \right)$.

where the chainrule is used to resolve the differentiation. The equation is rewritten using (1.15)⁵

$$\delta\mathcal{H} = \int_{\Omega} d^3\mathbf{r} \left(\frac{\partial\mathcal{L}}{\partial\Psi^*} \delta\Psi^* + \frac{\partial\mathcal{L}}{\partial(\nabla\Psi^*)} \cdot \nabla\delta\Psi^* \right) \quad (1.19)$$

In order to proceed, the term $\nabla\delta\Psi^*$ needs to be removed. This is achieved by integration by parts⁶, and the last term in rewritten as

$$\int_{\Omega} d^3\mathbf{r} \frac{\partial f}{\partial(\nabla\Psi^*)} \nabla\delta\Psi^* = \int_{\partial\Omega} d^2\mathbf{r} \frac{\partial f}{\partial(\nabla\Psi^*)} \cdot \mathbf{n} \delta\Psi^* - \int_{\Omega} d^3\mathbf{r} \nabla \left(\frac{\partial f}{\partial(\nabla\Psi^*)} \right) \delta\Psi^* \quad (1.20)$$

such that the variation of \mathcal{H} is

$$\delta\mathcal{H} = \int_{\Omega} d^3\mathbf{r} \left(\frac{\partial\mathcal{L}}{\partial\Psi^*} - \nabla \left(\frac{\partial\mathcal{L}}{\partial(\nabla\Psi^*)} \right) \right) \delta\Psi^* + \int_{\partial\Omega} d^2\mathbf{r} \frac{\partial\mathcal{L}}{\partial(\nabla\Psi^*)} \cdot \mathbf{n} \delta\Psi^* \quad (1.21)$$

In order to solve the variation problem the two derivatives in the above equation are calculated as

$$\frac{\partial\mathcal{L}}{\partial\Psi^*} = \frac{1}{2m} \left([q\mathbf{A}]^2 \Psi - \frac{\hbar}{i} q\mathbf{A} \cdot \nabla\Psi \right) - \alpha\Psi + \beta|\Psi|^2\Psi \quad (1.22a)$$

$$\frac{\partial\mathcal{L}}{\partial(\nabla\Psi^*)} = \frac{1}{2m} \left(-\frac{\hbar^2}{i^2} \nabla\Psi + \frac{\hbar}{i} q\mathbf{A}\Psi \right) \quad (1.22b)$$

Inserting the derivatives into (1.21) and rearranging yields⁷

$$\begin{aligned} \delta\mathcal{H} = \int_{\Omega} d^3\mathbf{r} \left(\frac{1}{2m} \left[\frac{\hbar}{i} \nabla - q\mathbf{A}_0 \right]^2 \Psi_0 - \alpha\Psi_0 + \beta|\Psi_0|^2\Psi_0 \right) \delta\Psi^* \\ - \int_{\partial\Omega} d^2\mathbf{r} \frac{1}{2m} \frac{\hbar}{i} \left(\frac{\hbar}{i} \nabla\Psi_0 - q\mathbf{A}_0\Psi_0 \right) \cdot \mathbf{n} \delta\Psi^* \end{aligned} \quad (1.23)$$

This concludes the variation of the order parameter and now the same procedure is used with the vector potential. Of the terms where the vector potential features in equation (1.16), it is seen that \mathcal{L} depends only on \mathbf{A} and $\nabla \times \mathbf{A}$. Using the defined functions in (1.15), differentiating equation (1.14) with respect to ε and multiplying with ε yields⁸

$$\delta\mathcal{H} = \int_{\Omega} d^3\mathbf{r} \left(\frac{\partial\mathcal{L}}{\partial\mathbf{A}} \delta\mathbf{A} + \frac{\partial\mathcal{L}}{\partial(\nabla \times \mathbf{A})} \cdot \nabla \times \delta\mathbf{A} \right) \quad (1.24)$$

In order to continue the following rule is used

$$\mathbf{Q} \cdot (\nabla \times \mathbf{W}) = \mathbf{W} \cdot (\nabla \times \mathbf{Q}) - \nabla \cdot (\mathbf{Q} \times \mathbf{W}) \quad (1.25)$$

⁵It is used that $\frac{\partial(\nabla\Psi^*)}{\partial\varepsilon} = \nabla \frac{\partial\Psi^*}{\partial\varepsilon}$.

⁶Integration by parts are calculated using $\int_{\Omega} (\nabla f) \cdot \mathbf{V} d\Omega = \int_{\partial\Omega} \mathbf{n} \cdot \mathbf{V} f dS - \int_{\Omega} f \nabla \cdot \mathbf{V} d\Omega$, which is derived using Gauss' theorem.

⁷In order to obtain $\delta\mathcal{H}$ we use the fact that $\delta\mathbf{A} = 0$ and $\delta\Psi = 0$, as they are not being varied. Thus $\mathbf{A} = \mathbf{A}_0$ and $\Psi = \Psi_0$.

⁸It is used that $\frac{\partial(\nabla \times \mathbf{A})}{\partial\varepsilon} = \nabla \times \frac{\partial\mathbf{A}}{\partial\varepsilon}$.

which turn the last term of equation (1.24) into

$$\frac{\partial \mathcal{L}}{\partial(\nabla \times \mathbf{A})} \cdot (\nabla \times \delta \mathbf{A}) = \delta \mathbf{A} \cdot \left(\nabla \times \frac{\partial \mathcal{L}}{\partial(\nabla \times \mathbf{A})} \right) - \nabla \cdot \left(\frac{\partial \mathcal{L}}{\partial(\nabla \times \mathbf{A})} \times \delta \mathbf{A} \right) \quad (1.26)$$

By making the substitution in (1.24) and using Gauss' rule⁹ a formula for the variation is obtained as

$$\delta \mathcal{H} = \int_{\Omega} d^3 \mathbf{r} \left(\frac{\partial \mathcal{L}}{\partial \mathbf{A}} + \nabla \times \frac{\partial \mathcal{L}}{\partial(\nabla \times \mathbf{A})} \right) \delta \mathbf{A} - \int_{\partial \Omega} d^2 \mathbf{r} \mathbf{n} \cdot \left(\frac{\partial \mathcal{L}}{\partial(\nabla \times \mathbf{A})} \times \delta \mathbf{A} \right) \quad (1.27)$$

The derivatives are calculated as

$$\frac{\partial \mathcal{L}}{\partial \mathbf{A}} = \frac{1}{2m} \left(2q^2 |\Psi|^2 \mathbf{A} + \frac{\hbar}{i} q (\Psi \nabla \Psi^* - \Psi^* \nabla \Psi) \right) \quad (1.28a)$$

$$\frac{\partial \mathcal{L}}{\partial(\nabla \times \mathbf{A})} = -\frac{1}{\mu_0} (\mathbf{B}_a - \nabla \times \mathbf{A}) \quad (1.28b)$$

To calculate the last derivative it is used that neither magnetic fields are complex, thus $|\mathbf{B}_a - \nabla \times \mathbf{A}|^2 = (\mathbf{B}_a - \nabla \times \mathbf{A})^2$. Using the calculated derivatives the variation with respect to \mathbf{A} becomes

$$\delta \mathcal{H} = \int_{\Omega} d^3 \mathbf{r} \left(\frac{1}{2m} \left[2q^2 |\Psi_0|^2 \mathbf{A} + \frac{\hbar}{i} q (\Psi_0 \nabla \Psi_0^* - \Psi_0^* \nabla \Psi_0) \right] - \frac{1}{\mu_0} \nabla \times (\mathbf{B}_a - \nabla \times \mathbf{A}) \right) \delta \mathbf{A} + \int_{\partial \Omega} d^2 \mathbf{r} \frac{1}{\mu_0} \mathbf{n} \cdot (\mathbf{B}_a - \nabla \times \mathbf{A}) \times \delta \mathbf{A} \quad (1.29)$$

Now the Ginzburg–Landau equations can be read from (1.23) and (1.29). In order to achieve minima of \mathcal{H} it is required that $\delta \mathcal{H} = 0$. Since the variations are arbitrary the integrands must vanish. The surface integrals are used to establish boundary conditions.

$$\frac{1}{2m} \left(\frac{\hbar}{i} \nabla - q \mathbf{A}_0 \right)^2 \Psi_0 - \alpha \Psi_0 + \beta |\Psi_0|^2 \Psi_0 = 0 \quad \text{in } \Omega \quad (1.30a)$$

$$\left(\frac{\hbar}{i} \nabla \Psi_0 - q \mathbf{A}_0 \Psi_0 \right) \cdot \mathbf{n} = 0 \quad \text{on } \partial \Omega \quad (1.30b)$$

$$\frac{1}{2m} \left(2q^2 |\Psi_0|^2 \mathbf{A} + \frac{\hbar}{i} q [\Psi_0 \nabla \Psi_0^* - \Psi_0^* \nabla \Psi_0] \right) - \frac{1}{\mu_0} \nabla \times (\mathbf{B}_a - \nabla \times \mathbf{A}) = 0 \quad \text{in } \Omega \quad (1.30c)$$

$$\mathbf{B}_a - \nabla \times \mathbf{A} = 0 \quad \text{on } \partial \Omega \quad (1.30d)$$

⁹Gauss' rule can be written as $\int_{\Omega} \nabla \cdot \mathbf{V} d\Omega = \int_{\partial \Omega} \mathbf{n} \cdot \mathbf{V} dS$.

Note that the third equation (1.30c) contains the term $\nabla \times \nabla \times \mathbf{A}$. From (1.6) we have that this term equals $\nabla \times \mathbf{B}_i$ and this term also exists in Ampere’s law (from Maxwell’s equations):

$$\frac{1}{\mu_0} \nabla \times \mathbf{B} = \mathbf{j} + \epsilon_0 \frac{\partial \mathbf{E}}{\partial t} \quad (1.31)$$

where \mathbf{E} is the electric field and \mathbf{j} is the current. Since the Ginzburg–Landau equations are steady state, the steady state Ampere’s law will be used which means the time derivative vanish. By using the time-independent Ampere’s law, the relation $\mathbf{B}_i = \nabla \times \mathbf{A}$ and dropping the variation subscripts the equations can be put on a more familiar form

$$\frac{1}{2m} \left(\frac{\hbar}{i} \nabla - q\mathbf{A} \right)^2 \Psi - \alpha\Psi + \beta|\Psi|^2\Psi = 0 \quad \text{in } \Omega \quad (1.32a)$$

$$\left(\frac{\hbar}{i} \nabla \Psi - q\mathbf{A}\Psi \right) \cdot \mathbf{n} = 0 \quad \text{on } \partial\Omega \quad (1.32b)$$

$$\frac{q\hbar}{2mi} (\Psi^* \nabla \Psi - \Psi \nabla \Psi^*) - \frac{q^2}{m} |\Psi|^2 \mathbf{A} + \frac{1}{\mu_0} \nabla \times \mathbf{B}_a = \mathbf{j}_s \quad \text{in } \Omega \quad (1.32c)$$

$$\mathbf{B}_a = \mathbf{B}_i \quad \text{on } \partial\Omega \quad (1.32d)$$

The boundary conditions can be given some physical meaning. The first boundary condition (1.32b) states that no current can flow out of the superconducting sample if the applied magnetic field is uniform, which mathematically means that the curl of the applied magnetic field is zero. The second boundary condition (1.32d) states that the magnetic field must be continuous.

To show that the boundary condition (1.32b) enforces what is claimed, the boundary condition is multiplied by Ψ^* . This yields

$$\Psi^* \left(\frac{\hbar}{i} \nabla \Psi - q\Psi\mathbf{A} \right) \cdot \mathbf{n} = 0 \quad \Leftrightarrow \quad \Psi \left(-\frac{\hbar}{i} \nabla \Psi^* - q\Psi^*\mathbf{A} \right) \cdot \mathbf{n} = 0 \quad (1.33)$$

If these two terms are added together and multiplied by $\frac{q}{2m}$ one gets

$$\frac{q}{2m} \left(\Psi^* \left[\frac{\hbar}{i} \nabla \Psi - q\Psi\mathbf{A} \right] \cdot \mathbf{n} + \Psi \left[-\frac{\hbar}{i} \nabla \Psi^* - q\Psi^*\mathbf{A} \right] \cdot \mathbf{n} \right) = 0 \quad (1.34)$$

The left hand side of the above equation is equivalent to the left hand side of (1.32c) if the curl of \mathbf{B}_a is zero, hence it is proved that from the first boundary it follows that $\mathbf{j}_s \cdot \mathbf{n} = 0$.

A looser boundary condition can actually be used to enforce that no current can flow out of the superconducting sample. If a real valued function γ is defined such that

$$\left(\frac{\hbar}{i} \nabla \Psi - q\Psi\mathbf{A} \right) \cdot \mathbf{n} = \nu\gamma \quad \text{on } \partial\Omega \quad (1.35)$$

a new boundary condition is formed. Provided that the applied magnetic field is uniform it can be readily verified that the above equation indeed satisfy $\mathbf{j}_s \cdot \mathbf{n} = 0$ by inserting it into (1.32d). The boundary condition (1.35) can be derived from BCS theory, from where it follows that $\gamma = 0$ for a superconductor-insulator

(or vacuum) interface and $\gamma \neq 0$ for a superconductor-normal conductor interface [13]. Note that (1.35) equals (1.32b) when γ is 0 and therefore the boundary condition derived from the variational process is only valid for a superconductor-insulator interface.

It is noted by Qiang, Gunzburger and Peterson that by adding $\int_{\partial\Omega} -v\gamma dS$ to (1.14) the boundary condition (1.35) directly follows from the variational process [13]. However they also state that to their knowledge there is no physical justification for this addition to the free energy.

1.4 Characteristic lengths

Within the theory of superconductivity two important length scales appear. First the length scale the *London penetration depth* is treated and secondly the *Ginzburg-Landau coherence length* is given attention.

1.4.1 London penetration depth

The London penetration depth was introduced in the London theory formulated by the London brothers in 1935 [5]. London theory describes superconductors in the Meissner phase, which means that the applied magnetic field does not penetrate the superconducting sample. An expression for the London penetration depth can be found from the Ginzburg-Landau equations. The starting point is to find an expression for the density of Cooper pairs, when the superconductor is in the Meissner phase. Since we are dealing with stationary equations it is required that the superconductor is in equilibrium state. This leads to $dg_s/d|\Psi|^2 = 0$ as the energy density is not allowed to change anywhere when the superconductor is in the equilibrium state. The energy density was found in equation (1.4) and from $dg_s/d|\Psi|^2$ we get

$$-\alpha + \beta|\Psi|^2 + q^2\mathbf{A} \cdot \mathbf{A} = 0 \quad (1.36)$$

Since the superconductor is in the Meissner phase the vectorpotential \mathbf{A} can be chosen to vanish. If this is done an expression for the density of Cooper pairs for superconductors in Meissner phase denoted Ψ_∞ is found as

$$|\Psi_\infty|^2 = \frac{\alpha}{\beta} \quad (1.37)$$

This expression is inserted into equation (1.32c). The first term of (1.32c) vanishes since the gradient of Ψ_∞ equals zero as both α and β are constants. Furthermore in London theory the applied magnetic field is required uniform so the curl of \mathbf{B}_a also vanishes. Thus by inserting the expression for Ψ_∞ into equation (1.32c) it reduces to

$$\mathbf{j}_s = -\frac{q^2\alpha}{m\beta}\mathbf{A} \quad (1.38)$$

Taking the curl of both sides and using the fact that $\nabla \times \mathbf{A} = \mathbf{B}_i$ yields

$$\mathbf{B}_i = -\frac{m\beta}{q^2\alpha}\nabla \times \mathbf{j}_s \quad (1.39)$$

The above equations is the second London equations [8]. The London penetration depth is introduced as

$$\lambda_L = \sqrt{\frac{m\beta}{\mu_0 q^2 \alpha}} \quad (1.40)$$

λ_L has dimension [length] as it should have¹⁰. By using the London penetration depth the second London equation can be written in the well-known form

$$\mathbf{B}_i = -\mu_0 \lambda_L \nabla \times \mathbf{j}_s \quad (1.41)$$

The meaning of λ_L can be illustrated by solving the second London equation. To solve the equation it is rewritten using Amperes law (1.31) without the time derivatives. Amperes law is changed into

$$\nabla \times \mathbf{B}_i = \mu_0 \mathbf{j}_s \quad (1.42)$$

by using that $\mathbf{B}_i = \mu \mathbf{B}$ with $\mu \approx 1$ for non-magnetic superconductors and $\mathbf{j} = \mathbf{j}_s$ [8]. Now the curl of both sides of equation (1.42) is taken

$$\nabla \times \nabla \times \mathbf{B}_i = \mu_0 \nabla \times \mathbf{j}_s \quad (1.43)$$

This equation is rewritten by using the following standard formula found from mathematical analysis

$$\nabla \times \nabla \times \mathbf{B}_i = \nabla(\nabla \cdot \mathbf{B}_i) - \nabla^2 \mathbf{B}_i \quad (1.44)$$

From Maxwells equations we have $\nabla \cdot \mathbf{B}_i = 0$ [11]. Using this fact equation (1.43) is finally written as

$$\nabla^2 \mathbf{B}_i = -\mu_0 \nabla \times \mathbf{j}_s \quad (1.45)$$

This result is combined with the second London equation (1.39) and a new equation is formed

$$\nabla^2 \mathbf{B}_i = \frac{1}{\lambda_L^2} \mathbf{B}_i \quad (1.46)$$

This equation is simplified to make it easier to solve. We consider a very large two-dimensional superconductor where the applied magnetic field only has a z component. The superconductor is positioned so $x = 0$ is the boundary of the superconductor and the right halfspace is inside the superconducting sample. This reduces (1.46) to the differential equation

$$\frac{d^2 B_{iz}(x)}{dx^2} = \frac{1}{\lambda_L^2} B_{iz}(x) \quad (1.47)$$

This equation is solved by using standard methods for second order differential equations¹¹. The equation has two solutions however only one of them has

¹⁰The dimensions of the entities in λ_L are $m = [\text{kg}]$, $\beta = [\text{J} \cdot \text{m}^3]$, $\mu_0 = [\text{kg} \cdot \text{m} \cdot \text{C}^{-2}]$, $q = [\text{C}]$ and $\alpha = [\text{J}]$. Inserting these dimensions in the expression for λ_L leads to $\lambda_L = [\text{m}]$.

¹¹The associated characteristic equation $R^2 - \lambda_L^{-2} = 0$ is formed and solved. The solution is $R = \pm \frac{1}{\lambda_L}$, and the solution to the differential equation is $B_{iz}(x) = c_1 e^{\frac{x}{\lambda_L}} + c_2 e^{-\frac{x}{\lambda_L}}$.

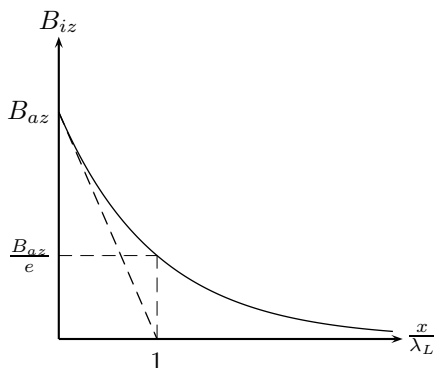


Figure 1.2: Decrease of the magnetic field inside a superconductor which is in the Meissner phase.

physical meaning. In the discarded solution the magnetic field inside the superconductor approaches infinity as x approaches infinity. With the boundary condition $B_{iz}(0) = B_{az}$ the acceptable solution is found to be

$$B_{iz}(x) = B_{az}e^{-\frac{x}{\lambda_L}} \quad (1.48)$$

Note that in this solution the magnetic field approaches zero as x approaches infinity. The solution is shown on figure 1.2. From this solution it is concluded that λ_L is the length it takes for the applied magnetic field to decrease with a factor e from the interface. Another interpretation of λ_L can be made by calculating the derivative of $B_{iz}(x)$

$$B'_{iz}(x) = -\frac{B_{az}}{\lambda_L}e^{-\frac{x}{\lambda_L}} \quad (1.49)$$

Then at $x = 0$ the derivative is $B'_{iz}(0) = -B_{az}\lambda_L^{-1}$. This means that when drawing a line $B_{iz}(x) = -B_{az}\lambda_L^{-1}x + B_{az}$ it will cross the x -axis at $x = \lambda_L$.

1.4.2 Ginzburg–Landau coherence length

The other characteristic length is found directly from the Ginzburg–Landau equations and is called the *Ginzburg–Landau coherence length*. This length is found by normalising equation (1.32a) to Ψ_∞ by making the following transformation

$$\psi = \frac{\Psi}{\Psi_\infty} \quad (1.50)$$

where Ψ_∞ was found in equation (1.37). Making the transformation yields

$$\frac{1}{2m} \left(\frac{\hbar}{i} \nabla - q\mathbf{A} \right)^2 \psi \Psi_\infty - \alpha \psi \Psi_\infty + \beta |\psi|^2 |\Psi_\infty|^2 \psi \Psi_\infty = 0 \quad (1.51)$$

Since Ψ_∞ is spatially constant, we are free to remove it from the equation in spite of the ∇ -operator. Dividing the equation with $\alpha\Psi_\infty$ and using equation (1.37) to replace $\beta|\Psi_\infty|^2$ with α in the last term yields

$$\frac{\hbar^2}{2m\alpha} \left(\frac{1}{i} \nabla - \frac{q}{\hbar} \mathbf{A} \right)^2 \psi - \psi + |\psi|^2 \psi = 0 \quad (1.52)$$

The \hbar^2 that appears in front of the brackets is just a reorganisation of the first term. The quantity in front of the first term has units of $[\text{length}]^2$, so this may yield a characteristic length¹². If the vector potential and the higher order term is disregarded, the resulting equation has the solution $e^{i\frac{x}{\xi_{GL}}}$ where ξ_{GL} is

$$\xi_{GL} = \sqrt{\frac{\hbar^2}{2m\alpha}} \quad (1.53)$$

This solution is a wave with a period of order ξ_{GL} , so ξ_{GL} is indeed a characteristic length. This length is the Ginzburg–Landau coherence length and to illustrate what this length represents, the first Ginzburg–Landau equation is solved for the Meissner phase. Disregarding \mathbf{A} in (1.52) and using the newly found coherence length, equation (1.52) becomes

$$-\xi_{GL}^2 \nabla^2 \psi - \psi + |\psi|^2 \psi = 0 \quad (1.54)$$

To make matters more simple we consider the case where the superconductor extends the x direction from zero to infinity, and in the y and z direction the superconductor is extended to infinity. Thus the superconductor only has an interface at $x = 0$. If we only consider the real case the Ginzburg–Landau equation reduces to

$$\xi_{GL}^2 \frac{d^2 \psi(x)}{dx^2} + \psi(x) - \psi^3(x) = 0 \quad (1.55)$$

For $x > 0$ this equation has the real solution [8]

$$\psi(x) = \tanh\left(\frac{x}{\sqrt{2}\xi_{GL}}\right) \quad (1.56)$$

This solution is shown on figure 1.3. We see that ξ_{GL} gives an indication of how fast the order parameter changes. At the boundary there are no Cooper pairs but after ξ_{GL} the Cooper pair density is 37% of the Meissner phase¹³. It turns out that ξ_{GL} also gives an indication of how big the vortices in a vortex phase superconductor are. This will be seen in chapter 3.

1.5 Critical magnetic fields

Three critical magnetic fields appears in the Ginzburg–Landau theory

- \mathbf{B}_c is the thermodynamical critical field where it becomes energy-wise more favourable for the superconductor to exist in the normal phase compared to the Meissner phase. This field only applies to type I superconductors.

¹²The dimensions of the units are $\hbar = [\text{J} \cdot \text{s}]$, $m = [\text{kg}]$ and $\alpha = [\text{J}]$. With $[\text{J}] = [\text{kg} \cdot \text{m}^2 \cdot \text{s}^{-2}]$ the dimension of $\frac{\hbar^2}{2m\alpha}$ is calculated to be $[\text{m}^2]$ which is $[\text{length}^2]$.

¹³The Cooper pair density is 37% since it is ψ^2 which is 0.61^2 .

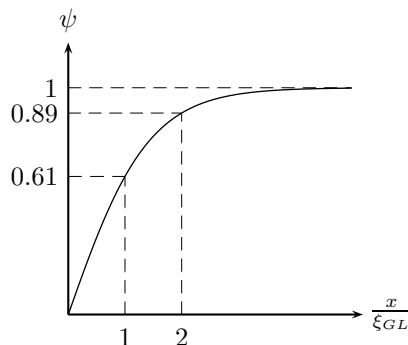


Figure 1.3: Increase in the density of Cooper pairs at the interface of the superconductor. The ψ axis is normalized to the Meissner phase according to equation (1.50), so the figure shows that the Cooper pair density asymptotically approaches the Meissner phase.

- \mathbf{B}_{c1} is the magnetic field where a type II superconductor switches from Meissner phase to vortex phase.
- \mathbf{B}_{c2} is the magnetic field where superconductivity can no longer exist in a type II superconductor.

With the knowledge of the Meissner effect it seems intuitively correct that strong magnetic fields will destroy superconductivity. If we have type I superconductor in the Meissner phase, it seems physical valid that at some point the superconductor can no longer resist the applied magnetic fields. The superconductor gives in to the applied magnetic field and superconductivity is destroyed. A type II superconductor is smarter however. Instead of letting the magnetic field destroy superconductivity entirely, the superconductor lets the applied magnetic field pass through in small regions and thus eases the “pressure” from the applied magnetic field. However, if the superconductor lets the magnetic field pass through in some areas, then at some point the magnetic field penetrates everywhere, and superconductivity is finally destroyed.

The above discussion does not hold any physical proof as it merely sees the phenomena from an intuitive point of view. \mathbf{B}_c and \mathbf{B}_{c2} will therefore be derived whereas \mathbf{B}_{c1} will only be cited due to the complexity of the derivation process.

1.5.1 The thermodynamic critical field

The thermodynamical critical field is the field where it is not longer favourable energy-wise for the superconductor to be in the Meissner phase. The value of this field is determined from the energy density found in equation (1.13). The energy density of the normal phase is calculated by letting $|\Psi|^2 = 0$, as there are no Cooper pairs present. Furthermore since the applied magnetic field penetrates the superconductor everywhere \mathbf{B}_a equals \mathbf{B}_i everywhere. The energy density

in this situation becomes

$$\mathcal{L}_n = 0 \quad (1.57)$$

The energy density of the Meissner phase is calculated by letting \mathbf{A} and \mathbf{B}_i vanish, as there is no magnetic field inside the superconductor. Furthermore the Cooper pair density for the Meissner phase was found in equation (1.37) so we let $|\Psi|^2 = |\Psi_\infty|^2$. The energy density for the Meissner phase then becomes

$$\mathcal{L}_m = -\frac{\alpha^2}{2\beta} + \frac{\mathbf{B}_a^2}{2\mu_0} \quad (1.58)$$

We have used the fact that the gradient of Ψ_∞ vanishes since Ψ_∞ is spatially constant.

If \mathcal{L}_n is greater than \mathcal{L}_m the superconductor will be in the Meissner phase, and if it is smaller, it will be in the normal phase. The transition from Meissner phase to normal phase therefore happens when \mathcal{L}_n equals \mathcal{L}_m . Thus we solve equation (1.58) for \mathbf{B}_a when \mathcal{L}_n equals \mathcal{L}_m . This defines the thermodynamical critical field value which is

$$B_c = \sqrt{\mu_0 \frac{\alpha^2}{\beta}} \quad (1.59)$$

The value of B_c depends on the temperature since α is temperature-dependent. This temperature-dependency was introduced in equation (1.3) and a similar temperature-dependent expression can be formed for B_c as

$$B_c'(T) = 2B_c(0) \left(1 - \frac{T}{T_c}\right) \quad (1.60)$$

However this expression is only valid near T_c . An expression for $B_c(T)$ has been determined empirically as [8]

$$B_c(T) \propto B_c(0) \left(1 - \left[\frac{T}{T_c}\right]^2\right) \quad (1.61)$$

These two expressions has been plotted in figure 1.4. From the figure it is seen that (1.60) is a good approximation near T_c . The plot on figure 1.4 is valid for type I superconductors, but not necessarily for type II superconductors. The calculations made in this chapter, only considers when it becomes more attractive energy-wise to be in the normal phase compared to the Meissner phase. However, in order to calculate the magnetic field value, which destroys superconductivity for type II superconductors, the vortex phase needs to be taken into account. It could be, that the vortex phase is more attractive than both the Meissner phase and normal conducting phase at $B = B_c$. If this is the case, a type II superconductor will instead switch to the vortex phase. And for this reason, the plot made on figure 1.4 is not necessarily valid for type II superconductors.

1.5.2 The upper critical field

The calculations made in the previous section does only take two phases into account and is therefore only valid for type I superconductors. In type II superconductors there can exist three phases, so another approach has to be taken in

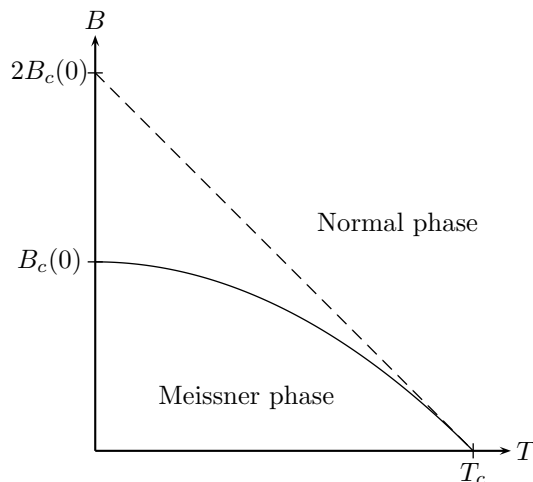


Figure 1.4: The dependency on temperature of the thermodynamic fields. The solid line is the empirically determined value (1.61) and the dashed line is the value which is valid near T_c (1.60).

order to calculate the upper critical field value for these superconductors. Since the Ginzburg–Landau equations are able to describe both type I and II superconductors, it seems natural to get the critical field value from these equations. It turns out that by solving the first Ginzburg–Landau equation under certain assumptions an upper critical field value can be determined. The derivation of the upper critical field value will now be shown.

Suppose we have a superconducting sample which is forced to be in the normal phase due to a strong magnetic field, and if the field is then lowered just enough for the superconductor to enter the vortex phase, it seems fair to assume that $|\Psi|^2$ is very small [14]. Since $|\Psi|^2$ is very small the term containing $|\Psi|^2$ in equation (1.32a) can be neglected and the following equation is obtained

$$\frac{1}{2m} \left(\frac{\hbar}{i} \nabla - q\mathbf{A} \right)^2 \Psi = \alpha\Psi \quad (1.62)$$

Writing out the brackets yields

$$-\frac{\hbar^2}{2m} \nabla^2 \Psi - \frac{\hbar q}{2mi} (\mathbf{A} \cdot \nabla \Psi + \nabla \cdot [\mathbf{A} \Psi]) + \frac{q^2 \mathbf{A} \cdot \mathbf{A}}{2m} \Psi = \alpha\Psi \quad (1.63)$$

And finally using that $\nabla \cdot (\mathbf{A} \Psi) = \mathbf{A} \cdot \nabla \Psi + \Psi \nabla \cdot \mathbf{A}$ the equation becomes

$$-\frac{\hbar^2}{2m} \nabla^2 \Psi - \frac{\hbar q}{2mi} (2\mathbf{A} \cdot \nabla \Psi + \Psi \nabla \cdot \mathbf{A}) + \frac{q^2 \mathbf{A} \cdot \mathbf{A}}{2m} \Psi = \alpha\Psi \quad (1.64)$$

Now since the system is only just in the vortex phase, very near to the normal phase, it must be fair to assume that the magnetic field penetrates the entire superconducting sample. From this observation follows that \mathbf{B}_i equals

\mathbf{B}_a throughout the superconducting sample. If the problem is reduced to a two-dimensional case where the applied magnetic field only has a z component then an expression for \mathbf{A} can be determined as

$$\mathbf{A} = (-yB_{az}, 0, 0) \quad (1.65)$$

With this choice of vector potential then by using the relation (1.6) the resulting magnetic field becomes¹⁴

$$\mathbf{B}_i = (0, 0, B_{az}) \quad (1.66)$$

According to (1.6) this choice of vector potential is not unique as we can always add a curlless vectorfield to the vector potential without altering the resulting magnetic field. Using the determined value of \mathbf{A} equation (1.64) becomes¹⁵

$$\left(-\frac{\hbar^2}{2m} \nabla^2 + \frac{\hbar q B_{az}}{m} y \frac{\partial}{\partial x} + \frac{q^2 B_{az}^2}{2m} y^2 \right) \Psi = \alpha \Psi \quad (1.67)$$

To solve the above equation quantum mechanics is revisited. The time-independent Schrödinger equation can be written as the eigenvalue equation

$$\hat{H}\psi = E\psi \quad (1.68)$$

where ψ is the wave-function which describes the particle in question, \hat{H} is the quantum mechanical Hamiltonian operator and E is the energy of the given particle. The Hamiltonian for a charged particle in a magnetic field was given in (1.9) and if this Hamiltonian is used with a vanishing scalar potential the resulting equation is formally equivalent to equation (1.67). With this analogy α corresponds to the energy eigenstates, so to solve equation (1.67) one needs to find the energy eigenstates of the Schrödinger equation for a charged particle in a magnetic field. This solution can be looked up in many textbooks however equation (1.67) will be solved here for completeness. To solve the equation an intelligent guess of Ψ is chosen to be [15]

$$\Psi(x, y, z) = e^{i(k_x x + k_z z)} \phi(y) \quad (1.69)$$

First the Laplace operator on Ψ and the derivative with respect to x is calculated

$$\begin{aligned} \nabla^2 \Psi &= -k_x^2 \Psi + \frac{\Psi}{\phi} \frac{d^2 \phi}{dy^2} - k_z^2 \Psi \\ \frac{\partial}{\partial x} \Psi &= i k_x \Psi \end{aligned} \quad (1.70)$$

If the derivatives (1.70) are inserted into (1.67), Ψ are present in all the terms. Inserting the derivatives and multiplying by $\phi \Psi^{-1}$ transforms (1.67) into an ordinary differential equation:

$$-\frac{\hbar^2}{2m} \frac{d^2 \phi}{dy^2} + \frac{q^2 B_{az}^2}{2m} y^2 \phi + \frac{\hbar q B_{az} k_x}{m} y \phi + \frac{\hbar^2}{2m} (k_x^2 + k_z^2) \phi = \alpha \phi \quad (1.71)$$

¹⁴ $\mathbf{B}_i = \nabla \times \mathbf{A} = \left(\frac{\partial A_z}{\partial y} - \frac{\partial A_y}{\partial z} \right) \mathbf{x} + \left(\frac{\partial A_x}{\partial z} - \frac{\partial A_z}{\partial x} \right) \mathbf{y} + \left(\frac{\partial A_y}{\partial x} - \frac{\partial A_x}{\partial y} \right) \mathbf{z}$.

¹⁵The operator ∇^2 also denoted as Δ is called the Laplace operator, and with three spatial coordinates it is $\nabla^2 = \frac{\partial^2}{\partial x^2} + \frac{\partial^2}{\partial y^2} + \frac{\partial^2}{\partial z^2}$.

This equation is reorganised into

$$-\frac{\hbar^2}{2m} \frac{d^2\phi}{dy^2} + \frac{m}{2} \frac{q^2 b_{az}^2}{m^2} \left(y^2 + \frac{\hbar^2 k_x^2}{q^2 B_{az}^2} - \frac{2\hbar k_x}{q B_{az}} y \right) \phi + \left(\frac{\hbar^2 k_z^2}{2m} - \alpha \right) \phi = 0 \quad (1.72)$$

and if the following variables are introduced

$$y_0 = \frac{\hbar k_x}{q B_{az}}, \quad \omega_c = \frac{q B_{az}}{m}, \quad E' = \alpha - \frac{\hbar^2 k_z^2}{2m} \quad (1.73)$$

the equation can be written as

$$-\frac{\hbar^2}{2m} \frac{d^2\phi}{dy^2} + \frac{m\omega_c^2}{2} (y - y_0)^2 \phi = E' \phi \quad (1.74)$$

This equation has the form of a harmonic oscillator with angular frequency ω_c . The Schrödinger equation for linear harmonic oscillator reads [12]

$$-\frac{\hbar^2}{2m} \frac{d^2\Psi(x)}{dx^2} + \frac{1}{2} k x^2 \Psi(x) = E \Psi(x) \quad (1.75)$$

The solution of this equation is basic quantum mechanics and is [12]

$$E_n = \left(n + \frac{1}{2} \right) \hbar \omega, \quad \omega = \sqrt{\frac{k}{m}} \quad n = 0, 1, 2, \dots \quad (1.76)$$

Where n is the *quantum number*. Using this result E'_n is determined as

$$E'_n = \left(n + \frac{1}{2} \right) \hbar \omega_c \quad n = 0, 1, 2, \dots \quad (1.77)$$

If equation (1.77) and (1.73) are combined an expression for B_{az} is found

$$B_{az} = \frac{2\alpha m - \hbar^2 k_z^2}{(2n + 1)\hbar q} \quad (1.78)$$

The interest here is to find the highest B_{az} which is when $n = 0$ and $k_z = 0$. This value is defined as B_{c2} and is the strongest magnetic field where a vortex phase can exist. B_{c2} becomes

$$B_{c2} = \frac{2\alpha m}{\hbar q} \quad (1.79)$$

B_{c2} can also be expressed in terms of B_c , where B_c was defined in equation (1.59). Doing this yields

$$B_{c2} = \frac{2\alpha m}{\hbar q} \sqrt{\frac{\beta}{\mu_0 \alpha^2}} B_c \quad (1.80)$$

This expression is simplified by introducing a new constant denoted κ which is called the *Ginzburg-Landau parameter* as

$$\kappa = \sqrt{\frac{2m^2 \beta}{\mu_0 \hbar^2 q^2}} \quad (1.81)$$

B_{c2} expressed using the Ginzburg–Landau parameter then becomes

$$B_{c2} = \sqrt{2}\kappa B_c \quad (1.82)$$

The Ginzburg–Landau parameter is a crucial parameter which can be used to divide superconductors into type I and II. If B_{c2} is greater than B_c , a vortex phase can appear as superconductivity survives beyond B_c . It can happen, because if we have an applied magnetic field value between B_{c2} and B_c , we know that the Ginzburg–Landau equations have a solution where Ψ is different from zero. This means that the superconductor is not in the normal conducting phase. It is not in the Meissner phase either, since we know that the normal conducting phase is preferred over the Meissner phase, when \mathbf{B}_a is greater than B_c . Therefore the superconductor must be in the Meissner phase. B_{c2} is greater than B_c if κ is greater than $1/\sqrt{2}$. If we consider the scenario where B_{c2} is smaller than B_c , the superconductor stays in the Meissner phase at least until B_{c2} is reached. At this point it becomes more attractive to be in the normal conducting phase compared to the vortex phase. However, when the applied magnetic field is weaker than B_c , the Meissner phase is preferred over the normal conductor phase. When the applied magnetic field reached B_c , however we know that the normal conducting phase is preferred over both the vortex phase and the Meissner phase. Therefore a superconductor which has B_{c2} lower than B_c will never enter a vortex phase. On this account superconductors are divided into two groups as [14]

$$\begin{aligned} \text{Type I superconductor} & \quad \text{if } \kappa < \frac{1}{\sqrt{2}} \\ \text{Type II superconductor} & \quad \text{if } \kappa \geq \frac{1}{\sqrt{2}} \end{aligned}$$

As a final note the Ginzburg–Landau parameter can also be written as

$$\kappa = \frac{\lambda_L}{\xi_{GL}} \quad (1.83)$$

So by measuring the London penetration depth and Ginzburg–Landau coherence length, the Ginzburg–Landau parameter can be determined. The typical value of κ for high T_c superconductors is $\kappa \approx 100$.

1.5.3 The lower critical field

For type II superconductors a critical field where the superconductor switches from normal phase to vortex phase exists. One could expect that this field is B_c , however this is not the case. A. A. Abrikosov calculated the critical field denoted B_{c1} in 1957 as [8, 16]

$$B_{c1} = \frac{1}{2\kappa}(\ln \kappa + 0.08)B_c \quad (1.84)$$

A phase diagram with B_{c1} and B_{c2} can be seen on figure 1.5. An interesting property of B_{c1} and B_{c2} is that with increasing κ B_{c1} lowers while B_{c2} increases. This leads to the conclusion that high T_c superconductors exist mostly in vortex phases. For $\kappa = 100$ we obtain the fields $B_{c1} = 0.023B_c$ and $B_{c2} = 141B_c$.

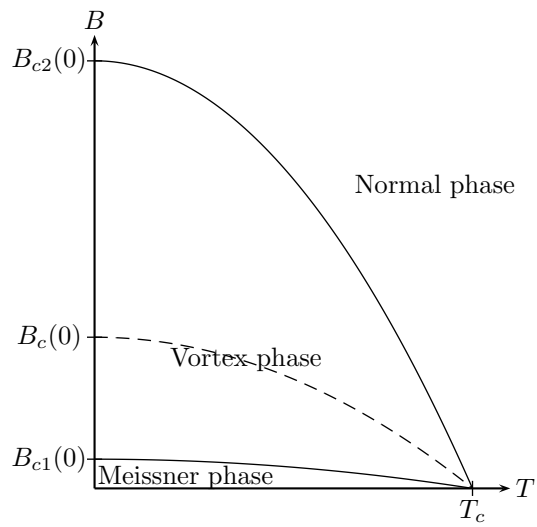


Figure 1.5: The critical fields dependency on temperature. The plot is made with $\kappa = 2$.

Chapter 2

Numerical formulation

Before the Ginzburg–Landau equations are solved, a few steps are made in order to reformulate them. First of all the equations have a freedom of gauge choice, so in order to solve them numerically we need to *fix the gauge*. Secondly the equations will be normalised in order to get rid of all the constants. This normalisation is not necessary in order to solve them, but it will make a nicer numeric formulation. Finally the equations are solved with the Finite Element method using a numerical software package called FEMLAB. In order to use FEMLAB the equations must be written in a very specific form.

2.1 Normalisation

The two most obvious choices are to normalise the length scale to either λ_L or ξ_{GL} . In this chapter both normalisations will be made as they have different advantages. These advantages will be discussed after the normalisations are made. From this point the Ginzburg–Landau coherence length and the London penetration depth are also written as ξ and λ .

2.1.1 Normalisation with $\mathbf{r} \rightarrow \xi_{GL}\mathbf{r}'$

The objective with the normalisation is to get rid of all the unnecessary variables. The energy density found in equation (1.13) is written for completeness

$$\mathcal{L} = \frac{1}{2m} \left| \left(\frac{\hbar}{i} \nabla - q\mathbf{A} \right) \Psi \right|^2 - \alpha |\Psi|^2 + \frac{\beta}{2} |\Psi|^4 + \frac{1}{2\mu_0} |\mathbf{B}_a - \mathbf{B}_i|^2 \quad (2.1)$$

The following transformations are introduced

$$(x, y, z) \rightarrow \xi(x, y, z)', \quad \mathbf{A} \rightarrow \frac{\hbar}{q\xi} \mathbf{A}', \quad \Psi \rightarrow \sqrt{\frac{\alpha}{\beta}} \Psi' \quad (2.2)$$

Since the spatial variables are transformed it is also required to rewrite the ∇ -operator. Using the chainrule the following identities follow¹:

$$\nabla = \frac{1}{\xi} \nabla', \quad d^3\mathbf{r} = d^3\mathbf{r}' \xi^3 \quad (2.3)$$

¹ $\frac{\partial}{\partial x} = \frac{\partial x'}{\partial x} \frac{\partial}{\partial x'} = \frac{1}{\xi} \frac{\partial}{\partial x'}$.

By using the above transformations the first term of the energy density (2.1) becomes

$$\frac{1}{2m} \left| \left(\frac{\hbar}{i} \nabla - q\mathbf{A} \right) \Psi \right|^2 = \frac{\hbar^2}{2m\xi^2} \frac{\alpha}{\beta} |({}_i\nabla' + \mathbf{A}') \Psi'|^2 \quad (2.4)$$

The multiplier is rewritten using (1.53):

$$\frac{\hbar^2}{2m\xi^2} \frac{\alpha}{\beta} = \frac{\alpha^2}{\beta} \quad (2.5)$$

The second and third term of (2.1) is transformed into

$$\begin{aligned} \alpha |\Psi|^2 &= \frac{\alpha^2}{\beta} |\Psi'|^2 \\ \frac{\beta}{2} |\Psi|^4 &= \frac{\alpha^2}{2\beta} |\Psi'|^4 \end{aligned} \quad (2.6)$$

Now the fourth term is normalised. From the transformations a new expression for \mathbf{B}_i is created

$$\mathbf{B}_i = \nabla \times \mathbf{A} = \frac{\hbar}{q\xi^2} \mathbf{B}'_i \quad (2.7)$$

By using the above transformations the last term in (2.1) becomes

$$\frac{1}{2\mu_0} |\mathbf{B}_a - \mathbf{B}_i|^2 = \frac{1}{2\mu_0} \frac{\hbar^2}{q^2\xi^4} |\mathbf{B}'_a - \mathbf{B}'_i|^2 \quad (2.8)$$

The multiplier is rewritten further by using the definitions of ξ (1.53) and κ (1.81)

$$\frac{1}{2\mu_0} \frac{\hbar^2}{q^2\xi^4} = \kappa^2 \frac{\alpha^2}{\beta} \quad (2.9)$$

Putting everything together transforms equation (2.1) into

$$\mathcal{L} = \frac{\alpha^2}{\beta} \left(|({}_i\nabla' + \mathbf{A}') \Psi'|^2 - |\Psi'|^2 + \frac{1}{2} |\Psi'|^4 + \kappa^2 |\mathbf{B}'_a - \mathbf{B}'_i|^2 \right) \quad (2.10)$$

Now the normalised Ginzburg–Landau equations can be found either by calculus of variation on (2.10) or by using the transformations on (1.32a)-(1.32d). To normalise equation (1.32a) and (1.32b) the transformations are used. The first Ginzburg–Landau equation in normalised form is

$$({}_i\nabla' + \mathbf{A}')^2 \Psi' - \Psi' + |\Psi'|^2 \Psi' = 0 \quad (2.11)$$

And the corresponding boundary condition becomes

$$({}_i\nabla' \Psi' + \mathbf{A}' \Psi') \cdot \mathbf{n} = 0 \quad (2.12)$$

The second Ginzburg–Landau equation is easiest to calculate using calculus of variations. First the function f_n is defined as (2.10) without the terms which are independent of \mathbf{A}' and $\nabla \times \mathbf{A}'$.

$$f_n = {}_i\mathbf{A}' \cdot (\Psi'^* \nabla \Psi' - \Psi' \nabla \Psi'^*) + \mathbf{A}' \cdot \mathbf{A}' |\Psi'|^2 + \kappa^2 |\mathbf{B}'_a - \nabla \times \mathbf{A}'|^2 \quad (2.13)$$

Note that the second Ginzburg–Landau equation is actually calculated in equation (1.27). Requiring that the integrands must vanish we have the equations as

$$\begin{aligned} \frac{\partial f}{\partial \mathbf{A}'} + \nabla \times \frac{\partial f}{\partial (\nabla \times \mathbf{A}')} &= 0 \quad \text{in } \Omega \\ \frac{\partial f}{\partial (\nabla \times \mathbf{A}')} &= 0 \quad \text{on } \partial\Omega \end{aligned} \quad (2.14)$$

And the derivatives are

$$\begin{aligned} \frac{\partial f}{\partial \mathbf{A}'} &= i(\Psi'^* \nabla \Psi' - \Psi' \nabla \Psi'^*) + 2\mathbf{A}' |\Psi'|^2 \\ \frac{\partial f}{\partial (\nabla \times \mathbf{A}')} &= -2\kappa^2 (\mathbf{B}'_a - \mathbf{B}'_i) \end{aligned} \quad (2.15)$$

First note that the boundary condition becomes $\mathbf{B}'_a = \mathbf{B}'_i$ so it has not changed by the normalisation. Now the inner equation is created by inserting the derivatives into (2.14):

$$\frac{1}{2\kappa^2} (i[\Psi' \nabla \Psi'^* - \Psi'^* \nabla \Psi'] - 2\mathbf{A}' |\Psi'|^2) + \nabla \times \mathbf{B}'_a = \nabla \times \mathbf{B}'_i \quad (2.16)$$

Since the right hand side is $\nabla \times \mathbf{B}'_i$ a transformation for the current is also needed. It is desirable that we get the relation $\nabla' \times \mathbf{B}'_i = \mathbf{j}'$. From Ampere's law (1.31):

$$\xi \nabla' \times \frac{q\xi^2}{\hbar} \mathbf{B}_i = \frac{\mu_0 q \xi^3}{\hbar} \mathbf{j} \quad (2.17)$$

An expression for \mathbf{j}' is read to be

$$\mathbf{j} = \frac{\hbar}{\mu_0 q \xi^2} \mathbf{j}' \quad (2.18)$$

All the equations has now been transformed. Dropping all the primes the normalised Ginzburg–Landau equations are

$$(i\nabla + \mathbf{A})^2 \Psi - \Psi + |\Psi|^2 \Psi = 0 \quad \text{in } \Omega \quad (2.19a)$$

$$(i\nabla \Psi + \mathbf{A}\Psi) \cdot \mathbf{n} = 0 \quad \text{on } \partial\Omega \quad (2.19b)$$

$$\frac{1}{2\kappa^2} (i[\Psi \nabla \Psi^* - \Psi^* \nabla \Psi] - 2\mathbf{A} |\Psi|^2) + \nabla \times \mathbf{B}_a = \mathbf{j}_s \quad \text{in } \Omega \quad (2.19c)$$

$$\mathbf{B}_a = \mathbf{B}_i \quad \text{on } \partial\Omega \quad (2.19d)$$

2.1.2 Normalisation with $\mathbf{r} \rightarrow \lambda_L \mathbf{r}'$

To normalise the length scale to the London penetration depth the following transformations are made

$$(x, y, z) \rightarrow \lambda(x, y, z)', \quad \mathbf{A} \rightarrow \frac{\hbar}{\xi q} \mathbf{A}', \quad \Psi = \sqrt{\frac{\alpha}{\beta}} \Psi' \quad (2.20)$$

from which it follows that

$$\nabla = \frac{1}{\lambda} \nabla', \quad \mathbf{B} = \frac{\hbar}{\lambda \xi q} \mathbf{B}', \quad \mathbf{j} = \frac{\hbar}{\mu_0 \lambda^2 \xi q} \mathbf{j}' \quad (2.21)$$

Without going into details of the calculations, the normalised Ginzburg–Landau equations using these transformations become

$$\left(\frac{\imath}{\kappa} \nabla + \mathbf{A} \right)^2 \Psi - \Psi + |\Psi|^2 \Psi = 0 \quad \text{in } \Omega \quad (2.22a)$$

$$\left(\frac{\imath}{\kappa} \nabla \Psi + \mathbf{A} \Psi \right) \cdot \mathbf{n} = 0 \quad \text{on } \partial\Omega \quad (2.22b)$$

$$\frac{\imath}{2\kappa} (\Psi \nabla \Psi^* - \Psi^* \nabla \Psi) - \mathbf{A} |\Psi|^2 + \nabla \times \mathbf{B}_a = \mathbf{j}_s \quad \text{in } \Omega \quad (2.22c)$$

$$\mathbf{B}_a = \mathbf{B}_i \quad \text{on } \partial\Omega \quad (2.22d)$$

Note that when $\kappa = 1$, the equations normalised with λ and ξ are identical as should be the case since κ equals λ_L / ξ_{GL} .

2.1.3 Choosing normalisation

Whether to normalise the length scale to λ_L or ξ_{GL} depends on which numerical simulations are made. If λ_L and ξ_{GL} are kept constant, it does not matter which normalisation is being used. However, if either λ_L or ξ_{GL} is varied then one normalisation scheme is better than the other. Which normalisation scheme to choose is made clear by a few thoughts.

Suppose that the normalisation $x' \rightarrow \lambda_L x$ is used. Having this normalisation leads to $L' = \lambda_L L$ where L is the actual physical length of the system and L' is the length of the normalised system. Now the value of λ_L is chosen to be altered. This is achieved by changing κ appropriately since κ is the only constant that appears in the normalised Ginzburg–Landau equations. If these thoughts are expressed in equations where κ_0 is the value of κ before the value is changed we get

$$\kappa_0 = \frac{\lambda_0}{\xi_0}, \quad x' \rightarrow \lambda_L x \quad \Rightarrow \quad L = \frac{L'}{\lambda_L} \quad (2.23)$$

Now λ_L is changed but at the same time it is also a priority to hold the actual physical dimensions of the system constant. This can be written as $L_1 = L_0$, where L_0 denotes the length before κ is changed and L_1 is the length after λ_L is changed. If λ_L is chosen to be doubled it is achieved by doubling the value of κ . This can be written in two ways

$$\kappa_1 = \frac{\lambda_1}{\xi_1}, \quad \kappa_1 = 2\kappa_0 = \frac{\lambda_0}{\frac{1}{2}\xi_0} = \frac{2\lambda_0}{\xi_0} \quad (2.24)$$

Thus by doubling κ either λ can be doubled or ξ can be halved. Which scenario is chosen depends purely on the choice of the normalised length denoted L'_1 . Since $L_1 = L_0$ then by letting L'_1 be equal to L'_0 , we see from equation (2.23) that λ_1 is forced to be equal to λ_0 . Therefore having the length L' unchanged means that ξ_{GL} is halved. On the other hand by letting $L'_1 = 2L'_0$ we choose $\lambda_1 = 2\lambda_0$ which means that ξ_{GL} is unchanged. From this observation we conclude that to achieve simulations for the same physical system with different ξ_{GL} , normalisation with

$x' \rightarrow \lambda_L x$ is the best choice since the normalised length remains unchanged. Similar calculations show the same scenario for $x' \rightarrow \xi_{GL} x$, where the length remains unchanged with changing λ_L .

2.2 Gauge transformation

The Ginzburg–Landau equations have the property of gauge invariance. Given a function $\chi(x, y, z)$ the linear transformation G_χ is defined as

$$G_\chi(\Psi, \mathbf{A}) = (\Psi', \mathbf{A}') \quad (2.25)$$

where

$$\Psi' = \Psi e^{i\kappa\chi}, \quad \mathbf{A}' = \mathbf{A} + \nabla\chi \quad (2.26)$$

Gauge invariance means that by making the transformations (2.26) the resulting equations will be formally equivalent to the former equations. The proof that the Ginzburg–Landau equations are invariant under the transformations can be found in appendix B.1.

From the gauge invariance it follows that having a solution (Ψ_0, \mathbf{A}_0) then $G_\chi(\Psi_0, \mathbf{A}_0)$ is also a solution to the Ginzburg–Landau equations, and so is any choice (Ψ', \mathbf{A}') that can be obtained through a gauge transformation. In this way it is possible to define an equivalence class of solutions, that is solutions that can be obtained from each other by making the gauge transformation. By *fixing the gauge* one chooses a particular set of solutions which is needed to obtain mathematically well-posed equations [13]. The gauge is fixed by choosing χ . It turns out to be an advantage to choose $\nabla^2\chi = \nabla \cdot \mathbf{A}'$ from which it follows that

$$\nabla \cdot \mathbf{A} = 0 \quad (2.27)$$

This gauge choice is called the *Coulomb gauge* and is a common choice in the solution of the stationary equations [11]. The gauge choice can be used to reduce the first Ginzburg–Landau equation (2.19a) to

$$-\nabla^2\Psi + 2i\mathbf{A} \cdot \nabla\Psi + \mathbf{A} \cdot \mathbf{A}\Psi - \Psi + |\Psi|^2\Psi = 0 \quad (2.28)$$

The Ginzburg–Landau equations can be reduced further by making some physical assumptions about the environment. First, only two dimensional devices will be simulated, thus Ψ is independent of z . Secondly the external magnetic field \mathbf{B}_a is assumed to have a z -component only. Furthermore we assume that the applied magnetic field is a static uniform field which means that the curl of \mathbf{B}_a vanish. Using these assumptions equation (2.19d) and (2.22d) can be written as²

$$A_{y,x} - A_{x,y} = B_{az} \quad \text{on} \quad \partial\Omega \quad (2.29)$$

Notice that the left hand side corresponds the the curl of \mathbf{A} . Putting everything together and reorganising the Ginzburg–Landau equations normalised with ξ_{GL}

² $\mathbf{B}_i = \nabla \times \mathbf{A} = \left(\frac{\partial A_z}{\partial y} - \frac{\partial A_y}{\partial z}\right)\mathbf{x} + \left(\frac{\partial A_x}{\partial z} - \frac{\partial A_z}{\partial x}\right)\mathbf{y} + \left(\frac{\partial A_y}{\partial x} - \frac{\partial A_x}{\partial y}\right)\mathbf{z}$.

(2.19) becomes

$$-\nabla^2\Psi + 2i\mathbf{A} \cdot \nabla\Psi + \mathbf{A} \cdot \mathbf{A}\Psi - \Psi + |\Psi|^2\Psi = 0 \quad \text{in } \Omega \quad (2.30a)$$

$$(i\nabla\Psi + \mathbf{A}\Psi) \cdot \mathbf{n} = 0 \quad \text{on } \partial\Omega \quad (2.30b)$$

$$\frac{1}{2\kappa^2} (i[\Psi\nabla\Psi^* - \Psi^*\nabla\Psi] - 2\mathbf{A}|\Psi|^2) = \mathbf{j}_s \quad \text{in } \Omega \quad (2.30c)$$

$$A_{y,x} - A_{x,y} = B_{az} \quad \text{on } \partial\Omega \quad (2.30d)$$

The Ginzburg–Landau equations normalised with λ_L (2.22) becomes

$$-\frac{1}{\kappa^2}\nabla^2\Psi + i\frac{2}{\kappa}\mathbf{A} \cdot \nabla\Psi + \mathbf{A} \cdot \mathbf{A}\Psi - \Psi + |\Psi|^2\Psi = 0 \quad \text{in } \Omega \quad (2.31a)$$

$$\left(\frac{i}{\kappa}\nabla\Psi + \mathbf{A}\Psi\right) \cdot \mathbf{n} = 0 \quad \text{on } \partial\Omega \quad (2.31b)$$

$$\frac{i}{2\kappa} (\Psi\nabla\Psi^* - \Psi^*\nabla\Psi) - \mathbf{A}|\Psi|^2 = \mathbf{j}_s \quad \text{in } \Omega \quad (2.31c)$$

$$A_{y,x} - A_{x,y} = B_{az} \quad \text{on } \partial\Omega \quad (2.31d)$$

2.3 FEMLAB

The normalized Ginzburg–Landau equations will be solved using FEMLAB v3.1a. FEMLAB is a numerical analysis product by COMSOL where FEM stand for “Finite Element Method”. The finite element method is a numerical method for solving partial differential equation with boundary value problems. How the method works will only be discussed briefly, for a deeper treatment refer to [17, 18].

2.3.1 The Finite Element Method

In a numerical method there are always two steps to complete; writing the equations in a way suitable for a computer, and when this is done use a method to solve the equations. When writing equations suitable for computers the equations are *discretised*. When the equations are discretised the solution is obviously also discretised. To discretise the equations, a computational grid called a *mesh* is constructed. This mesh is made by dividing the definition space into smaller subspaces. How this can be done is best illustrated by an example in a one dimensional case.

Suppose we have an equation with the solution $u(x)$ and we want to compute the solution for $0 \leq x \leq 2$. This interval is then discretised by dividing it into smaller intervals. To keep it simple, a mesh consisting of two mesh intervals is constructed. This is done by creating points at $x_1 = 0$, $x_2 = 1$ and $x_3 = 2$. These the points are called *node* points. At these node points, the value of the solution is then calculated and the solution values are denoted as $U_1 = u(x_1)$, $U_2 = u(x_2)$ and $U_3 = u(x_3)$. Suppose that the solution to our equation is $u(x) = -0.25x^2 + 1.25x$, then we get the solution values $U_1 = 0$, $U_2 = 1$ and $U_3 = 1.5$. In order to construct a function based on our calculated solution points, we need to make interpolation between the function values. This could for example be linear interpolation, which is shown on figure 2.1. If the two interpolation

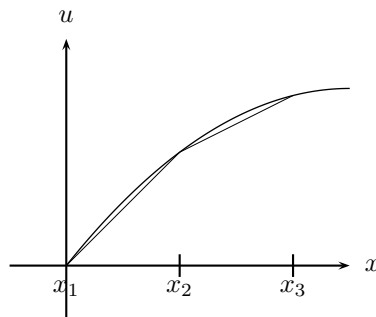


Figure 2.1: Linear interpolation example. The function u is defined as $u(x) = -0.25x^2 + 1.25x$.

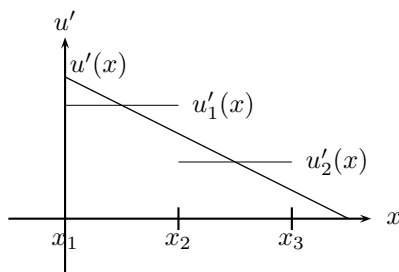


Figure 2.2: Approximation of the first derivative of $u(x)$ using linear interpolation.

functions are denoted $u_1(x)$ and $u_2(x)$, and both functions vanish outside the interpolation area, the solution can be approximated as

$$u(x) \approx u_1(x) + u_2(x) \quad (2.32)$$

It is crucial that as the amount of node points approaches infinity, the approximated solution approaches the exact solution. It is clear that this is the case with this approximation scheme. However using linear functions as interpolation function has a very unfortunate effect. The first derivative of $u(x)$ is not approximated with great precision, which is quite clear on figure 2.2. Therefore depending on the niceness of solution, one might want to use higher order interpolation functions, in order to achieve greater precision. However, in order to use for example second order polynomials as interpolation functions, three solution points must be known. Thus using higher order interpolation function also requires more computational power, as more solution points are needed.

The finite element method uses a similar approach as above. In the finite element method the solution is written as

$$u(x) = U_1\varphi_1(x) + U_2\varphi_2(x) + U_3\varphi_3(x) \quad (2.33)$$

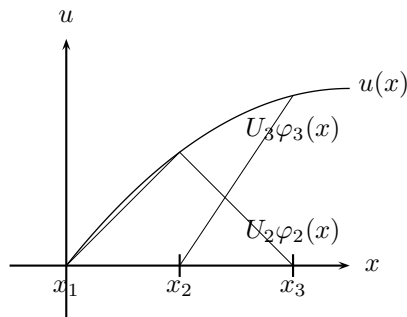


Figure 2.3: The finite element approximation using linear Lagrange elements. The triangle is $U_2\varphi_2(x)$ and the straight line is $U_3\varphi_3(x)$.

where $\varphi_i(x)$ are certain piecewise functions which are called the *basis functions*. These functions are defined such that $\phi(x)_i$ is one at node i and zero at all other node points. These functions could for example be chosen as linear functions. If linear functions are used, the functions are defined as

$$\begin{aligned}\phi_1(x) &= \begin{cases} -x + 1 & \text{if } 0 \leq x \leq 1 \\ 0 & \text{otherwise} \end{cases} \\ \phi_2(x) &= \begin{cases} x & \text{if } 0 \leq x \leq 1 \\ -x + 2 & \text{if } 1 \leq x \leq 2 \\ 0 & \text{otherwise} \end{cases} \\ \phi_3(x) &= \begin{cases} x - 1 & \text{if } 1 \leq x \leq 2 \\ 0 & \text{otherwise} \end{cases}\end{aligned}\quad (2.34)$$

With linear functions each function $\varphi_i(x)$, except those at the boundary (here $\varphi_1(x)$ and $\varphi_3(x)$), constructs a triangle in the mesh interval i and $i + 1$. Thus the solution $u(x)$ is actually approximated by a series of triangles multiplied by the coefficients U_i . This approximation method is illustrated in figure 2.3. Notice that

$$U_1\varphi_1(x) + U_2\varphi_2(x) + U_3\varphi_3(x) = u_1(x) + u_2(x) \quad (2.35)$$

so the finite element method does actually use linear interpolation between the solution points. The linear functions $\phi_i(x)$ used in this context are called the *Lagrange element* of order one. One can also use higher order functions, for example the Lagrange element of order two which consists of a second order polynomial. This Lagrange element is also called *quadratic Lagrange*. When quadratic Lagrange elements are used additional node points are needed. Those are laid at the median of the interval, in this case at $x_4 = 0.5$ and $x_5 = 1.5$. The mesh resolution and choice of basis functions are entirely up to the user of the Finite Element method.

In the two-dimensional case the mesh consists of triangles, but the basis principles are exactly the same. An example mesh can be seen on figure 2.4. On

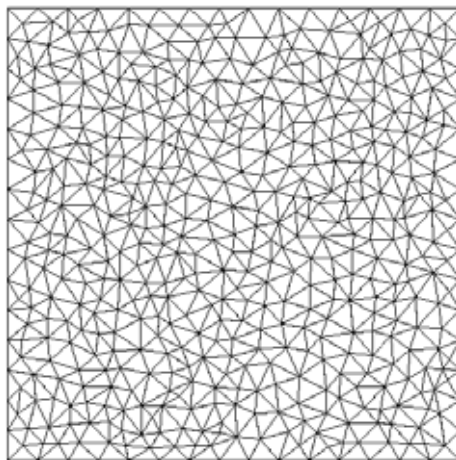


Figure 2.4: A mesh generated by FEMLAB.

the figure a square is plotted and it is evident that the mesh does not preserve the symmetry of the square. However while this can be seen as insufficient, then from a numerical point of view a mesh that contained symmetry would not be very desirable. In case of degenerated solutions it would be very hard to get the numerical solution to converge as only roundoff errors would break the symmetry of the mesh. From a numerical point of view it is therefore convenient to have a mesh that breaks the symmetry of a symmetric geometry. If one wants to preserve the symmetry of the chosen geometry, FEMLAB is capable of making symmetry lines which ensures this [19].

So far only step one of the numerical method has been discussed, namely how the solution is approximated by using a mesh. We have not described how the equations are reformulated, in order to be implemented on a computer. This has been omitted, since it does not provide any useful information about the general concepts of the finite element method.

The approximation of the solution requires the values of $u(x)$ at all the node points. These values are calculated using an iteration process, which in order to begin needs an initial guess. The user of the numerical method has to provide the initial values of $u(x)$. How close to the exact solution these values need to be, is entirely dependent on the equation system. When the initial values are given the iteration process can begin, and FEMLAB uses a variant of the *damped Newton method*. How it works will not be discussed due to the complexity of the method, however the general concepts of an iteration method will be briefly discussed. When FEMLAB has discretised the equations, the task is to solve a nonlinear algebraic system. Such a system can be written on the form

$$\mathbf{U} = h\mathbf{g}(\mathbf{U}) + \mathbf{b} \quad (2.36)$$

where \mathbf{U} is the solution vector, and the function \mathbf{g} and vector \mathbf{b} are determined, based on the equation system that is going to be solved. h is an unknown factor, usually called the stepsize. If $h = 1$, the above equation system should reduce

to the original equation system. Now, in general an iteration algorithm can be written as

$$\mathbf{U}^{[i+1]} = \mathcal{A}(\mathbf{U}^{[i]}), \quad i = 0, 1, \dots \quad (2.37)$$

where i denotes the iteration number. The superscript denotes the solution vector at iteration i . The most simple approach is to choose \mathcal{A} as the right hand side of (2.36), and with $h = 1$ we get the equation

$$\mathbf{U}^{[i+1]} = \mathbf{g}(\mathbf{U}^{[i]}) + \mathbf{b}, \quad i = 0, 1, \dots \quad (2.38)$$

When the left hand side is sufficiently close to the right hand side, the solution has converged. This simple algorithm works by inserting the initial solution into the right hand side of the equation system, and then calculates a new solution based on this. This new solution vector is then used in the next iteration, in order to calculate the next solution. This process can be made more sophisticated, for example by using stepsize control. The damped Newton method is an example of a more sophisticated algorithm, but the basic concepts are the same. Refer to the book by Iserles for a full treatment of this method [18].

2.3.2 Modelling

In order to use FEMLAB the equations must be put on a specific form. FEMLAB supports two different forms where it is recommend to use the so-called *general*³ form for nonlinear problems. With Neumann boundary conditions³ (which is what we have) the general form is [17]

$$\begin{aligned} \mathbf{d}_a \frac{\partial u}{\partial t} + \nabla \cdot \mathbf{\Gamma} &= \mathbf{F} & \text{in } \Omega \\ -\mathbf{n} \cdot \mathbf{\Gamma} &= \mathbf{G} & \text{on } \partial\Omega \end{aligned} \quad (2.39)$$

\mathbf{d}_a is a mass matrix which in this case is zero as we are dealing with stationary equations. The u 's are the solution variables. \mathbf{F} and \mathbf{G} are vectors and they have as many components as there are solution variables. If four solution variables are used, \mathbf{F} and \mathbf{G} end up having four component, where each component is a scalar. Finally $\mathbf{\Gamma}$ is also a vector with the amount of components as solution variables. However each component of $\mathbf{\Gamma}$ is also a vector of the spatial variables. The three vectors $\mathbf{\Gamma}$, \mathbf{F} and \mathbf{G} can be functions of the solution u and the spatial derivative of u .

2.3.3 Formulation with $\mathbf{r} \rightarrow \xi_{GL}\mathbf{r}'$

The Ginzburg–Landau equations normalised with ξ_{GL} (2.30) are formulated as a FEMLAB problem. To solve the Ginzburg–Landau equations in FEMLAB $|\Psi|^2$ is divided into a real and imaginary part by defining $\Psi \equiv u_1 + iu_2$. This is required since $|\Psi|^2$ is *not* an analytic function.

First the boundary conditions are written on the form prescribed by (2.39). By inserting $\Psi \equiv u_1 + iu_2$ equation (2.30b) is written as

$$-(\nabla u_2 - \mathbf{A}u_1) \cdot \mathbf{n} - i(-\nabla u_1 - \mathbf{A}u_2) \cdot \mathbf{n} = 0 \quad \text{on } \partial\Omega \quad (2.40)$$

³When the boundary condition specifies the derivative $\mathbf{n} \cdot \nabla f$ it is called a Neumann boundary condition. The expression $\mathbf{n} \cdot \nabla f$ can also be written as $\frac{\partial f}{\partial n}$.

By writing

$$-\mathbf{\Gamma}_1 \cdot \mathbf{n} - i\mathbf{\Gamma}_2 \cdot \mathbf{n} = G_1 + iG_2 \quad (2.41)$$

we see that the boundary condition is written in the general form. The vectors are found to be $\mathbf{\Gamma}_1 = (\nabla u_2 - \mathbf{A}u_1)$ and $\mathbf{\Gamma}_2 = (-\nabla u_1 - \mathbf{A}u_2)$ and the scalars G_1 and G_2 are found to be zero.

The second boundary condition (2.30d) does not contain Ψ so it does not need to be rewritten in terms of $u_{1,2}$. The boundary condition can be implemented directly as Γ_{3x} however this does not suffice. If we choose this approach the corresponding FEMLAB implementation becomes

$$-n_x \cdot \mathbf{\Gamma}_3 = 0 \quad \Rightarrow \quad -n_x(A_{y,x} - A_{x,y} - B_{az}) = 0 \quad (2.42)$$

The above equation is solved for either $n_x = 0$ or $A_{y,x} - A_{x,y} - B_{az} = 0$. The last expression is our boundary condition, so we must ensure this is always the solution chosen. However, if we have a geometry where $n_x = 0$ exists, the boundary condition will vanish. This implies that we do not have a boundary condition for the magnetic field where n_x vanishes. For this reason we also need to have Γ_{4y} to represent the boundary condition. It would not be correct to have both Γ_{3x} and Γ_{3y} equal to the boundary condition, since $-\mathbf{n} \cdot \mathbf{\Gamma}_3 = 0$ would construct the equation

$$-n_x(A_{y,x} - A_{x,y} - B_{az}) - n_y(A_{y,x} - A_{x,y} - B_{az}) = 0 \quad (2.43)$$

which clearly only enforces $A_{y,x} - A_{x,y} - B_{az} = 0$ when either n_x or n_y vanishes. Therefore we are forced to use two vectors in order to implement (2.30d). However it turns out to be an advantage to incorporate the curl of \mathbf{A} into $\mathbf{\Gamma}_{3,4}$. This is done by constructing the two linearly independent⁴ vectors

$$\mathbf{\Gamma}_3 = \begin{pmatrix} \nabla \cdot \mathbf{A} \\ -A_{y,x} + A_{x,y} + B_{a,z} \end{pmatrix}, \quad \mathbf{\Gamma}_4 = \begin{pmatrix} A_{y,x} - A_{x,y} - B_{a,z} \\ \nabla \cdot \mathbf{A} \end{pmatrix} \quad (2.44)$$

If G_3 and G_4 are chosen to be zero it is quite clear that $\mathbf{\Gamma}_{3,4}$ implements equation (2.30d) since the curl of \mathbf{A} vanishes everywhere in space. To summarise the boundary conditions are implemented in FEMLAB by choosing $\mathbf{G} = \mathbf{0}$ and the complete form of $\mathbf{\Gamma}$ is

$$\begin{aligned} \mathbf{\Gamma}_1 &= \nabla u_2 - \mathbf{A}u_1 & \mathbf{\Gamma}_2 &= -\nabla u_1 - \mathbf{A}u_2 \\ \mathbf{\Gamma}_3 &= \begin{pmatrix} A_{x,x} + A_{y,y} \\ -A_{y,x} + A_{x,y} + B_{a,z} \end{pmatrix} & \mathbf{\Gamma}_4 &= \begin{pmatrix} A_{y,x} - A_{x,y} - B_{a,z} \\ A_{x,x} + A_{y,y} \end{pmatrix} \end{aligned} \quad (2.45)$$

To determine \mathbf{F} the starting point is to calculate the left hand side of (2.39)⁵:

$$\nabla \cdot \mathbf{\Gamma} = \begin{pmatrix} \nabla^2 u_2 - \nabla(\mathbf{A}u_1) \\ -\nabla^2 u_1 - \nabla(\mathbf{A}u_2) \\ A_{x,xx} + A_{y,yy} - A_{y,xy} + A_{x,yy} + B_{a,z,y} \\ A_{y,xx} - A_{x,yx} + A_{x,xy} + A_{x,yy} - B_{a,z,x} \end{pmatrix} = \begin{pmatrix} \nabla^2 u_2 - \mathbf{A} \cdot \nabla u_1 \\ -\nabla^2 u_1 - \mathbf{A} \cdot \nabla u_2 \\ A_{x,xx} + A_{x,yy} \\ A_{y,xx} + A_{y,yy} \end{pmatrix} \quad (2.46)$$

⁴A set of vectors are linearly independent if $a_i \mathbf{V}_i + a_i \mathbf{V}_i + \dots \neq 0$ where a_i are constants and not all are zero. Furthermore, by having a vector $\mathbf{V}_1 = (a, b)$ a linearly independent vector $\mathbf{V}_2 = (-b, a)$ can be constructed.

⁵It is used that $\frac{\partial^2}{\partial x \partial y} = \frac{\partial^2}{\partial y \partial x}$.

In the last equality it is used that the curl of \mathbf{A} vanishes and B_{az} is a constant. In order to determine \mathbf{F} the new solution form $\Psi = u_1 + \imath u_2$ is inserted into equation (2.30a) and (2.30c). The first Ginzburg–Landau equation becomes

$$\begin{aligned} & (-\nabla^2 u_1 - 2\mathbf{A} \cdot \nabla u_2 + \mathbf{A} \cdot \mathbf{A} u_1 - u_1 + |u_1 + \imath u_2|^2 u_1) \\ & + \imath(-\nabla^2 u_2 + 2\mathbf{A} \cdot \nabla u_1 + \mathbf{A} \cdot \mathbf{A} u_2 - u_2 + |u_1 + \imath u_2|^2 u_2) = 0 \end{aligned} \quad (2.47)$$

If the above equation is split into a real and imaginary part then two new equations are obtained as

$$\begin{aligned} \nabla^2 u_2 - \mathbf{A} \cdot \nabla u_1 &= \mathbf{A} \cdot \nabla u_1 + \mathbf{A} \cdot \mathbf{A} u_2 - u_2 + |u_1 + \imath u_2|^2 u_2 & (\Im) \\ -\nabla^2 u_1 - \mathbf{A} \cdot \nabla u_2 &= \mathbf{A} \cdot \nabla u_2 - \mathbf{A} \cdot \mathbf{A} u_1 + u_1 - |u_1 + \imath u_2|^2 u_1 & (\Re) \end{aligned} \quad (2.48)$$

We see that the left hand sides are equal to the divergence of $\mathbf{\Gamma}_{1,2}$ which means that $F_{1,2}$ is found as the right hand sides. To determine $F_{3,4}$ the new solution form $\Psi = u_1 + \imath u_2$ is inserted into equation (2.30c)

$$\mathbf{j} = \frac{1}{\kappa^2} (u_1 \nabla u_2 - u_2 \nabla u_1 - |u_1 + \imath u_2|^2 \mathbf{A}) \quad (2.49)$$

As the calculations show equation (2.19c) is transformed into a purely real two–component vector equation and therefore needs to be implemented as two equations. The left hand side, $\mathbf{j} = \nabla \times \nabla \times \mathbf{A}$ can be rewritten in terms of \mathbf{A} . Notice that the left hand side of equation (2.29) is the curl of \mathbf{A} , so taking the curl of the left hand side of equation (2.29) gives

$$\mathbf{j} = \nabla \times (A_{y,x} - A_{x,y}) \mathbf{z} = (A_{y,xy} - A_{x,yy}) \mathbf{x} + (-A_{y,xx} + A_{x,yx}) \mathbf{y} \quad (2.50)$$

To rewrite (2.49) into FEMLAB form some identities are derived from (2.27)

$$\begin{aligned} A_{x,x} = -A_{y,y} &\Rightarrow A_{x,xx} = -A_{y,yx} \\ A_{x,x} = -A_{y,y} &\Rightarrow A_{x,xy} = -A_{y,yy} \end{aligned} \quad (2.51)$$

Using the above identities and equation (2.50), then by making one equation for the x -component and one for the y -component, the second Ginzburg–Landau equation (2.49) is split into two equations

$$A_{x,xx} + A_{x,yy} = \frac{1}{\kappa^2} (u_2 u_{1,x} - u_1 u_{2,x} + |u_1 + \imath u_2|^2 A_x) \quad \hat{\mathbf{x}} \quad (2.52)$$

$$A_{y,xx} + A_{y,yy} = \frac{1}{\kappa^2} (u_2 u_{1,y} - u_1 u_{2,y} + |u_1 + \imath u_2|^2 A_y) \quad \hat{\mathbf{y}} \quad (2.53)$$

We see that the left hand side equals the divergence of $\mathbf{\Gamma}_{3,4}$ so $F_{3,4}$ becomes the right hand sides of the above equation. Writing \mathbf{F} in full it becomes

$$\mathbf{F} = \begin{pmatrix} \mathbf{A} \cdot \nabla u_1 + \mathbf{A} \cdot \mathbf{A} u_2 - u_2 + |u_1 + \imath u_2|^2 u_2 \\ \mathbf{A} \cdot \nabla u_2 - \mathbf{A} \cdot \mathbf{A} u_1 + u_1 - |u_1 + \imath u_2|^2 u_1 \\ \frac{1}{\kappa^2} (u_2 u_{1,x} - u_1 u_{2,x} + |u_1 + \imath u_2|^2 A_x) \\ \frac{1}{\kappa^2} (u_2 u_{1,y} - u_1 u_{2,y} + |u_1 + \imath u_2|^2 A_y) \end{pmatrix} \quad (2.54)$$

The above equation system is implemented using MATLAB. MATLAB has an interface for FEMLAB, so that all the functions and methods in FEMLAB can be accessed by MATLAB scripts. The script which implements the equations found in this section can be found in appendix C.1.

2.3.4 Formulation with $\mathbf{r} \rightarrow \lambda_L \mathbf{r}'$

The Ginzburg–Landau equations normalised with λ_L is also implemented in FEMLAB. However since the implementation procedure is exactly the same as in the previous section, only the results will be written. The vector \mathbf{G} is still found to be zero. $\mathbf{\Gamma}$ is found to be

$$\begin{aligned} \Gamma_1 &= \frac{1}{\kappa} \nabla u_2 - \mathbf{A} u_1 & \Gamma_2 &= -\frac{1}{\kappa} \nabla u_1 - \mathbf{A} u_2 \\ \Gamma_3 &= \begin{pmatrix} A_{x,x} + A_{y,y} \\ -A_{y,x} + A_{x,y} + B_{a,z} \end{pmatrix} & \Gamma_4 &= \begin{pmatrix} A_{y,x} - A_{x,y} - B_{a,z} \\ A_{x,x} + A_{y,y} \end{pmatrix} \end{aligned} \quad (2.55)$$

and \mathbf{F} is found as

$$\mathbf{F} = \begin{pmatrix} \mathbf{A} \cdot \nabla u_1 + \kappa (\mathbf{A} \cdot \mathbf{A} u_2 - u_2 + |u_1 + u_2|^2 u_2) \\ \mathbf{A} \cdot \nabla u_2 - \kappa (\mathbf{A} \cdot \mathbf{A} u_1 - u_1 + |u_1 + u_2|^2 u_1) \\ \frac{1}{\kappa} (u_2 u_{1,x} - u_1 u_{2,x}) + |u_1 + u_2|^2 A_x \\ \frac{1}{\kappa} (u_2 u_{1,y} - u_1 u_{2,y}) + |u_1 + u_2|^2 A_y \end{pmatrix} \quad (2.56)$$

This implementation is also found in appendix C.1.

Chapter 3

Numerical results

Having implemented the Ginzburg–Landau equations we can now try to solve them numerically for “any” geometry. Three geometries are chosen; a square, a circle and a triangle. Before solving the equations a few numerical decisions needs to be made. All numerical simulations will be made with a relative tolerance of 10^{-6} . As mentioned in the previous chapter, the solution is found with a iteration method. An iteration method calculates the solution in steps, and when having an error tolerance of 10^{-6} , it roughly means that the difference of the solution at step n and $n - 1$ must be below 10^{-6} . The estimated error is calculated by the Euclidean norm

$$Relative\ error = \left(\frac{1}{N} \sum_i |E_i|^2 \right)^{\frac{1}{2}} \quad (3.1)$$

where N is the amount of node points and E_i is the estimated error at node point i . The error E_i is calculated based on the solution U_i at step n and $n - 1$. When the relative error becomes lower than the relative error tolerance the solution will be accepted as converged. The mesh quality needs to be determined and it turned out using about 5000-12000 mesh points was enough to calculate a fairly precise solution. Finally the type of element needs to be chosen. It turned out that it was very hard to get FEMLAB to converge when using the quadratic Langrange elements. For this reason the linear Lagrange elements are used in all simulations in this chapter. All plots are made with Gnuplot 4.0 and the gnuplot scripts can be seen in appendix D. To solve the equations an initial guess must be provided. To begin with we try to make a solution where the superconductor is in the Meissner phase. The Ginzburg–Landau equations normalised with λ_L (2.22) are written for completeness

$$\left(\frac{i}{\kappa} \nabla + \mathbf{A} \right)^2 \Psi - \Psi + |\Psi|^2 \Psi = 0 \quad in \quad \Omega \quad (3.2a)$$

$$\left(\frac{i}{\kappa} \nabla \Psi + \mathbf{A} \Psi \right) \cdot \mathbf{n} = 0 \quad on \quad \partial\Omega \quad (3.2b)$$

$$\frac{i}{2\kappa} (\Psi \nabla \Psi^* - \Psi^* \nabla \Psi) - \mathbf{A} |\Psi|^2 + \nabla \times \mathbf{B}_a = \mathbf{j}_s \quad in \quad \Omega \quad (3.2c)$$

$$\mathbf{B}_a = \mathbf{B}_i \quad on \quad \partial\Omega \quad (3.2d)$$

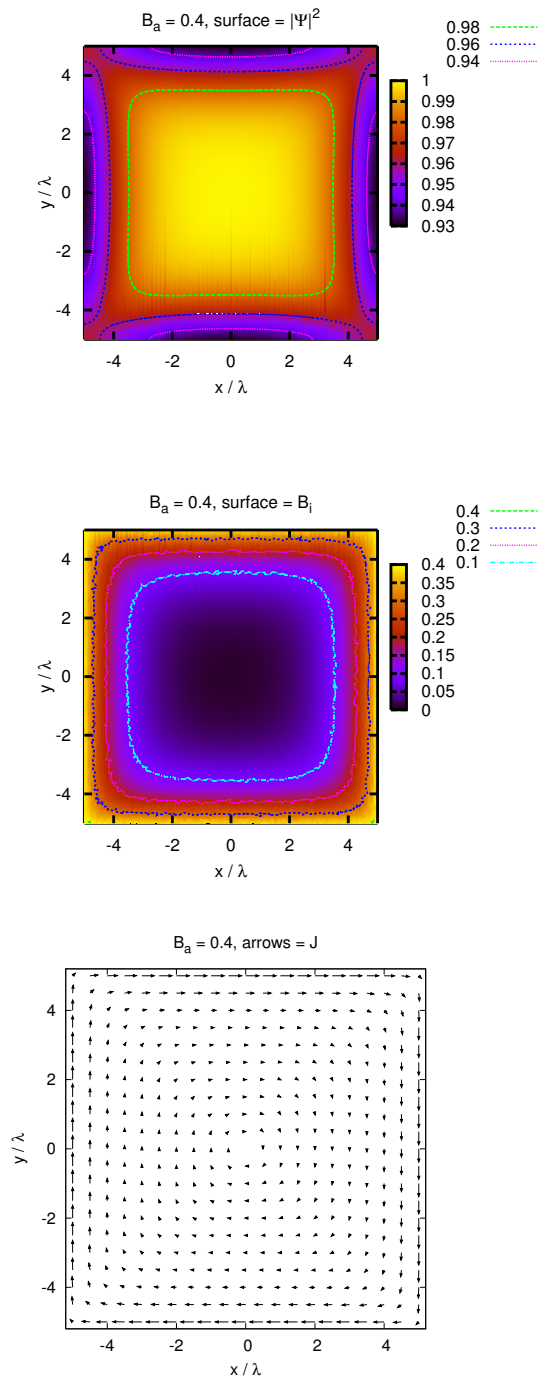


Figure 3.1: Plot made with $\kappa = 1$ and $B_{az} = 0.4$. The first plot is the order parameter squared, the second is the inner magnetic field B_{iz} and the third plot is the supercurrent \mathbf{j}_s . The length of the arrows denote the amplitude of the current.

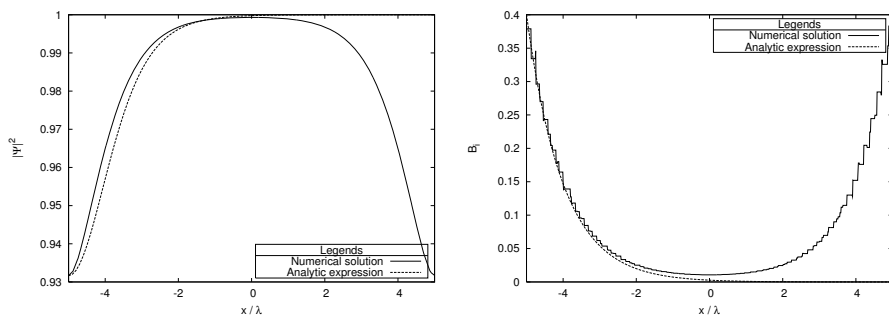


Figure 3.2: Plot made with $\kappa = 1$ and $B_{az} = 0.4$. The line plot is made of the square plotted in figure 3.1 with a cut at $y = 0$. The left plot is the Cooper pair density and the right plot is the magnetic field inside the superconductor.

The initial guess used to calculate solutions in the Meissner phase is

$$\begin{aligned} u_1(x, y) &= u_2(x, y) = \sqrt{0.5} \\ A_x(x, y) &= A_y(x, y) = 0 \end{aligned} \quad (3.3)$$

This choice implies that $B_{iz} = 0$ and $|\Psi|^2 = 1$. Using this solution as an initial guess and having $\kappa = 1$ and the applied magnetic field at $B_a = 0.4$, FEMLAB successfully solves the equations. The solutions normalised with λ_L can be seen on figure 3.1. It does not make any difference however which equations are used as the value of κ is one. When $\kappa = 1$ the equations normalised to λ_L and ξ_{GL} are identical so the solutions on the plots are actually normalised to both λ_L and ξ_{GL} . The first plot is the order parameter squared, and as expected it is near one sufficiently far from the boundary. However having determined an expression for Ψ in equation (1.56) it would be expected that the Cooper pair density near the boundary was lower than 93%. It is also quite surprising that the Cooper pair density is higher at the corners compared to the edges. The second plot is the magnetic field value B_i which is seen to be vanishing in the centre of the superconductor and as expected the magnetic field penetrates into the superconductor. The supercurrent that induces the screening magnetic field may be seen on the third plot. The current is strong near the boundary and low at the centre which is also expected.

Having calculated a solution numerically, we can investigate if the assumptions made in section 1.4 was profound. To do this, two new lineplots at the center of the device, at $y = 0$, are made. These can be seen on figure 3.2. The left plot is the Cooper pair density plotted together with an altered analytic function described below. First of all we see that at the interface the Cooper pair density is 0.93% and not zero as the function found in equation (1.56) is. However, we can still test if the function accurately estimates the rate of change of the order parameter by altering the function to

$$\Psi_0(x) = 0.07 \tanh\left(\frac{x+5}{\sqrt{2}\xi_{GL}}\right) + 0.93 \quad (3.4)$$

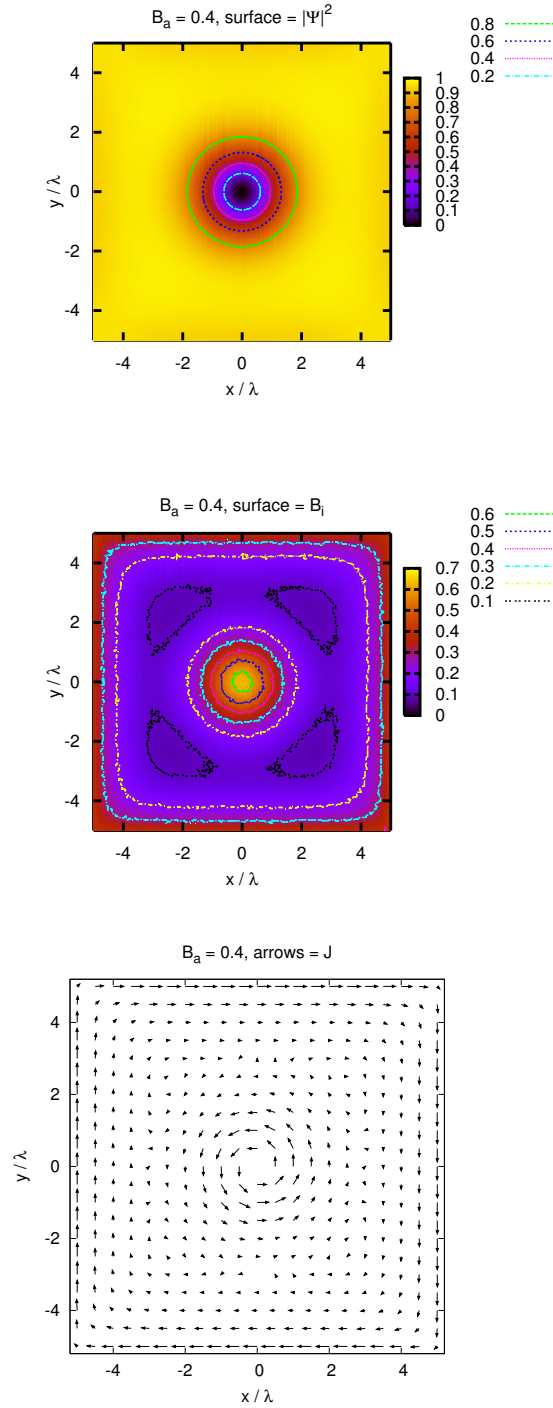


Figure 3.3: The plots are made with $\kappa = 1$ and $B_{az} = 0.4$. The first plot is the order parameter squared, the second is the inner magnetic field B_{iz} and the third plot is the supercurrent \mathbf{j}_s .

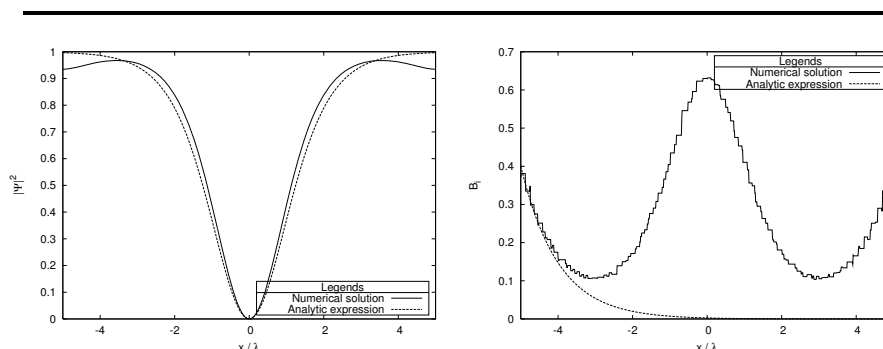


Figure 3.4: Lineplot made with $\kappa = 1$ and $B_{az} = 0.4$. The left plot is the Cooper pair density and the right plot is the magnetic field inside the superconductor. The lineplots are made at $y = 0$.

This altered function fits the numerical solution. The expression is altered with three terms. First $x \rightarrow x + 5$ which just shift the origin to $x = -5$. Secondly the solution is multiplied by 0.07. This is done to make the function have a range on 0.07. Finally we add 0.93 since the numerical solution has a minimum value that is 0.93.

The second plot is the inner magnetic field value plotted with the analytic expression found for the magnetic field in equation (1.48). On this plot the unfortunate consequence of using linear functions is very visible, however in spite of an imprecise numerical solution, it is clear that the analytic expression fits the numerical solution well.

Having made a solution in the Meissner phase we can try to calculate a solution for the vortex phase. This is done with the initial guess

$$\begin{aligned}
 u_1 &= \frac{x}{\sqrt{x^2 + y^2}} \\
 u_2 &= \frac{y}{\sqrt{x^2 + y^2}} \\
 A_x &= A_y = 0
 \end{aligned} \tag{3.5}$$

Using an applied magnetic field value of $B_{az} = 0.4$ a vortex solution is found. This solution can be seen for a square with $\kappa = 1$ on figure 3.3, and this is indeed numerical evidence that the solutions to the equations are not unique. This means that having an applied magnetic field of $B_{az} = 0.4$, it is actually possible for the superconductor to be both in the Meissner phase and vortex phase. It depends on the initial condition. This could also suggest that hysteresis is possible. This will be investigated in chapter 5. The first plot displays the Cooper pair density and the second plot the magnetic field inside the superconductor. At the vortex we see that the Cooper pair density is close to zero, which confirms that a superconductor in the vortex phase is in superconducting state in some areas and in normal state the remaining areas. The third plot reveals that current circulates the vortex, which creates a screening magnetic field inside the superconductor. It seems that the current around the vortex actually

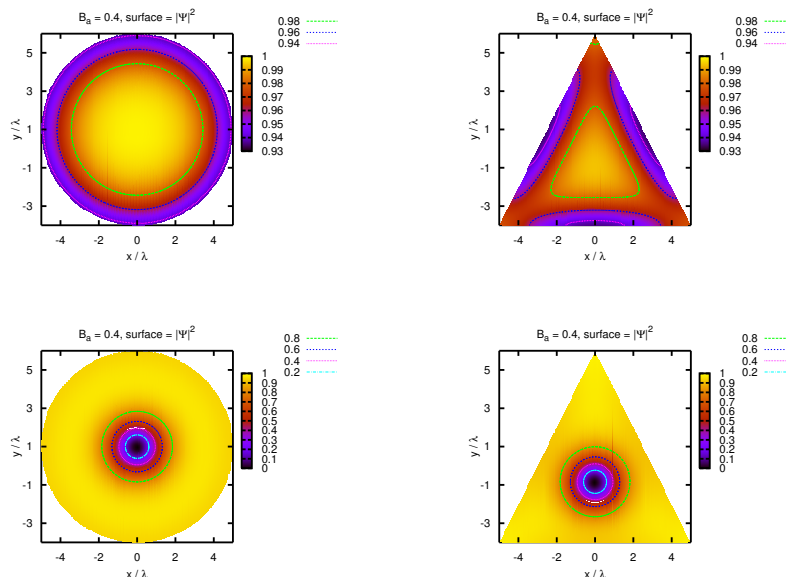


Figure 3.5: The Cooper pair density made with $\kappa = 1$ and $B_{az} = 0.4$.

induces a magnetic field, since the magnetic field in the vortex is stronger than the applied magnetic field. Notice that the current inside the superconductor runs in the opposite direction of the surface current.

Two lineplots of the numerical solution together with the expressions found in (1.56) and (1.48) can be seen on figure 3.4. We see that there is a much better correspondence between the numerical solution and the expression found in (1.56) compared to figure 3.2. The effect of the vortex is roughly $4\xi_{GL}$ wide and fits the analytic expression well. The analytic expression found for B_{iz} is also fairly accurate close to the boundary. This shows, that the rate the applied magnetic field penetrates into the superconductor within λ_L , is the same for the Meissner phase and the vortex phase containing one vortex. That is, the analytic expression found for the inner magnetic field, is still accurate within one λ_L from the boundary.

Having found a solution for a vortex phase we could try to find solutions having more vortices. However FEMLAB was not able to find those solutions as the initial guesses were not accurate enough. To solve this problem the time-dependent model can be used to generate an initial guess. This model will be treated in chapter 4.

Having obtained solutions for a square, we can try to solve the equations for other geometries. This seems to be fairly easy as long the geometry is “nice” and we keep to solutions in the Meissner phase or vortex phase with one vortex only. The Cooper pair density for a circle and triangle can be seen in figure 3.5. Only the Cooper pair density has been plotted as it has been shown with the square plots how the corresponding supercurrent and magnetic field behaves.

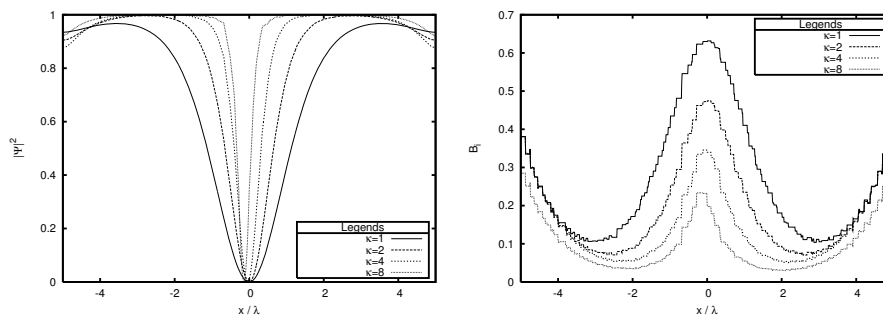


Figure 3.6: The Cooper pair density plotted for a square when $y = 0$. The plot is made with an applied magnetic field value of $B_{az} = 0.3$ for $\kappa = 8$ and $B_{az} = 0.4$ for the remaining curves. The length scale is normalised to λ_L .

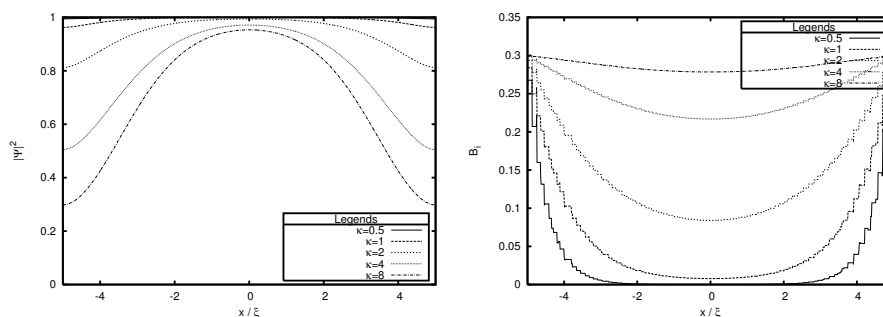


Figure 3.7: The Cooper pair density plotted for a square when $y = 0$. The solutions are made with an applied magnetic field value of $B_{az} = 0.3$. The length scale is normalised to ξ_{GL} .

In order to illustrate the effect of λ_L and ξ_{gL} we can try to change the value of κ to see the effect. This is done on figure 3.6 with the equations normalised to λ_L . This has the consequence that ξ_{GL} decreases as κ increases. The left plot clearly shows that the vortex size is determined with ξ_{GL} . In each step in the vortex size is roughly halved, that is the vortex with $\kappa = 2$ is about half the size of the vortex with $\kappa = 1$ etc. Unlike the solutions calculated with $B_{az} = 0.4$, the solution calculated with $\kappa = 8$ has an applied magnetic field on $B_{az} = 0.3$. This is due to lack of convergence with $B_{az} = 0.4$ so the applied magnetic field was reduced. We also see that the vortex for $\kappa = 8$ is not positioned exactly at the centre, which implies that the vortex is about to “leave” the superconductor. On the right plot the inner magnetic field value B_{iz} is plotted. We see that the magnetic field value in the vortex is also dependent of the value of κ . It is also clear on the right plot that the London penetration depth remains fixed.

In order to study what effects it has to change λ_L we can solve the equations normalised to ξ_{GL} . This has been done for the Meissner phase and the results

can be seen on figure 3.7. On the left figure we clearly see that the value of λ_L has a impact on the Cooper pair density. However notice that all five curves has the same basefunction, namely the one found in equation (1.56) (the solution with $\kappa = 0.5$ is hard to see as it has a Cooper pair density near one throughout the superconductor). On the right plot we see as expected that the slope of the curves roughly doubles as κ doubles. This is expected, since when κ is doubled, it implies that the London penetration depth is also doubled.

It turned out that calculating solutions with different κ while having the applied magnetic field fixed was a challenge. On one occasion it failed (on figure 3.6) where we had to change the applied magnetic field. During the simulations made on figure 3.7 FEMLAB failed to converge several times, however it turned out that on few occasions we could make the solution converge by simply restarting the solver with the exact same parameters.

It is very hard to investigate solutions containing more that one vortex, due to the fact that we must provide the numerical solver with a good initial guess. It is not easy to make such an analytic expression containing more than one vortex. We have tried to use the superposition principle on our initial guess for one vortex however all attempts failed to converge. To solve this problem we turn our attention to the time-dependent Ginzburg-Landau model, which should not have these kind of problems. This also enables the study of vortex dynamics.

Chapter 4

Time-Dependent Ginzburg-Landau Theory

The time-dependent Ginzburg Landau equations can be written as [20]¹

$$\begin{aligned}\frac{\hbar^2}{2mD} \left(\frac{\partial}{\partial t} + i \frac{q}{\hbar} \Phi \right) \Psi &= - \frac{\delta \mathcal{L}}{\delta \Psi^*} \\ \sigma \left(\frac{\partial \mathbf{A}}{\partial t} + \nabla \Phi \right) &= - \frac{\delta \mathcal{L}}{\delta \mathbf{A}}\end{aligned}\tag{4.1}$$

where \mathcal{L} was found in chapter 1 as equation (1.13):

$$\mathcal{L} = \frac{1}{2m} \left| \left(\frac{\hbar}{i} \nabla - q \mathbf{A} \right) \Psi \right|^2 - \alpha |\Psi|^2 + \frac{\beta}{2} |\Psi|^4 + \frac{1}{2\mu_0} |\mathbf{B}_a - \mathbf{B}_i|^2\tag{4.2}$$

Compared to the stationary equations a couple of new variables are introduced; D is a phenomenological diffusion coefficient, Φ is the electric potential and σ is the conductivity constant which is assumed constant. Furthermore the order parameter becomes $\Psi = \Psi(x, y, z, t)$ and the vector potential $\mathbf{A} = \mathbf{A}(x, y, z, t)$.

An important property of the time-dependent model is that the current density is [20]

$$\mathbf{J} = \sigma \mathbf{E} + \mathbf{J}_s\tag{4.3}$$

where \mathbf{J}_s is the supercurrent which is found in equation (1.32c) and \mathbf{E} is the electric field. The electric field is found in electromagnetics from Faraday's law as [11]

$$\mathbf{E} = - \frac{\partial \mathbf{A}}{\partial t} - \nabla \Phi\tag{4.4}$$

If \mathbf{J} is viewed as the normal current which obeys Ohm law, σ may be interpreted as the coefficient of normal conductivity.

¹These equations are given in cgs units in the cited paper. Refer to appendix A for the conversion from cgs to SI units.

To obtain the full form of the time-dependent equations the variational derivatives needs to be written out. From equation (1.21) and (1.27) the derivatives are found to be

$$\begin{aligned}\frac{\delta\mathcal{L}}{\delta\Psi^*} &= \frac{\partial\mathcal{L}}{\partial\Psi^*} - \nabla \cdot \left(\frac{\partial\mathcal{L}}{\partial(\nabla\Psi^*)} \right) \\ \frac{\delta\mathcal{L}}{\delta\mathbf{A}} &= \frac{\partial\mathcal{L}}{\partial\mathbf{A}} + \nabla \times \left(\frac{\partial\mathcal{L}}{\partial(\nabla \times \mathbf{A})} \right)\end{aligned}\quad (4.5)$$

The derivatives has been calculated in equation (1.22) and (1.28). When using the above equations together with the derivatives then the full form of (4.1) is found as

$$\frac{\hbar^2}{2mD} \left(\frac{\partial}{\partial t} + i\frac{q}{\hbar}\Phi \right) \Psi = -\frac{1}{2m} \left(\frac{\hbar}{i}\nabla - q\mathbf{A} \right)^2 \Psi + \alpha\Psi - \beta|\Psi|^2\Psi \quad (4.6a)$$

$$\sigma \left(\frac{\partial\mathbf{A}}{\partial t} + \nabla\Phi \right) = \frac{q\hbar}{2mi} (\Psi^*\nabla\Psi - \Psi\nabla\Psi^*) - \frac{q^2}{m} |\Psi|^2\mathbf{A} - \frac{1}{\mu_0} \nabla \times \nabla \times \mathbf{A} \quad (4.6b)$$

Note that the differentiation in (4.6a) also applies to Ψ . To obtain (4.6b) it is assumed that the applied magnetic field is an uniform static field, which formally means that the curl of \mathbf{B}_a vanishes. If this is not the case the term $\frac{1}{\mu_0} \nabla \times \nabla \times \mathbf{B}_a$ needs to be added to the right hand side of equation (4.6b).

At the interface of the superconducting sample the following boundary conditions are imposed [21]:

$$\left(\frac{\hbar}{i}\nabla\Psi - q\mathbf{A}\Psi \right) \cdot \mathbf{n} = 0 \quad \text{on } \partial\Omega \quad (4.7a)$$

$$\mathbf{B}_a = \mathbf{B}_i \quad \text{on } \partial\Omega \quad (4.7b)$$

$$\left(\frac{\partial\mathbf{A}}{\partial t} + \nabla\Phi \right) \cdot \mathbf{n} = 0 \quad \text{on } \partial\Omega \quad (4.7c)$$

Equation (4.7a) and (4.7b) are also the boundary conditions in the stationary situation. For a discussion about the physical consequences of these boundary conditions refer to section 1.3. Equation (4.7c) can also be written as $\mathbf{E} \cdot \mathbf{n} = 0$ with \mathbf{E} given in equation (4.4). A justification of this boundary condition is that the current is always parallel to the electric field [11], so this boundary condition is a physical consequence of $\mathbf{j}_s \cdot \mathbf{n} = 0$.

As a final remark before proceeding to the numerical formulation, the theoretical validity of the time-dependent model is arguable. Beside the limitation that Ginzburg–Landau theory is only valid near T_c (as discussed in chapter 1), the model also requires the superconductor to be *gapless* [2]. What this means is beyond the scope of this text, but we refer to the book by Tinkham for details [2]. In spite of these limitations the experimental results over a wide range of temperatures are in excellent agreement with the model [20].

4.1 Normalisation

As in the stationary case the Ginzburg–Landau equations are normalised before they are solved numerically. As discussed during the normalisation process of the

stationary equations, two different normalisation schemes are natural choices. Only the normalisation with λ_L will be made since the numerical calculations will be conducted with a fixed Ginzburg–Landau parameter. The normalisation are made using the following transformations

$$\begin{aligned} (x, y, z) &\rightarrow \lambda(x, y, z)', & t &\rightarrow \frac{\xi^2}{D}t, & \mathbf{A} &\rightarrow \frac{\hbar}{q\xi}\mathbf{A}' \\ \Psi &\rightarrow \sqrt{\frac{\alpha}{\beta}}\Psi', & \Phi &\rightarrow \alpha D\kappa^2\sqrt{\frac{2\mu_0}{b}}\Phi', & \sigma &\rightarrow \frac{1}{\mu_0 D\kappa^2}\sigma' \end{aligned} \quad (4.8)$$

from which the following transformation follows by use of the chain rule

$$\nabla = \frac{1}{\lambda}\nabla', \quad \frac{\partial}{\partial t} = \frac{D}{\xi^2}\frac{\partial}{\partial t'} \quad (4.9)$$

Furthermore by using that $\mathbf{B} = \nabla \times \mathbf{A}$ a transformation for the magnetic field is obtained as

$$\mathbf{B} = \frac{\hbar}{q\xi\lambda}\mathbf{B}' \quad (4.10)$$

First the left hand side of (4.6a) is normalised using the defined transformations

$$\frac{\hbar^2}{2mD} \left(\frac{\partial}{\partial t} + i\frac{q}{\hbar}\Phi \right) \Psi = \alpha\sqrt{\frac{\alpha}{\beta}} \left(\frac{\partial}{\partial t'} + i\kappa\Phi' \right) \Psi' \quad (4.11)$$

Now the right hand side is normalised. The first term is transformed into

$$\frac{1}{2m} \left(\frac{\hbar}{i}\nabla - q\mathbf{A} \right)^2 \Psi = \alpha\sqrt{\frac{\alpha}{\beta}} \left(\frac{i}{\kappa}\nabla' + \mathbf{A}' \right)^2 \Psi' \quad (4.12)$$

The second and the third term on the right hand side are found to be

$$\begin{aligned} \alpha\Psi &= \alpha\sqrt{\frac{\alpha}{\beta}}\Psi' \\ \beta|\Psi|^2\Psi &= \alpha\sqrt{\frac{\alpha}{\beta}}|\Psi'|^2\Psi' \end{aligned} \quad (4.13)$$

After the transformations both sides of (4.6a) has the same multiplier, $\alpha\sqrt{\alpha/\beta}$, which can be eliminated from the equation. When this is done the only constant that features in the equation is κ . Now the second Ginzburg–Landau equation is normalised. The left hand side of the second equation (4.6b) is transformed into

$$\sigma \left(\frac{\partial \mathbf{A}}{\partial t} + \nabla\Phi \right) = \frac{q\alpha}{\beta} \sqrt{\frac{2\alpha}{m}} \sigma' \left(\frac{\partial \mathbf{A}'}{\partial t'} + \nabla'\Phi' \right) \quad (4.14)$$

The supercurrent \mathbf{J}_s is transformed as

$$\mathbf{J}_s = \frac{q\hbar}{2mi} \frac{\alpha}{\beta\lambda} (\Psi'^*\nabla'\Psi' - \Psi'\nabla'\Psi'^*) - \frac{q^2}{m} \frac{\alpha\hbar}{\beta q\xi} |\Psi'|^2 \mathbf{A}' \quad (4.15)$$

The multipliers are rewritten into

$$\begin{aligned}\frac{q\hbar}{2m\iota} \frac{\alpha}{\beta\lambda} &= \frac{q\alpha}{\beta} \sqrt{\frac{\alpha}{2m}} \frac{1}{\iota\kappa} \\ \frac{q^2}{m} \frac{\alpha\hbar}{\beta q\xi} &= \frac{q\alpha}{\beta} \sqrt{\frac{2\alpha}{m}}\end{aligned}\quad (4.16)$$

and the final form of \mathbf{J}_s becomes

$$\mathbf{J}_s = \frac{q\alpha}{\beta} \sqrt{\frac{2\alpha}{m}} \left(\frac{1}{2\iota\kappa} [\Psi'^*\nabla'\Psi' - \Psi'\nabla'\Psi'^*] - |\Psi'|^2 \mathbf{A}' \right) \quad (4.17)$$

The second term on the right hand side of (4.6b) is rewritten as

$$-\frac{1}{\mu_0} \nabla \times \nabla \times \mathbf{A} = -\frac{\hbar}{\mu_0 q \xi \lambda^2} \nabla' \times \nabla' \times \mathbf{A}' \quad (4.18)$$

where the multiplier is reduced to

$$\frac{\hbar}{\mu_0 q \xi \lambda^2} = \frac{q\alpha}{\beta} \sqrt{\frac{2\alpha}{m}} \quad (4.19)$$

Both sides of (4.6b) end up having the same multiplier so this is removed from the equation.

To summarise the normalised equations when omitting the primes are

$$\left(\frac{\partial}{\partial t} + \iota\kappa\Phi \right) \Psi = - \left(\frac{\iota}{\kappa} \nabla + \mathbf{A} \right)^2 \Psi + \Psi - |\Psi|^2 \Psi \quad (4.20a)$$

$$\sigma \left(\frac{\partial \mathbf{A}}{\partial t} + \nabla \Phi \right) = \frac{1}{2\iota\kappa} (\Psi^* \nabla \Psi - \Psi \nabla \Psi^*) - |\Psi|^2 \mathbf{A} - \nabla \times \nabla \times \mathbf{A} \quad (4.20b)$$

and the boundary conditions becomes

$$\left(\frac{\iota}{\kappa} \nabla \Psi + \mathbf{A} \Psi \right) \cdot \mathbf{n} = 0 \quad \text{on } \partial\Omega \quad (4.21a)$$

$$\mathbf{B}_a = \mathbf{B}_i \quad \text{on } \partial\Omega \quad (4.21b)$$

$$\left(\frac{\partial \mathbf{A}}{\partial t} + \nabla \Phi \right) \cdot \mathbf{n} = 0 \quad \text{on } \partial\Omega \quad (4.21c)$$

4.2 Gauge invariance

The time-dependent Ginzburg–Landau equations like the stationary equations have the property of gauge invariance. Given a function $\chi(x, y, z, t)$, the linear transformation G_χ is defined as

$$G_\chi(\Psi, \mathbf{A}, \Phi) = (\Psi', \mathbf{A}', \Phi') \quad (4.22)$$

where

$$\Psi' = \Psi e^{\iota\kappa\chi}, \quad \mathbf{A}' = \mathbf{A} + \nabla\chi, \quad \Phi' = \Phi - \frac{\partial\chi}{\partial t} \quad (4.23)$$

The proof of gauge invariance can be found in appendix B.2.

As in the stationary case we need to fix the gauge in order to obtain well-posed equations [21]. The most convenient choice when solving the time-dependent equations turns out to be the *zero electric potential gauge* where Φ is chosen to be zero. From the transformations given in (4.23) we then have

$$\frac{\partial \chi}{\partial t} = -\Phi' \quad (4.24)$$

Knowing that the equations are gauge invariant we can simply let Φ vanish in all the equations. The boundary condition (4.21c) however is rewritten further. Letting Φ vanish we get

$$\left(\frac{\partial \mathbf{A}}{\partial t} \right) \cdot \mathbf{n} = 0 \quad (4.25)$$

This equation can be integrated and the integration constant chosen to be zero, which turns the equation into $\mathbf{A} \cdot \mathbf{n} = 0$ [21]. This relation is used to reduce equation (4.21a). The equations to solve with the primes omitted becomes

$$\frac{\partial \Psi}{\partial t} = - \left(\frac{\imath}{\kappa} \nabla + \mathbf{A} \right)^2 \Psi + \Psi - |\Psi|^2 \Psi \quad (4.26a)$$

$$\sigma \frac{\partial \mathbf{A}}{\partial t} = \frac{1}{2\imath\kappa} (\Psi^* \nabla \Psi - \Psi \nabla \Psi^*) - |\Psi|^2 \mathbf{A} - \nabla \times \nabla \times \mathbf{A} \quad (4.26b)$$

with the boundary conditions

$$\nabla \Psi \cdot \mathbf{n} = 0 \quad \text{on } \partial\Omega \quad (4.27a)$$

$$\mathbf{B}_a = \mathbf{B}_i \quad \text{on } \partial\Omega \quad (4.27b)$$

$$\mathbf{A} \cdot \mathbf{n} = 0 \quad \text{on } \partial\Omega \quad (4.27c)$$

4.3 Correspondence with stationary equations

One important goal with the time-dependent equations is to find stabilised stationary solutions. In order to be sure it is a valid stationary solution, the stabilised solution will be used as an initial guess to the stationary equations. This will only work if the time-dependent equations (4.26) reduces to the stationary equations (2.31) when such a solution is found. Since the stationary equations written in (2.31) are found using the Coulomb gauge, we need to prove that the zero potential gauge implies the Coulomb gauge when having a stationary state. This is done by taking the divergence of equation (4.26b) which yields

$$\sigma \frac{\partial}{\partial t} \nabla \cdot \mathbf{A} = \frac{1}{2\imath\kappa} (\Psi^* \nabla^2 \Psi - \Psi \nabla^2 \Psi^*) - \nabla \cdot (|\Psi|^2 \mathbf{A}) \quad (4.28)$$

To obtain the result it is used that the divergence of $\nabla \times \mathbf{V}$ vanishes for any vectorfield \mathbf{V} . To rewrite the above equation further the first Ginzburg–Landau equation is used. Reorganising (4.26a) yields

$$\nabla^2 \Psi = \kappa^2 \frac{\partial \Psi}{\partial t} + \kappa^2 \Psi \mathbf{A} \cdot \mathbf{A} + \imath\kappa (2\mathbf{A} \cdot \nabla \Psi + \Psi \nabla \cdot \mathbf{A}) - \kappa^2 \Psi + \kappa^2 |\Psi|^2 \Psi \quad (4.29)$$

This result is used to rewrite (4.28) into

$$\sigma \frac{\partial}{\partial t} \nabla \cdot \mathbf{A} = \frac{1}{2i\kappa} \left(\Psi^* \frac{\partial \Psi}{\partial t} - \Psi \frac{\partial \Psi^*}{\partial t} \right) \quad (4.30)$$

We now see that having a divergence free vector potential requires either that the order parameter is either zero or its phase is independent of time. In the stationary state the phase is obviously independent of time and there we have a divergence free vector potential. This means that the time-dependent equations indeed reduces to the stationary equations when a stationary solution is found.

4.4 FEMLAB formulation

To solve the time-dependent model the equations must be given on the form

$$\begin{aligned} \mathbf{d}_a \frac{\partial u}{\partial t} + \nabla \cdot \mathbf{\Gamma} &= \mathbf{F} \quad \text{in} \quad \Omega \\ -\mathbf{n} \cdot \mathbf{\Gamma} &= \mathbf{G} \quad \text{on} \quad \partial\Omega \end{aligned} \quad (4.31)$$

For a discussion about the parameters in the above equations refer to section 2.3.2.

The vector $\mathbf{\Gamma}$ is the first one to be determined which is done by handling the boundary conditions. As in chapter 2 the order parameter is written as $\Psi = u_1 + iu_2$ which changes (4.27a) into

$$\nabla u_1 \cdot \mathbf{n} + i \nabla u_2 \cdot \mathbf{n} = 0 \quad (4.32)$$

With the above equation $\mathbf{\Gamma}_{1,2}$ can immediately be determined, however it turns out to be an advantage to multiply (4.27a) with κ^{-2} . Doing this $\mathbf{\Gamma}_{1,2}$ are found as $\mathbf{\Gamma}_1 = -\frac{1}{\kappa^2} \nabla u_1$ and $\mathbf{\Gamma}_2 = -\frac{1}{\kappa^2} \nabla u_2$. The scalars $G_{1,2}$ are found to be zero. By the same considerations made in section 2.2, the second boundary condition (4.27b) is reduced to

$$A_{y,x} - A_{x,y} - B_{az} = 0 \quad (4.33)$$

As discussed in 2.3.2 two vectors are needed to represent this boundary condition. The last boundary condition (4.27c) is left untouched, and since the right hand side of all the boundary conditions is zero, it is only natural to choose $\mathbf{G} = \mathbf{0}$. When this is done $\mathbf{\Gamma}$ is written as

$$\begin{aligned} \mathbf{\Gamma}_1 &= -\frac{1}{\kappa^2} \nabla u_1 \\ \mathbf{\Gamma}_2 &= -\frac{1}{\kappa^2} \nabla u_2 \\ \mathbf{\Gamma}_3 &= \begin{pmatrix} 0 \\ A_{y,x} - A_{x,y} - B_{az} \end{pmatrix} \\ \mathbf{\Gamma}_4 &= \begin{pmatrix} -A_{y,x} + A_{x,y} + B_{az} \\ 0 \end{pmatrix} \\ \mathbf{\Gamma}_5 &= \begin{pmatrix} A_x \\ A_y \end{pmatrix} \end{aligned} \quad (4.34)$$

We see that opposed to the stationary equations a vector of five components is needed to implement the boundary conditions in FEMLAB.

To determine the vector \mathbf{F} and the matrix \mathbf{d}_a the divergence of $\mathbf{\Gamma}$ needs to be determined, which is

$$\nabla \cdot \mathbf{\Gamma} = \begin{pmatrix} -\frac{1}{\kappa^2} \nabla^2 u_1 \\ -\frac{1}{\kappa^2} \nabla^2 u_2 \\ A_{y,xy} - A_{x,yy} \\ A_{x,yx} - A_{y,xx} \\ A_{x,x} + A_{x,y} \end{pmatrix} \quad (4.35)$$

The scalars $F_{1,2}$ are determined by inserting $\Psi = u_1 + u_2$ into equation (4.26a) and then splitting the resulting equation into a real and imaginary part. When this is done we get

$$\begin{aligned} \frac{\partial u_1}{\partial t} - \frac{1}{\kappa^2} \nabla^2 u_1 &= -\mathbf{A} \cdot \mathbf{A} u_1 + \frac{1}{\kappa} (2\mathbf{A} \cdot \nabla u_2 + u_2 \nabla \cdot \mathbf{A}) + u_1 - |u_1 + u_2|^2 u_1 \\ \frac{\partial u_2}{\partial t} - \frac{1}{\kappa^2} \nabla^2 u_2 &= -\mathbf{A} \cdot \mathbf{A} u_2 - \frac{1}{\kappa} (2\mathbf{A} \cdot \nabla u_1 + u_1 \nabla \cdot \mathbf{A}) + u_2 - |u_1 + u_2|^2 u_2 \end{aligned} \quad (4.36)$$

where the first equation is the real part and the second is the imaginary part. The scalars $F_{1,2}$ are found as the right hand sides of the above equations. To obtain $F_{3,4}$ the solution $\Psi = u_1 + u_2$ is inserted into equation (4.26b), which yields

$$\sigma \frac{\partial \mathbf{A}}{\partial t} = \frac{1}{2\kappa} (u_1 \nabla u_2 - u_2 \nabla u_1) - |u_1 + u_2|^2 \mathbf{A} - \nabla \times \nabla \times \mathbf{A} \quad (4.37)$$

As in the stationary case this equation is divided into two new equations by making one for the x -component and one for the y -component. From equation (2.50) we have

$$\nabla \times \nabla \times \mathbf{A} = (A_{y,xy} - A_{x,yy}) \mathbf{x} + (-A_{y,xx} + A_{x,yx}) \mathbf{y} \quad (4.38)$$

and the two new equations becomes

$$\begin{aligned} \sigma \frac{\partial A_x}{\partial t} + A_{y,xy} - A_{x,yy} &= \frac{1}{2\kappa} (u_1 u_{2,x} - u_2 u_{1,x}) - |u_1 + u_2|^2 A_x \\ \sigma \frac{\partial A_y}{\partial t} + A_{x,yx} - A_{y,xx} &= \frac{1}{2\kappa} (u_1 u_{2,y} - u_2 u_{1,y}) - |u_1 + u_2|^2 A_y \end{aligned} \quad (4.39)$$

The scalars $F_{3,4}$ are determined as the right hand sides. One scalar still needs to be found which is F_5 however only four equations are needed to implement the Ginzburg–Landau equations, but five are needed for the boundary conditions. This problems is solved by letting F_5 be equal to the divergence of $\mathbf{\Gamma}_5$ with only the solution variable u_5 added. If the fifth row of \mathbf{d}_a only contain zeros the fifth FEMLAB equation then becomes $0 = u_5$. The complete form of \mathbf{F} becomes

$$\mathbf{F} = \begin{pmatrix} -\mathbf{A} \cdot \mathbf{A} u_1 + \frac{1}{\kappa} (2\mathbf{A} \cdot \nabla u_2 + u_2 \nabla \cdot \mathbf{A}) + u_1 - |u_1 + u_2|^2 u_1 \\ -\mathbf{A} \cdot \mathbf{A} u_2 - \frac{1}{\kappa} (2\mathbf{A} \cdot \nabla u_1 + u_1 \nabla \cdot \mathbf{A}) + u_2 - |u_1 + u_2|^2 u_2 \\ \frac{1}{2\kappa} (u_1 u_{2,x} - u_2 u_{1,x}) - |u_1 + u_2|^2 A_x \\ \frac{1}{2\kappa} (u_1 u_{2,y} - u_2 u_{1,y}) - |u_1 + u_2|^2 A_y \\ A_{x,x} + A_{y,y} + u_5 \end{pmatrix} \quad (4.40)$$

and the mass matrix becomes

$$\mathbf{d}_a = \mathit{diag}(1, 1, \sigma, \sigma, 0) \quad (4.41)$$

where *diag* is the diagonal of a square matrix. The remaining elements of \mathbf{d}_a is zero. The MATLAB implementation can be seen in appendix C.3.

Chapter 5

Time-dependent results

With the time-dependent model implemented in FEMLAB, we can try to find solutions containing more than one vortex. These solutions were calculated with an error tolerance of 10^{-6} . During the simulations, it turned out that using linear Lagrange functions was a bad idea. The solutions found with linear elements were simply incorrect, as the Cooper pair density was in the region of 1.5 several places. However when quadratic Lagrange elements were used, the time-dependent solver worked satisfactory.

To begin with, we would like to illustrate the impact of using quadratic Lagrange elements. The square which was solved in chapter 3, figure 3.3 and 3.4, is also solved using the time-dependent equations. The equations are solved to $t = 250$, where the solution seems to be stabilised. This solution is used as initial guess to the stationary equations, and the stationary equations converge. The results can be seen on figure 5.1. On this figure, we see that the magnetic field inside the superconductor has a much better approximation. However, it is also the case, that even though the solution seems to have stabilised, the magnetic field calculated using the stationary equations is stronger than the field calculated using the time-dependent equations. Whether the solution at $t = 250$ is truly a stationary state is not known, since the stationary equations fail to converge when using quadratic elements. Thus, we can conclude one of two scenarios; either the solution has not truly stabilised at $t = 250$, or if it has stabilised, then linear Lagrange elements might not be sufficient to calculate an accurate solution for the magnetic field inside the superconductor. We will not delve more into this issue, but just conclude, that there might be some numerical issues that requires further investigation. Our original point has been shown, namely that the inner magnetic field is approximated better when using quadratic Lagrange elements.

Using the time-dependent model, we do not suffer from the lack of making adequate initial guesses. Therefore we can try to solve more challenging scenarios. We could for example investigate the behaviour just around $\kappa = 1/\sqrt{2}$, which is the value that separates type I and II superconductors. If κ is less than $\kappa = 1/\sqrt{2}$, a vortex solution should not be possible. To investigate this, we try to make a solution where $\kappa = 0.71$, which is just enough to make a vortex

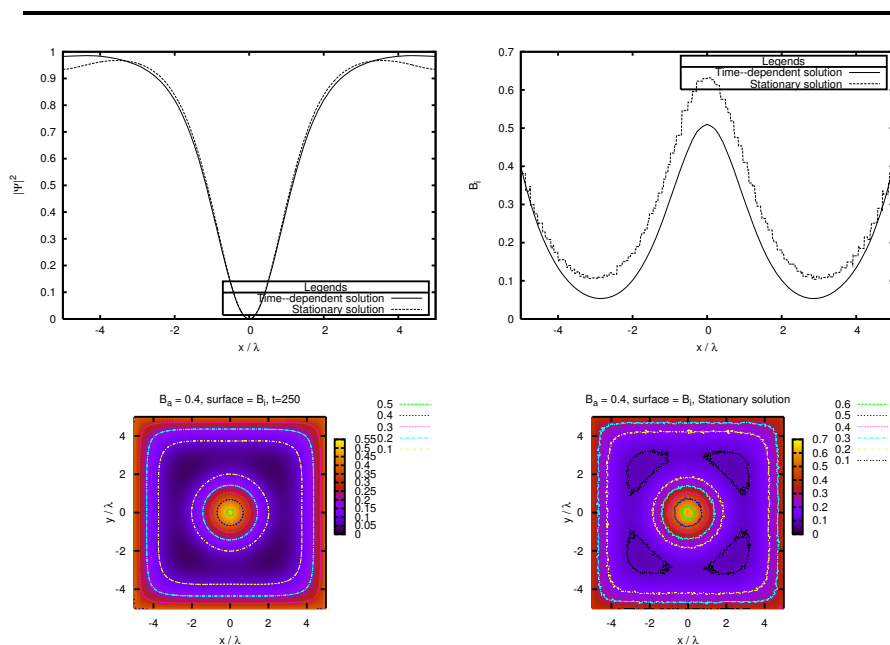


Figure 5.1: Comparison between the solutions found by the time-dependent equations and stationary equations. The top left figure, is the Cooper pair density at the centre of the device. The top right is the inner magnetic field, likewise at the centre of the device. The surface plots are plots of the inner magnetic field.

solution legal. If we use the following initial condition

$$\begin{aligned}
 u_1 &= \frac{x}{\sqrt{x^2 + y^2}} \\
 u_2 &= \frac{y}{\sqrt{x^2 + y^2}} \\
 A_x &= A_y = 0
 \end{aligned} \tag{5.1}$$

at $t = 0$, a solution containing one vortex is recovered. Now κ is reduced to 0.4, which is below the limit $\kappa = 1/\sqrt{2}$, a vortex solution is still found. This is obviously wrong! Whether the numerical calculation is inadequate, or the Ginzburg–Landau equations indeed allow such solution, is not investigated due to lack of time. However, since κ is a fixed value for a superconductor, this numerical simulation is not a realistic scenario, as we are using a vortex solution as an initial guess, for a superconductor which would never enter a vortex phase in the first place. The results can be seen on figure 5.2.

Now we turn our attention to vortex dynamics. To begin with, we can try to solve a square for $\kappa = 4$ and $B_{az} = 0.75$, which can be seen on figure 5.3. At $t = 0$ the superconductor is in the Meissner phase. This is achieved by the

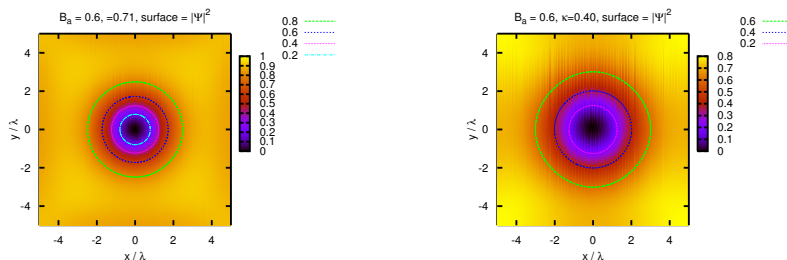


Figure 5.2: The Cooper pair density of a square. On the left plot we have $\kappa = 0.71$ and on the right $\kappa = 0.4$.

initial condition

$$\begin{aligned} u_1(x, y) &= u_2(x, y) = \sqrt{0.5} \\ A_x(x, y) &= A_y(x, y) = 0 \end{aligned} \quad (5.2)$$

The physical setup this solution illustrates, is that we have a superconductor with a magnetic field weak enough to let the superconductor be in the Meissner phase. What happens, is that the vortices make entry at the centre of the sides. This does not come as a surprise, since we saw in chapter 3, that this was the area with lowest Cooper pair density. After the vortices have entered the superconductor, they begin to form a square of their own ($t = 450$), from where two of the vortices are pushed into the centre of the superconductor. This happens in order for the vortices to be as far away from each other as possible, while also taking the magnetic field at boundary into account. A movie sequence of this scenario can be found on the attached CD, refer to appendix D. The solution at $t = 2000$ has reached a stationary state, which is used as an initial guess for the stationary equations. The solution computed by the stationary equations can be seen on the figure in the bottom-right corner.

In the previous simulation, it is very helpful to have a non-symmetric mesh, as the vortices could have converged to a vertical alignment instead. We see, that the solution in this scenario have a degeneracy of two, and the only reason one of the solutions is chosen above the other, is because of a non-symmetric mesh. In this way, we can say that the mesh used is biased towards the solution seen on the figure. If we try to solve the model with a lower applied magnetic field, no vortices enter the superconductor. We have tried to begin with an applied magnetic field at $B_{az} = 0.4$, and then increase the value with an interval of 0.05, and the superconductor stays in the Meissner phase until $B_{az} = 0.75$ is reached. We can try make further calculations on this solution, by changing the applied magnetic field at $t = 2000$.

If the magnetic field is lowered to a value of 0.45, with an interval of 0.10, the vortices stay in the superconductor. This fact is numerical evidence that hysteresis exists, that is, the superconductor does not return to the Meissner phase, even though the magnetic field is lowered to a value, where the superconductor has previously been in the Meissner phase. If the magnetic field is

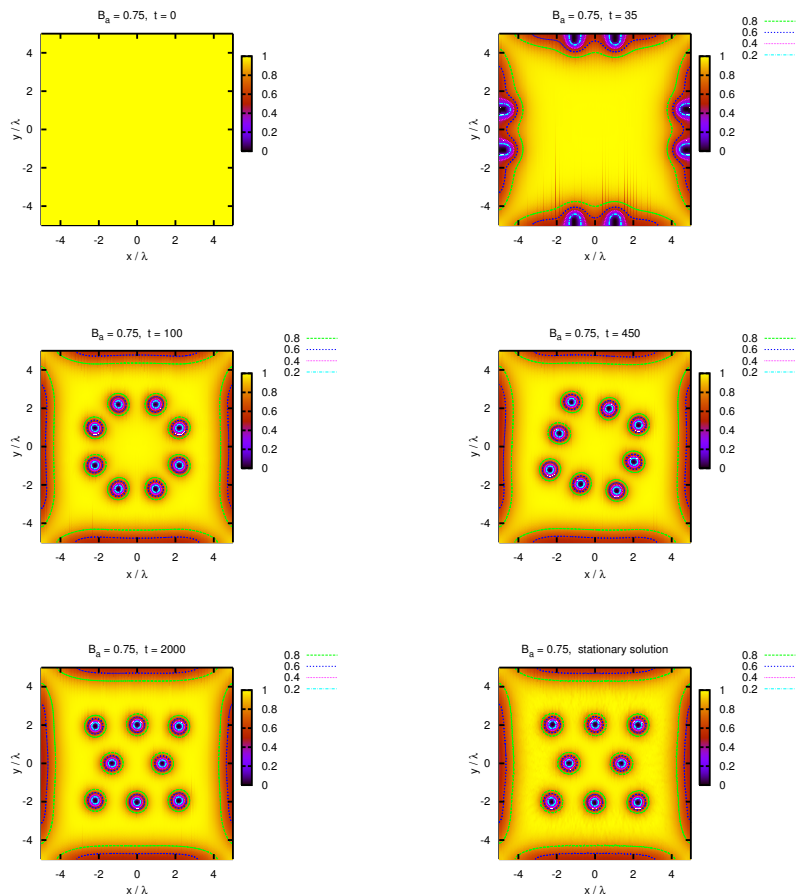


Figure 5.3: The Cooper pair density made with $\kappa = 1$ and $B_{az} = 0.4$.

lowered further, to a value of 0.05, the vortices are finally pushed out of the superconductor. The solutions for an applied magnetic field value of 0.65, 0.55 and 0.45 did also converge in the stationary equations. The solutions between 0.05 and 0.45 did not converge in the stationary solver, but due to lack of time, this issue was not investigated further.

Armed with the time-dependent equations, we can also try to solve more difficult geometries. This could for example be a rectangle, which are divided into two sections by making cuts at the centre. This can be seen in figure 5.4. With an applied magnetic field of $B_{az} = 0.75$, we see that 4 vortices enter the superconductor. This solution becomes stable at $t = 100$. If the magnetic field is increased with a interval of 0.05, nothing new happens until b_{az} reaches 0.9. At this point, 4 additional vortices enter the superconductors. This scenario can be seen on figure 5.5. After the four vortices has entered, the solution appears to have stabilised at $t = 100$, however at $t = 700$ the vortices begin

to move. They order each other differently, and the solution does not become stable before $t = 1500$.

We can calculate another solution with $B_{az} = 0.9$, by choosing the Meissner phase as initial condition. When this is done, only 6 vortices enter the superconductor. This simulation can be seen on 5.6. This scenario is another example of hysteresis. However, the time-dependent equations might not be completely accurate in this case. While the solution with 6 vortices converged in the stationary equations, the solution with 8 vortices did not. However, if this lack of convergence is due to using different finite elements remains to be investigated.

Using this geometry, we can try to create a solution, containing as many vortices as possible. This is done by beginning with an magnetic field value of $B_{az} = 1$, and then increasing it with an interval of 0.1. This was done, and some of the simulations are shown on figure 5.7. All simulations are made with the Meissner phase as initial condition. The solutions are calculated to $t = 250$, but since they might not be stable at this point, they will not be tested with the stationary equations. Notice the plot were the applied magnetic field is $B_{az} = 4$. On this plot, very little superconductivity remains. This is in agreement with the assumptions made in section 1.5.2, where a upper critical magnetic field value was calculated. Here we assumed, that just before superconductivity siezed to exist, the Cooper pair density was very low.

Another defect geometry geometry is investigated, which is a circle with a small triangular defect. If an applied magnetic field value of $B_{az} = 0.8$ is used, all vortices enter the superconductor through this defect. This is illustrated on figure 5.8. In this scenario, it takes a long time for the solution to stabilise, which happens at about $t = 15000$.

A different scenario is seen, if the applied magnetic field is $B_{az} = 0.9$. This simulation is shown on figure 5.9. While some of the vortices enter the superconductor through the defect, most of the vortices enter through the remaining boundary. The applied magnetic field is simply too strong for the superconductor to resist. This solution is also quite slow in reaching stability, however it is nothing in the range of the previous scenario. Movies of the two scenarios involving the circle, can be found on the attached CD.

The solutions found with the time-dependent algorithm has not truly converged for the stationary equations, as has been stated in this chapter. However, FEMLAB exhibits a very odd behaviour just before the solver terminates. The estimated error gets as low as 10^{-8} , however instead of declaring the solution for converged, it makes a huge stepsize and gets a new estimated error in the area 10^{20} . After this happens the solver declares that it is unable to solve the equations and terminates. However we suspect that the solution did actually converge, but for some reason FEMLAB fails to acknowledge this. With this odd behaviour of FEMLAB, we cannot know for sure if any of the stationary solutions found in this chapter also solves the stationary equations. This problem may be solved in future version of FEMLAB, but to know the true reason why the numerical method exhibits this behaviour, we would probably need to write our own software.

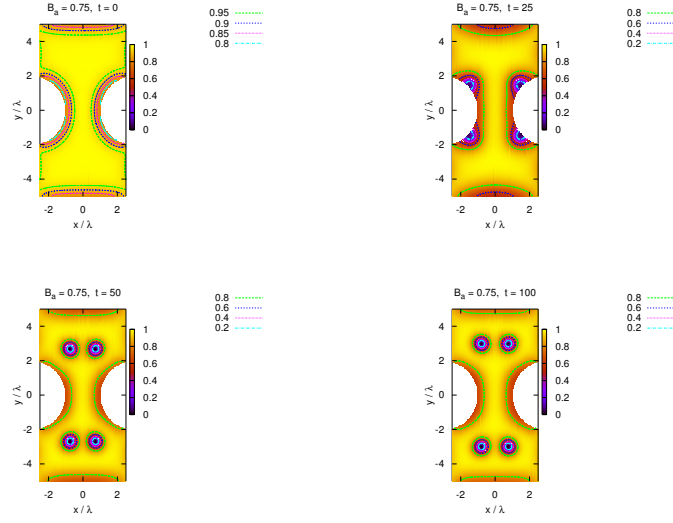


Figure 5.4: The Cooper pair density made with $\kappa = 4$ and $B_{az} = 0.75$.

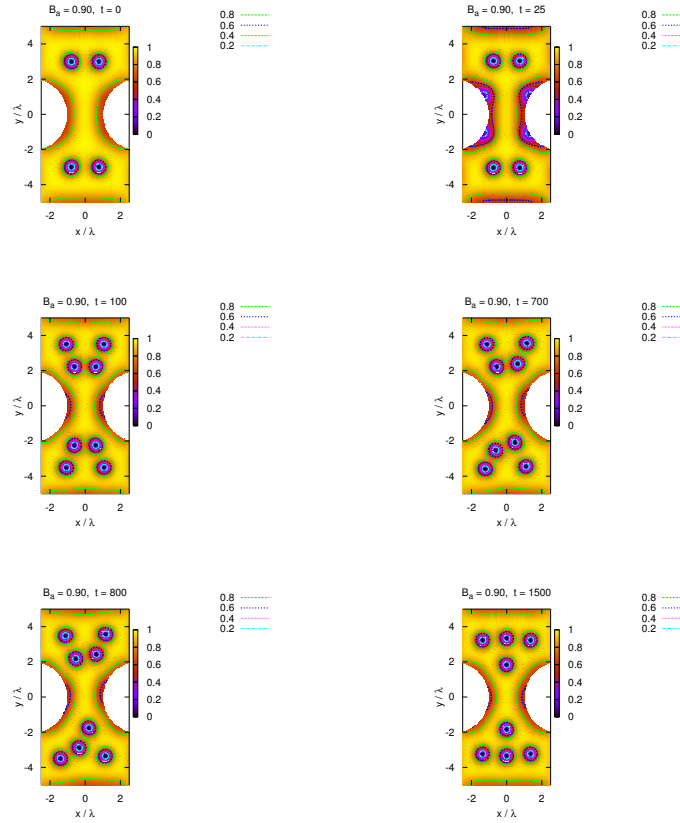


Figure 5.5: The Cooper pair density made with $\kappa = 4$ and $B_{az} = 0.90$.

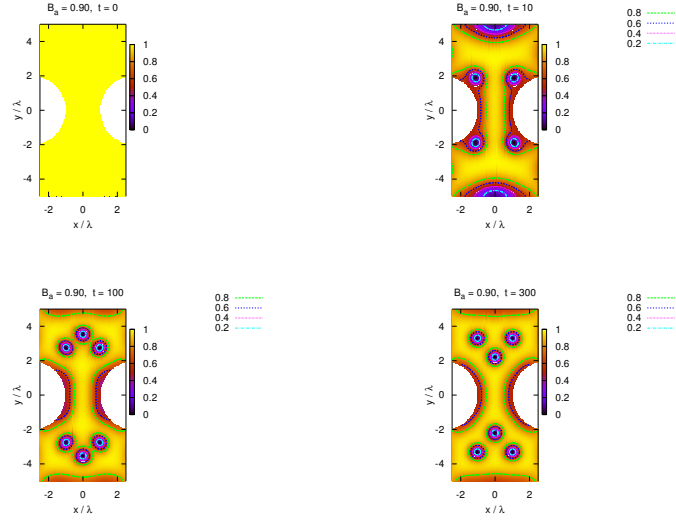


Figure 5.6: The Cooper pair density made with $\kappa = 4$ and $B_{az} = 0.90$.

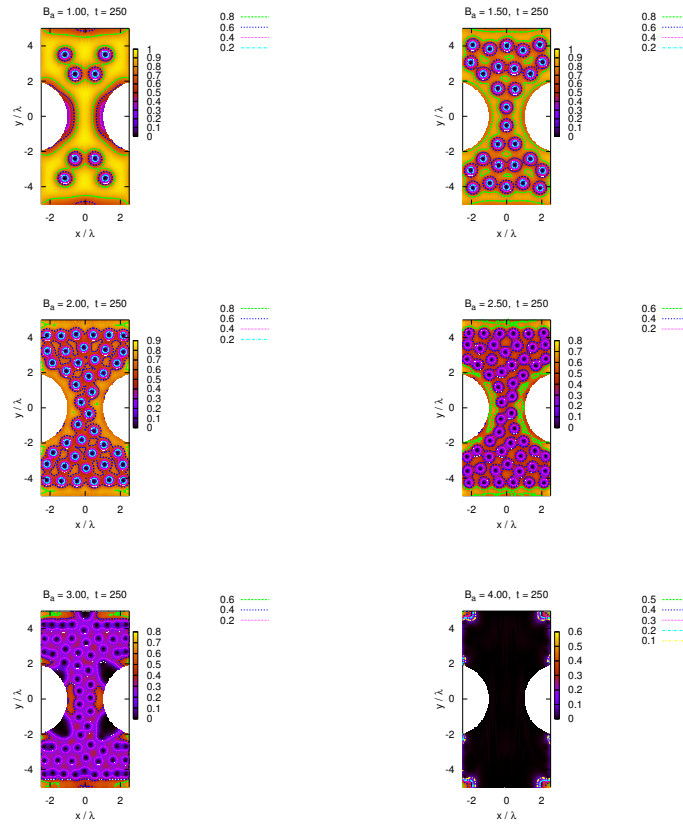


Figure 5.7: The Cooper pair density made with $\kappa = 4$ and different B_{az} .

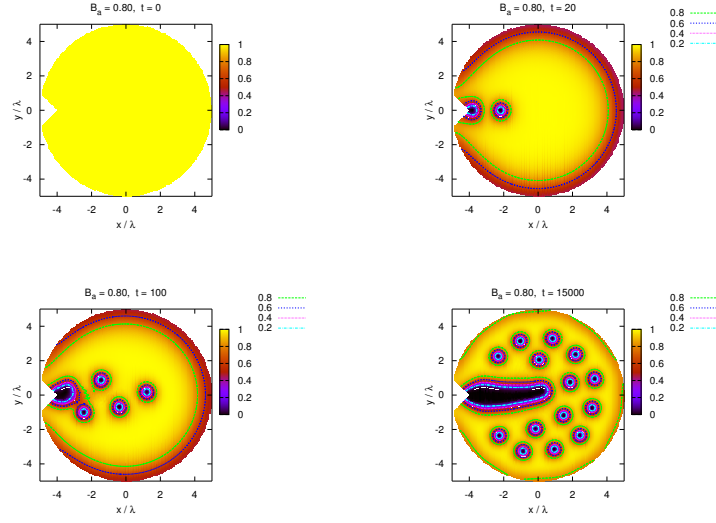


Figure 5.8: The Cooper pair density made with $\kappa = 4$ and $B_{az} = 0.80$.

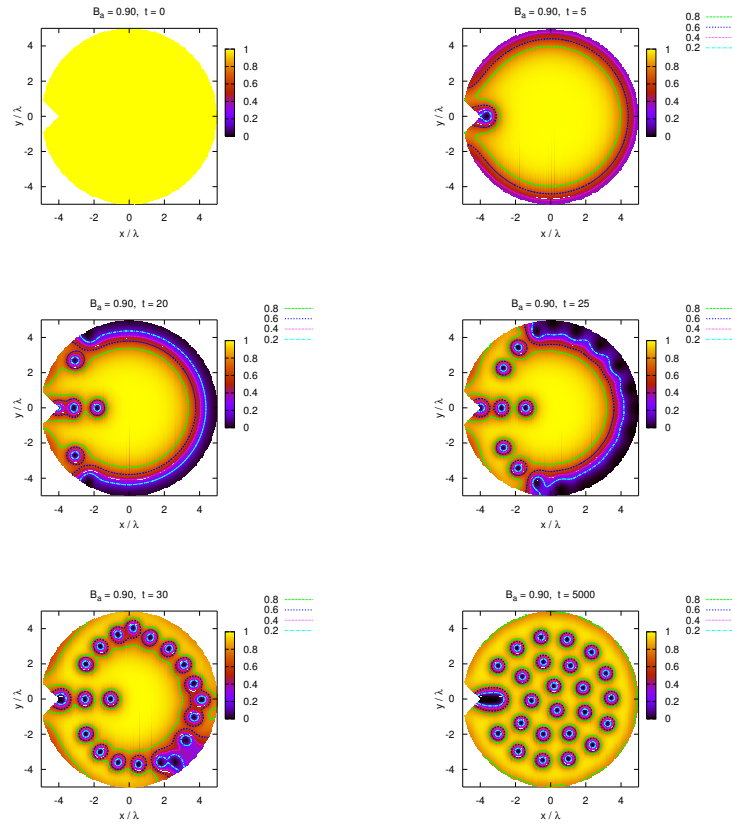


Figure 5.9: The Cooper pair density made with $\kappa = 4$ and $B_{az} = 0.90$.

Conclusion

We have solved the stationary Ginzburg–Landau equations for a square, both in the Meissner phase and vortex phase. Based on these solutions, we have concluded that the assumptions made in deriving the London penetration depth and Ginzburg–Landau coherence length are valid. Unfortunately, it turned out, that the possibilities to calculate multi-vortex systems using the stationary model is very limited. We were not able to give FEMLAB an initial guess, which was accurate enough in order for FEMLAB to converge. One can also question the usability of such a model. It is not very interesting to have a model, which can only be solved when we know exactly what to expect (that is, when we are able to provide an initial guess sufficiently close to the solution).

In order to eliminate these difficulties, the time–dependent model was used. This model pretty much solves everything. However, it became evident that not all solutions produced should be taken for valid solution. This was illustrated with a vortex solution, calculated for $\kappa = 0.4$.

When using a time–dependent model in search of an equilibrium state, one problem comes to mind; when has the solution computed truly stabilised? In order to answer this question, every solution calculated using the time–dependent model, was used as an initial guess to the stationary equations. On this account, the stationary equations are very usable, as they become the numerical proof of stable solutions.

In the process of seeking numerical proof that the calculated solution has indeed stabilised, a new problem arose. FEMLAB did not truly converge once. By this, we mean the very odd behaviour exhibited described in chapter 5. Due to this behaviour, just before the numerical algorithm terminated, is it very likely that the solution has converged. In order to be sure of this, additional numerical study must be made. Perhaps other basefunctions than Lagrange element are much better suited to solve the Ginzburg–Landau equations. Perhaps the solution to this problem, is to write a numerical solver, in order to get complete control of the algorithm, and thereby be able to customize it to this particular problem.

In spite of the difficulties with convergence, the time–dependent model has still provided insight on vortex dynamics and the existence of hysteresis. We have seen how defects in geometries can be used to control, or at least have an influence on where and how vortices enter a superconductor.

Appendices

Appendix A

Ginzburg–Landau in cgs

The Ginzburg–Landau equations often appear written in cgs (Gaussian) units. In this appendix both the stationary and the time-dependent equations is converted to SI units.

A.1 Stationary equations

In the textbook by Singer [14] the free energy density is written as

$$\mathcal{L}_{cgs} = \frac{\hbar^2}{2m} \left| \left(\nabla + \frac{2\pi}{\Phi_0} \mathbf{A} \right) \Psi \right|^2 - \alpha |\Psi|^2 + \frac{\beta}{2} |\Psi|^4 + \frac{|\mathbf{H} - \mathbf{B}|^2}{8\pi} \quad (\text{A.1})$$

This equation can be converted to SI units by using the conversion table in the book by Barone and Paterno [22]. The needed expressions are written in table A.1 and A.2. To begin with the first term is rewritten and Φ_0 is replaced as indicated in table A.1:

$$\begin{aligned} \frac{\hbar^2}{2m} \left| \left(\nabla + \frac{2\pi}{\Phi_0} \mathbf{A} \right) \Psi \right|^2 &= \frac{1}{2m} \left| \hbar \left(\nabla + \frac{2q\pi}{ch} \mathbf{A} \right) \Psi \right|^2 \\ &= \frac{1}{2m} \left| \left(\hbar \nabla - \frac{q}{c} \mathbf{A} \right) \Psi \right|^2 \end{aligned} \quad (\text{A.2})$$

Now q , c and \mathbf{A} is replaced as stated in table A.2:

$$\begin{aligned} \frac{1}{2m} \left| \left(\hbar \nabla - \frac{q}{c} \mathbf{A} \right) \Psi \right|^2 &= \frac{1}{2m} \left| \left(\hbar \nabla - \frac{\sqrt{\mu_0 \epsilon_0}}{\sqrt{4\pi \epsilon_0}} \sqrt{\frac{4\pi}{\mu_0}} q' \mathbf{A}' \right) \Psi \right|^2 \\ &= \frac{1}{2m} \left| \left(\hbar \nabla - q' \mathbf{A}' \right) \Psi \right|^2 \end{aligned} \quad (\text{A.3})$$

The last term in (A.1) is rewritten by inserting the SI expression for \mathbf{B} and \mathbf{H} :

$$\begin{aligned} \frac{|\mathbf{H} - \mathbf{B}|^2}{8\pi} &= \frac{\left| (\sqrt{4\pi \mu_0} \mathbf{H}' - \sqrt{\frac{4\pi}{\mu_0}} \mathbf{B}'_i) \right|^2}{8\pi} \\ &= \frac{1}{2\mu_0} |\mathbf{B}'_a - \mathbf{B}'_i|^2 \end{aligned} \quad (\text{A.4})$$

Quantity	Symbol	SI	cgs
Flux quantum	Φ_0	$\frac{h}{q}$	$\frac{hc}{q}$
Plank's constant divided by 2π	\hbar	$\frac{h}{2\pi}$	$\frac{h}{2\pi}$

Table A.1: Abbreviated symbol table from Barone and Paterno[22]. Before converting a formula the above symbols must be replaced by the expression in the cgs column. The expressions in the SI column are for formulas given in SI units.

where \mathbf{B}_i is the magnetic field inside the superconducting sample and \mathbf{B}_a is the applied magnetic field. In the last line the relation from electromagnetism $\mathbf{B} = \mu_0\mathbf{H}$ is used. By inserting the two converted expressions in (A.1), equation (1.13) from chapter 1 is obtained.

A.2 Time-dependent equations

In chapter 4 the time-dependent equations are taken from the article by Kaper et al [20]. In the paper they are written as

$$\begin{aligned} \frac{\hbar^2}{2mD} \left(\frac{\partial}{\partial t} + i\frac{q}{\hbar}\Phi \right) \Psi &= -\frac{\delta\mathcal{L}_{tcgs}}{\delta\Psi^*} \\ \frac{\sigma}{c} \left(\frac{1}{c} \frac{\partial\mathbf{A}}{\partial t} + \nabla\Phi \right) &= -\frac{\delta\mathcal{L}_{tcgs}}{\delta\mathbf{A}} - \frac{1}{4\pi} \nabla \times \nabla \times \mathbf{A} \end{aligned} \quad (\text{A.5})$$

and \mathcal{L}_{tcgs} is defined as

$$\mathcal{L}_{tcgs} = \alpha|\Psi|^2 + \frac{1}{2}\beta|\Psi|^4 + \frac{1}{2m} \left| \left(\frac{\hbar}{i} - \frac{q}{c}\mathbf{A} \right) \Psi \right|^2 \quad (\text{A.6})$$

First notice that the above definition of \mathcal{L}_{tcgs} is similar to (A.1). In chapter 1 the coefficients were investigated, and the sign of α depends on whether α is chosen to be positive or negative in the superconducting state. In the discussion in Singers textbook, α is chosen to be positive when $T < T_c$ and in the paper by Kaper [20] α is chosen to be negative when $T < T_c$, so the sign of α in (A.6) must be changed. A new \mathcal{L} is now defined as

$$\mathcal{L}_{tcgs1} = -\alpha|\Psi|^2 + \frac{1}{2}\beta|\Psi|^4 + \frac{1}{2m} \left| \left(\frac{\hbar}{i} - \frac{q}{c}\mathbf{A} \right) \Psi \right|^2 \quad (\text{A.7})$$

Besides the sign of α the energy contribution from the magnetic field is absent in (A.6) compared to equation (A.1). In equation (A.5) the contribution from

Quantity	SI	cgs
Charge, current density	$\frac{1}{\sqrt{4\pi\epsilon_0}}(q, \mathbf{J})$	(q, \mathbf{J})
Conductivity	$\frac{\sigma}{4\pi\epsilon_0}$	σ
Electric potential	$\sqrt{4\pi\epsilon_0}\Phi$	Φ
Magnetic induction	$\sqrt{\frac{4\pi}{\mu_0}}\mathbf{B}$	\mathbf{B}
Magnetic field	$\sqrt{4\pi\mu_0}\mathbf{H}$	\mathbf{H}
Vector Potential	$\sqrt{\frac{4\pi}{\mu_0}}\mathbf{A}$	\mathbf{A}
Velocity of light	$\frac{1}{\sqrt{\mu_0\epsilon_0}}$	c

Table A.2: Abbreviated conversion table from Barone and Paterno[22]. Each entry expresses the relation between a quantity in formulas written in cgs and SI units. To convert an equation from cgs to SI, every quantity in the cgs column is replaced by the equivalent expression in the SI column.

\mathcal{L}_{tcgs} is written as variational derivatives. Calculating the difference yields

$$\begin{aligned}
-\frac{\delta(\mathcal{L}_{cgs} - \mathcal{L}_{tcgs1})}{\delta\Psi^*} &= 0 \\
-\frac{\delta(\mathcal{L}_{cgs} - \mathcal{L}_{tcgs1})}{\delta\mathbf{A}} &= \frac{1}{4\pi}\nabla \times (\mathbf{H} - \nabla \times \mathbf{A})
\end{aligned}
\tag{A.8}$$

The equations are obtained by using the same techniques as used in section 1.3, where the Ginzburg Landau equations was derived. If we assume that the external magnetic field is constant, then the difference of using \mathcal{L}_{cgs} compared to \mathcal{L}_{tcgs1} is $-\frac{1}{4\pi}\nabla \times \nabla \times \mathbf{A}$. Based on this information a new model equivalent to (A.5) which uses \mathcal{L}_{cgs} can be defined as

$$\begin{aligned}
\frac{\hbar^2}{2mD} \left(\frac{\partial}{\partial t} + i\frac{q}{\hbar}\Phi \right) \Psi &= -\frac{\delta\mathcal{L}_{cgs}}{\delta\Psi^*} \\
\frac{\sigma}{c} \left(\frac{1}{c} \frac{\partial\mathbf{A}}{\partial t} + \nabla\Phi \right) &= -\frac{\delta\mathcal{L}_{cgs}}{\delta\mathbf{A}}
\end{aligned}
\tag{A.9}$$

To convert (A.9) to SI units table A.2 is used. The first equation of (A.9) is converted by inserting the expressions for q and Φ , however the multipliers cancel out so the equation is the same in SI units. To convert the second equation we need to look at $\delta\mathbf{A}$, which is defined in (1.15) as

$$\delta\mathbf{A} = \frac{\partial\mathbf{A}}{\partial\varepsilon}\varepsilon
\tag{A.10}$$

We see that $\delta\mathbf{A}$ must be converted as it was just a vector potential \mathbf{A} . Making the proper replacements yields

$$\begin{aligned} \frac{\sqrt{\mu_0\epsilon_0}}{4\pi\epsilon_0}\sigma' \left(\sqrt{\mu_0\epsilon_0}\sqrt{\frac{4\pi}{\mu_0}}\frac{\partial\mathbf{A}'}{\partial t} + \sqrt{4\pi\mu_0}\nabla\Phi' \right) &= -\sqrt{\frac{\mu_0}{4\pi}}\frac{\delta\mathcal{L}}{\delta\mathbf{A}'} \quad \Leftrightarrow \\ \sigma' \left(\frac{\partial\mathbf{A}'}{\partial t} + \nabla\Phi' \right) &= -\frac{\delta\mathcal{L}}{\delta\mathbf{A}'} \end{aligned} \quad (\text{A.11})$$

To summarise the time-dependent Ginzburg–Landau model in SI units is

$$\begin{aligned} \frac{\hbar^2}{2mD} \left(\frac{\partial}{\partial t} + i\frac{q}{\hbar}\Phi \right) \Psi &= -\frac{\delta\mathcal{L}}{\delta\Psi^*} \\ \sigma \left(\frac{\partial\mathbf{A}}{\partial t} + \nabla\Phi \right) &= -\frac{\delta\mathcal{L}}{\delta\mathbf{A}} \end{aligned} \quad (\text{A.12})$$

where \mathcal{L} is equation (1.13) defined in chapter 1 as

$$\mathcal{L} = \frac{1}{2m} \left| \left(\frac{\hbar}{i}\nabla - q\mathbf{A} \right) \Psi \right|^2 - \alpha|\Psi|^2 + \frac{\beta}{2}|\Psi|^4 + \frac{1}{2\mu_0}|\mathbf{B}_a - \mathbf{B}_i|^2 \quad (\text{A.13})$$

Appendix B

Gauge invariance

B.1 Proof for stationary equations

It was written in section 2.2 that the stationary Ginzburg–Landau equations are gauge invariant under the linear transformation G_χ defined as

$$G_\chi(\Psi, \mathbf{A}) = (\Psi', \mathbf{A}') \quad (\text{B.1})$$

where

$$\Psi' = \Psi e^{i\kappa\chi}, \quad \mathbf{A}' = \mathbf{A} + \nabla\chi \quad (\text{B.2})$$

and $\chi = \chi(x, y, z)$. To prove the gauge invariance the equations normalised with λ_L are used

$$-\frac{1}{\kappa^2}\nabla^2\Psi + i\frac{2}{\kappa}\mathbf{A} \cdot \nabla\Psi + \mathbf{A} \cdot \mathbf{A}\Psi - \Psi + |\Psi|^2\Psi = 0 \quad \text{in } \Omega \quad (\text{B.3a})$$

$$\left(\frac{i}{\kappa}\nabla\Psi + \mathbf{A}\Psi\right) \cdot \mathbf{n} = 0 \quad \text{on } \partial\Omega \quad (\text{B.3b})$$

$$\frac{i}{2\kappa}(\Psi\nabla\Psi^* - \Psi^*\nabla\Psi) - \mathbf{A}|\Psi|^2 = \mathbf{j}_s \quad \text{in } \Omega \quad (\text{B.3c})$$

$$A_{y,x} - A_{x,y} = B_{az} \quad \text{on } \partial\Omega \quad (\text{B.3d})$$

The gauge invariance is proved by making the transformations (B.2) in (B.3), and if the transformed equations formally equals the original equations, then the gauge invariance is proved. In order to calculate the transformed equations the following relations will be needed. The gradient of Ψ'

$$\nabla(\Psi' e^{-i\kappa\chi}) = e^{-i\kappa\chi}(\nabla\Psi' - i\kappa\Psi'\nabla\chi) \quad (\text{B.4})$$

The Laplace operator on Ψ' is also needed which is

$$\nabla^2(\Psi' e^{-i\kappa\chi}) = \nabla \cdot \nabla(\Psi' e^{-i\kappa\chi}) \quad (\text{B.5})$$

By using the calculated expression for $\nabla\Psi$ we obtain

$$\nabla^2(\Psi' e^{-i\kappa\chi}) = e^{-i\kappa\chi}(\nabla^2\Psi' - i\kappa\Psi'\nabla^2\chi - \kappa^2\Psi'\nabla\chi\nabla\chi - 2i\kappa\nabla\Psi'\nabla\chi) \quad (\text{B.6})$$

The inner product $\mathbf{A} \cdot \mathbf{A}$ also needs to be calculated

$$\mathbf{A} \cdot \mathbf{A} = \mathbf{A}' \cdot \mathbf{A}' + \nabla\chi \nabla\chi - 2\mathbf{A}' \cdot \nabla\chi \quad (\text{B.7})$$

And finally the rotation of \mathbf{A} becomes

$$\nabla \times \mathbf{A} = \nabla \times (\mathbf{A}' - \nabla\chi) = \nabla \times \mathbf{A}' \quad (\text{B.8})$$

It is used that the curl of ∇f vanishes for any function f .

First equation (B.3a) is transformed. Before this is done the equation is reorganised by writing out the brackets

$$-\frac{1}{\kappa^2} \nabla^2 \Psi + \mathbf{A} \cdot \mathbf{A} \Psi + \frac{i}{\kappa} (2\mathbf{A} \cdot \nabla \Psi + \Psi \nabla \cdot \mathbf{A}) - \Psi + |\Psi|^2 \Psi = 0 \quad (\text{B.9})$$

If the transformations are made we get

$$\begin{aligned} e^{-i\kappa\chi} \left(-\frac{1}{\kappa^2} \nabla^2 \Psi' + \frac{i}{\kappa} \Psi' \nabla^2 \chi + \Psi' \nabla \chi \nabla \chi + \frac{2i}{\kappa} \nabla \Psi' \nabla \chi \right. \\ \left. + \mathbf{A}' \cdot \mathbf{A}' \Psi' + \Psi' \nabla \chi \nabla \chi - 2\Psi' \mathbf{A}' \cdot \nabla \chi \right. \\ \left. \frac{2i}{\kappa} \mathbf{A}' [\nabla \Psi' - i\kappa \Psi' \nabla \chi] - \frac{2i}{\kappa} \nabla \chi [\nabla \Psi' - i\kappa \Psi' \nabla \chi] + \frac{i}{\kappa} \Psi' \nabla [\mathbf{A}' - \nabla \chi] \right. \\ \left. - \Psi' + |\Psi'|^2 \Psi' \right) = 0 \end{aligned} \quad (\text{B.10})$$

The first line corresponds to the first term transformed, the second line to the second term and so on. We see that all the terms which contain χ cancel each other out, so by removing all terms with χ we get

$$e^{-i\kappa\chi} \left(-\frac{1}{\kappa^2} \nabla^2 \Psi' + \mathbf{A}' \cdot \mathbf{A}' \Psi' + \frac{i}{\kappa} (2\mathbf{A}' \cdot \nabla \Psi' + \Psi' \nabla \cdot \mathbf{A}') - \Psi' + |\Psi'|^2 \Psi' \right) = 0 \quad (\text{B.11})$$

If the equation is multiplied by $e^{i\kappa\chi}$ we obtain an equation which is formally equal to (B.3a) and therefore the first Ginzburg–Landau equation is gauge invariant. If the transformations are inserted into the second Ginzburg–Landau equation (B.3c) we obtain

$$\begin{aligned} \frac{i}{2\kappa} (\Psi' e^{-i\kappa\chi} e^{i\kappa\chi} [\nabla \Psi'^* + i\kappa \Psi'^* \nabla \chi] - \Psi'^* e^{i\kappa\chi} e^{-i\kappa\chi} [\nabla \Psi' - i\kappa \Psi' \nabla \chi]) \\ - \mathbf{A}' |\Psi'|^2 + \nabla \chi |\Psi'|^2 + \nabla \times \mathbf{B}_a = \nabla \times \nabla \times (\mathbf{A}' - \nabla \chi) \end{aligned} \quad (\text{B.12})$$

Again all the terms which contain χ cancel out and the resulting equation is

$$\frac{i}{2\kappa} (\Psi' \nabla \Psi'^* - \Psi'^* \nabla \Psi') - \mathbf{A}' |\Psi'|^2 + \nabla \times \mathbf{B}_a = \nabla \times \nabla \times \mathbf{A}' \quad (\text{B.13})$$

which is formally equivalent to the original equation. If the gauge transformation is made on the boundary conditions we get

$$e^{-i\kappa\chi} \left(\frac{i}{\kappa} [\nabla \Psi' - i\kappa \Psi' \nabla \chi] + \mathbf{A}' \Psi' - \Psi' \nabla \chi \right) \cdot \mathbf{n} = 0 \quad (\text{B.14})$$

The terms with χ cancel out and multiplying with $e^{i\kappa\chi}$ the resulting equation is formally equivalent to the original boundary condition. The second boundary condition is also gauge invariant as the curl of \mathbf{A} is equal to the curl of \mathbf{A}' . Hence the equations (B.3) are gauge invariant under the transformation written in (B.2).

B.2 Proof for time-dependent equations

The time-dependent equations are gauge invariant under the transformation

$$G_\chi(\Psi, \mathbf{A}, \Phi) = (\Psi', \mathbf{A}', \Phi') \quad (\text{B.15})$$

where

$$\Psi' = \Psi e^{i\kappa\chi}, \quad \mathbf{A}' = \mathbf{A} + \nabla\chi, \quad \Phi' = \Phi - \frac{\partial\chi}{\partial t} \quad (\text{B.16})$$

To prove the gauge invariance the transformations (B.16) are made in

$$\left(\frac{\partial}{\partial t} + i\kappa\Phi \right) \Psi = - \left(\frac{i}{\kappa} \nabla + \mathbf{A} \right)^2 \Psi + \Psi - |\Psi|^2 \Psi \quad (\text{B.17a})$$

$$\sigma \left(\frac{\partial \mathbf{A}}{\partial t} + \nabla\Phi \right) = \frac{1}{2i\kappa} (\Psi^* \nabla \Psi - \Psi \nabla \Psi^*) - |\Psi|^2 \mathbf{A} - \nabla \times \nabla \times \mathbf{A} \quad (\text{B.17b})$$

with the boundary conditions

$$\left(\frac{i}{\kappa} \nabla \Psi + \mathbf{A} \Psi \right) \cdot \mathbf{n} = 0 \quad \text{on } \partial\Omega \quad (\text{B.18a})$$

$$\mathbf{B}_a = \mathbf{B}_i \quad \text{on } \partial\Omega \quad (\text{B.18b})$$

$$\left(\frac{\partial \mathbf{A}}{\partial t} + \nabla\Phi \right) \cdot \mathbf{n} = 0 \quad \text{on } \partial\Omega \quad (\text{B.18c})$$

From the proof in B.1 we know that the boundary conditions (B.18a) and (B.18b) are gauge invariant. We also know that by using the gauge transformation the right hand side of (B.17a) has the multiplier $e^{-i\kappa\chi}$. The right hand side of (B.17b) is unchanged. To prove gauge invariance only the left hand sides of (B.17) needs to be calculated. The left hand side of (B.17a) is

$$\left(\frac{\partial}{\partial t} + i\kappa\Phi \right) \Psi = \left(\frac{\partial}{\partial t} + i\kappa \left[\Phi' + \frac{\partial\chi}{\partial t} \right] \right) \Psi' e^{-i\kappa\chi} \quad (\text{B.19})$$

The time-derivative are calculated as

$$\frac{\partial}{\partial t} \Psi' e^{-i\kappa\chi} = e^{-i\kappa\chi} \left(\frac{\partial \Psi'}{\partial t} - i\kappa \Psi' \frac{\partial\chi}{\partial t} \right) \quad (\text{B.20})$$

and we see that the terms having χ cancels out. The resulting equation is

$$\left(\frac{\partial}{\partial t} + i\kappa\Phi \right) \Psi = e^{-i\kappa\chi} \left(\frac{\partial}{\partial t} + i\kappa\Phi' \right) \Psi' \quad (\text{B.21})$$

Since the transformed left hand side and right hand side of (B.17a) have the same multiplier it is removed from the equation. When this is done we obtain (B.17a). The left hand side of (B.17b) becomes

$$\sigma \left(\frac{\partial \mathbf{A}}{\partial t} + \nabla\Phi \right) = \sigma \left(\frac{\partial(\mathbf{A}' - \nabla\chi)}{\partial t} + \nabla \left[\Phi' + \frac{\partial\chi}{\partial t} \right] \right) \quad (\text{B.22})$$

$$(\text{B.23})$$

Since the order of differentiation does not matter, then left hand side of (B.17b) remains unchanged by the gauge transformation, hence it is proved that (B.17) is gauge invariant. Having shown that the left hand side of (B.17b) is unchanged, it is clear that the third boundary condition (B.18c) is also gauge invariant.

Appendix C

MATLAB Code

In this appendix the MATLAB code which solves both the stationary and time-dependent equations is found. Five MATLAB functions are made which are

- `GLE.m` The implementation of the stationary Ginzburg–Landau equations.
- `glestart.m` The script that calls `GLE.m` with the proper geometry and afterwards plots the solution by using the constructed `plotter.m`. This script is used to construct all the figures made in chapter 3.
- `TDGL.m` This script is the implementation of the time-dependent Ginzburg–Landau equations.
- `tdglstart.m` This function is very similar to `glestart.m`. The script calls the time-dependent solver `TDGL.m` and optionally tries to use the output as initial guess in the stationary solver. This script was used to make all the simulations in chapter 5.
- `plotter.m` This script extracts the calculated solution from the FEMLAB structure and stores the result on disk. The results are datafiles suitable for Gnuplot.

In order for any of these scripts to work MATLAB must be able to use FEMLAB functions. In order to achieve this on a unix system, simply type `femlab matlab` in a console. Then the interactive FEMLAB launches and the console becomes a MATLAB prompt. The interactive FEMLAB should be closed and MATLAB can now access all the FEMLAB functions.

Only `glestart.m` and `glstart.m` are called by the user. The function `tdglstart` is defined as

```
function [varargout] = tdglstart(usergeom, Ba, fem,  
                                solform, kappa, vortex, time, glerun)
```

Example use is

```
[tdgl1ba7m gleba7] = tdglstart(3, 0.7, 0, 0, 4, 0, [0:1:100], 0);
```

The above command calls the time-dependent equations for geometry number 3 with an applied magnetic field value of 0.7. The solver integrates from $t = 0$ to 100 and stores the solutions with an interval of 1. This solution is stored in

tdglba7m. Having calculated the solution to $t = 100$ we can try to make this solution converge in the stationary equations. This is done with the command

```
[tdglba7t100 gleba7] =
    tdglstart(3, 0.7, tdglba7m, 1, 4, 0, [100:1000:10100], 1);
```

With this command the previously calculated solution at $t = 100$ is used and solved to $t = 10100$. This is done to make sure the found solutions is stabil, therefore we only store the solution with an interval of 1000. When the solution at $t = 10100$ is found, the solver uses this as an initial guess to the stationary equations.

In the MATLAB scripts A_x equals u_3 and A_y equals u_4 . When writing u_3y it means $A_{x,y}$.

C.1 GLE.m

```

1  % GLE - Steady state Ginzburg-Landau equations
2  % geom = geometry to solve.
3  % bndind = boundary vector for equ.bnd.ind
4  % initsol = Initial solution
5  % solform = 0 or 1. If 0 the solution is an formal initial solution. If 1
6  % the solution is given as a fem structure.
7  % mode = 'lambda' or 'xi'. If lambda, the equations normalized as x' =
8  % x/lambda id used. If xi, the other equations are used.
9  % kappa = kappa, the ginzburg landau parameter
10 % Ba = applied magnetic field
11 % geomid = Mesh generation parameter. Some of the defect geometries needs
12 % speciel refinement.
13 % Hauto = FEMLAB mesh variable. See manual for details.
14 function [vargout] = GLE(geom, bndind, initsol, solform,
15                        mode, kappa, Ba, geomid,Hauto)
16
17 %Set geometry
18 fem.draw=struct('s',geom);
19 fem.geom=geomcsg(fem);
20
21 % Set appliaction to PDE General form.
22 clear appl
23 appl.mode.class = 'F1PDEG';
24
25 % Set variables.
26 appl.dim = {'u1','u2','u3','u4','u5','u1_t','u2_t','u3_t','u4_t','u5_t'};
27
28 % Set variables as linear lagrange
29 appl.shape = {'shlag(1,''u1'')','shlag(1,''u2'')','shlag(1,''u3'')
30              ','shlag(1,''u4'')','shlag(1,''u5'')'};
31
32 appl.gporder = 2;
33 appl.cporder = 1;
34
35 % Set boundary conditions
36 appl.assignsuffix = '_g';
37 clear bnd
38 bnd.type = 'neu'; % Neumann conditions
39 bnd.ind = bndind;
40 appl.bnd = bnd;
41 clear equ
42
43 if solform==0
44     % Set initial solution

```

```

44     equ.init = initsol;
45 end
46
47 if strcmp(mode,'xi') == 1
48     equ.f = {...
49         'u3.*u1x+u4.*u1y+(u3.^2+u4.^2).*u2-u2+(u1.^2+u2.^2).*u2';...%F1
50         'u3.*u2x+u4.*u2y-(u3.^2+u4.^2).*u1+u1-(u1.^2+u2.^2).*u1';...%F2
51         '1./(kappa.^2).*(u2.*u1x-u1.*u2x+(u1.^2+u2.^2).*u3)';...%F3
52         '1./(kappa.^2).*(u2.*u1y-u1.*u2y+(u1.^2+u2.^2).*u4)';...%F4
53         'u5'}; %F5
54     equ.ga = {...
55         {'u2x-u3.*u1';'u2y-u4.*u1'};...%Gamma1
56         {'-u1x-u3.*u2';'-u1y-u4.*u2'};...%Gamma2
57         {'u3x+u4y';'-u4x+u3y+Ba'};...%Gamma3
58         {'u4x-u3y-Ba';'u3x+u4y'};...%Gamma4
59         {'0';'0'}}; %Gamma5
60 elseif strcmp(mode,'lambda') == 1
61     equ.f = {...
62         'kappa.*(u3.^2+u4.^2).*u2+u3.*u1x+u4.*u1y-kappa.*u2
63             +kappa.*(u1.^2+u2.^2).*u2';...%F1
64         '-kappa.*(u3.^2+u4.^2).*u1+u3.*u2x+u4.*u2y+kappa.*u1
65             -kappa.*(u1.^2+u2.^2).*u1';...%F2
66         '(1./kappa).*(u2.*u1x-u1.*u2x)+(u1.^2+u2.^2).*u3';...%F3
67         '(1./kappa).*(u2.*u1y-u1.*u2y)+(u1.^2+u2.^2).*u4';...%F4
68         'u5'}; %F5
69     equ.ga = {...
70         {'u2x./kappa-u3.*u1';'u2y./kappa-u4.*u1'};...%Gamma1
71         {'-u1x./kappa-u3.*u2';'-u1y./kappa-u4.*u2'};...%Gamma2
72         {'u3x+u4y';'-u4x+u3y+Ba'};...%Gamma3
73         {'u4x-u3y-Ba';'u3x+u4y'};...%Gamma4
74         {'0';'0'}}; %Gamma5
75 else
76     %Abort
77     error('Unknown mode!')
78 end
79
80 % Construct fem structure
81 equ.ind = [1];
82 appl.equ = equ;
83 fem.appl{1} = appl;
84 fem.border = 1;
85
86 % insert constants
87 fem.const={'Ba',sprintf('%d',Ba),'kappa',sprintf('%d',kappa)};
88
89 % Multiphysics
90 fem=multiphysics(fem);
91
92 % Initialize mesh
93 fem.mesh=meshinit(fem,'Hauto','Hauto');
94
95 fem.xmesh=meshextend(fem);
96
97 if solform == 0
98     % Evaluate initial value
99     init = assemnit(fem);
100 elseif solform == 1
101     % Mapping current solution to extended mesh
102     init = assemnit(fem,'init',initsol.sol,'xmesh',initsol.xmesh);
103 end
104
105 % Update model

```

```

106 fem.sol = init;
107
108 %Solve problem
109 fem.sol=femlin(fem, ...
110   'init',init, ...
111   'HnLin','on',...
112   'solcomp',{'u1','u2','u3','u4','u5'}, ...
113   'outcomp',{'u1','u2','u3','u4','u5'}, ...
114   'Ntol',1e-6,...
115   'maxiter',1000);
116
117 vargout = fem;

```

C.2 glestart.m

```

1 % function [varargout] = tdglstart(usergeom, Ba, fem, solform, kappa,
2                                     vortex, time, glerun)
3 function [varargout] = tdglstart(usergeom, Ba, fem, solform, kappa,
4                                     vortex, time, glerun)
5
6 % Geometry
7 % -----
8 % 1 = Square
9 % 2 = Square with link
10 % 3 = Circle
11 % 4 = Circle with defect
12 % 5 = Triangle
13
14 % Set mode
15 % mode = 'xi';
16 mode = 'lambda';
17
18 % Set variables.
19 if time == 0
20     time = [0:20:5000];
21 end
22 if kappa == 0
23     kappa = 4;
24 end
25
26 sigma = 1;
27 if Ba == 0
28     Ba = 0.1;
29 end
30 tdglH = 2;
31 gleH = 2;
32
33 % if solform = 1 then a femlab structure is passed as init
34 if solform == 1
35     init = fem;
36 else
37     if vortex == 1
38         %one Vortex at center
39         init = {'x./sqrt(x.^2+y.^2)';'y./sqrt(x.^2+y.^2)';0;0;0;0;0;0};
40     else
41         % No Vortex, Meissner phase
42         init = {'sqrt(0.5)';'sqrt(0.5)';0;0;0;0;0;0};
43     end
44 end
45

```

```

46 clear geom
47 switch usergeom
48     case 1
49         % A square
50         g1=rect2(10,10,'base','corner','pos',[-5,-5]);
51         geom.objs={g1};
52         bndind = [1,1,1,1];
53         diradd = 'square';
54         plotgeom = [-5,5,-5,5];
55     case 2
56         % Rect with defects as link.
57         % Geometry
58         g1=rect2(6,10,'base','corner','pos',[-3,-5]);
59         g2=ellip2(2,2,'base','center','pos',[-3,0]);
60         g3=ellip2(2,2,'base','center','pos',[3,0]);
61         g4=geomcomp({g1,g2,g3},'ns',{g1','g2','g3}','sf','g1-g2-g3',
62                     'edge','none');
63         bndind = [1,1,1,1,1,1,1,1,1,1];
64         geom.objs={g4};
65         diradd = 'squarelink';
66         plotgeom = [-2.5,2.5,-5,5];
67     case 3
68         % Circle with r=5 and x and y direction, with center at 0,0
69         g1=ellip2(5,5,'base','center','pos',[0,0]);
70         geom.objs={g1};
71         bndind = [1,1,1,1];
72         diradd = 'circle';
73         plotgeom = [-5,5,-5,5];
74     case 4
75         % A circle with a defect
76         % Circle with r=5 and x and y direction, with center at 0,0
77         g1=ellip2(5,5,'base','center','pos',[0,0]);
78         carr={curve2([-5,-4],[1,0],[1,1]), ... %Line from (-5,1)->(-4,0)
79               curve2([-4,-5],[0,-1],[1,1]), ...%Line from (-4,0)->(-5,-1)
80               curve2([-5,-5],[-1,1],[1,1])};%Line from (-5,1)->(-5,1)
81         g2=geomcoerce('solid',carr);%Make the geom solid
82         g3=geomcomp({g1,g2},'ns',{g1','g2}','sf','g1-g2','edge','none');
83         geom.objs={g3};
84         bndind = [1,1,1,1,1,1];
85         diradd = 'circledef';
86         plotgeom = [-5,5,-5,5];
87     case 5
88         % Triangle
89         carr={curve2([-5,0],[-4,6],[1,1]), ...
90               curve2([0,5],[6,-4],[1,1]), ...
91               curve2([6,-6],[-4,-4],[1,1])};
92         g1=geomcoerce('solid',carr);
93         bndind = [1,1,1];
94         geom.objs={g1};
95         diradd = 'triangle';
96         plotgeom = [-5,5,-4,6];
97     otherwise
98         error('Unknown geometry!')
99 end
100
101 geom.name={'R1'};
102 geom.tags={'g1'};
103
104 sprintf('TDGL for BA = %d',Ba)
105
106 [tdglfem] = TDGL(geom, bndind, init, solform, time, mode, kappa, Ba,
107                 sigma, usergeom, tddlH);

```

```

108
109 % Plot solution
110 dir = strcat('../data/',mode, '/', diradd, '/tdgl_');
111 plotter(tdglfem,time,mode,Ba,kappa,201,201,51,21,plotgeom,dir);
112 if glerun == 1
113     sprintf('GLE for BA = %d',Ba)
114     [glefem] = GLE(geom, bndind, tdglfem, 1, mode, kappa, Ba,
115                 usergeom, gleH);
116     dir = strcat('../data/',mode, '/', diradd, '/gle_');
117     plotter(glefem,0,mode,Ba,kappa,201,201,51,31,plotgeom,dir);
118 else
119     glefem = 0;
120 end
121
122 varargout{1} = tdglfem;
123 varargout{2} = glefem;

```

C.3 TDGL.m

```

1 % GLE - Steady state Ginzburg-Landau equations
2 % geom = geometry to solve.
3 % bndind = boundary vector for equ.bnd.ind
4 % initsol = Initial solution
5 % solform = 0 or 1. If 0 the solution is an formal initial solution. If 1
6 % the solution is given as a fem structure.
7 % mode = 'lambda' or 'xi'. If lambda, the equations normalized as x' =
8 % x/lambda id used. If xi, the other equations are used.
9 % kappa = kappa, the ginzburg landau parameter
10 % Ba = applied magnetic field
11 % geomid = Mesh generation parameter. Some of the defect geometries needs
12 % speciel refinement.
13 % Hauto = FEMLAB mesh variable. See manual for details.
14 function [vargout] = GLE(geom, bndind, initsol, solform, mode,
15                         kappa, Ba, geomid,Hauto)
16
17 %Set geometry
18 fem.draw=struct('s',geom);
19 fem.geom=geomcsg(fem);
20
21 % Set appliaction to PDE General form.
22 clear appl
23 appl.mode.class = 'F1PDEG';
24
25 % Set variables.
26 appl.dim = {'u1','u2','u3','u4','u5','u1_t','u2_t','u3_t','u4_t','u5_t'};
27
28 % Set variables as linear lagrange
29 appl.shape = {'shlag(1,'u1')','shlag(1,'u2')','shlag(1,'u3')'
30             , 'shlag(1,'u4')','shlag(1,'u5')'};
31
32 appl.gporder = 2;
33 appl.cporder = 1;
34
35 % Set boundary conditions
36 appl.assignsuffix = '_g';
37 clear bnd
38 bnd.type = 'neu'; % Neumann conditions
39 bnd.ind = bndind;
40 appl.bnd = bnd;
41 clear equ

```



```

42 if solform==0
43     % Set initial solution
44     equ.init = initsol;
45 end
46
47 if strcmp(mode,'xi') == 1
48     equ.f = {{...
49         'u3.*u1x+u4.*u1y+(u3.^2+u4.^2).*u2-u2+(u1.^2+u2.^2).*u2';...%F1
50         'u3.*u2x+u4.*u2y-(u3.^2+u4.^2).*u1+u1-(u1.^2+u2.^2).*u1';...%F2
51         '1./(kappa.^2).*(u2.*u1x-u1.*u2x+(u1.^2+u2.^2).*u3)';...%F3
52         '1./(kappa.^2).*(u2.*u1y-u1.*u2y+(u1.^2+u2.^2).*u4)';...%F4
53         'u5'}}; %F5
54     equ.ga = {{...
55         {'u2x-u3.*u1';'u2y-u4.*u1'};...%Gamma1
56         {'-u1x-u3.*u2';'-u1y-u4.*u2'};...%Gamma2
57         {'u3x+u4y';'-u4x+u3y+Ba'};...%Gamma3
58         {'u4x-u3y-Ba';'u3x+u4y'};...%Gamma4
59         {'0';'0'}}};%Gamma5
60 elseif strcmp(mode,'lambda') == 1
61     equ.f = {{...
62         'kappa.*(u3.^2+u4.^2).*u2+u3.*u1x+u4.*u1y-kappa.*u2
63             +kappa.*(u1.^2+u2.^2).*u2';...%F1
64         '-kappa.*(u3.^2+u4.^2).*u1+u3.*u2x+u4.*u2y+kappa.*u1
65             -kappa.*(u1.^2+u2.^2).*u1';...%F2
66         '(1./kappa).*(u2.*u1x-u1.*u2x)+(u1.^2+u2.^2).*u3';...%F3
67         '(1./kappa).*(u2.*u1y-u1.*u2y)+(u1.^2+u2.^2).*u4';...%F4
68         'u5'}}; %F5
69     equ.ga = {{...
70         {'u2x./kappa-u3.*u1';'u2y./kappa-u4.*u1'};...%Gamma1
71         {'-u1x./kappa-u3.*u2';'-u1y./kappa-u4.*u2'};...%Gamma2
72         {'u3x+u4y';'-u4x+u3y+Ba'};...%Gamma3
73         {'u4x-u3y-Ba';'u3x+u4y'};...%Gamma4
74         {'0';'0'}}};%Gamma5
75     else
76         %Abort
77         error('Unknown mode!')
78     end
79
80 % Construct fem structure
81 equ.ind = [1];
82 appl.equ = equ;
83 fem.appl{1} = appl;
84 fem.border = 1;
85
86 % insert constants
87 fem.const={'Ba',sprintf('%d',Ba),'kappa',sprintf('%d',kappa)};
88
89 % Multiphysics
90 fem=multiphysics(fem);
91
92 % Initialize mesh
93 fem.mesh=meshinit(fem,'Hauto',Hauto);
94
95 fem.xmesh=meshextend(fem);
96
97 if solform == 0
98     % Evaluate initial value
99     init = asseminit(fem);
100 elseif solform == 1
101     % Mapping current solution to extended mesh
102     init = asseminit(fem,'init',initsol.sol,'xmesh',initsol.xmesh);
103 end

```

```

104
105 % Update model
106 fem.sol = init;
107
108 %Solve problem
109 fem.sol=femlin(fem, ...
110   'init',init, ...
111   'HnLin','on',...
112   'solcomp',{'u1','u2','u3','u4','u5'}, ...
113   'outcomp',{'u1','u2','u3','u4','u5'}, ...
114   'Ntol',1e-6,...
115   'maxiter',1000);
116
117 varargout = fem;

```

C.4 tddlstart.m

```

1 % function [varargout] = tddlstart(usergeom, Ba, fem,
2   solform, kappa, vortex, time, glerun)
3 function [varargout] = tddlstart(usergeom, Ba, fem,
4   solform, kappa, vortex, time, glerun)
5
6 % Geometry
7 % -----
8 % 1 = Square
9 % 2 = Square with link
10 % 3 = Circle
11 % 4 = Circle with defect
12 % 5 = Triangle
13
14 % Set mode
15 % mode = 'xi';
16 mode = 'lambda';
17
18 % Set variables.
19 if time == 0
20   time = [0:20:5000];
21 end
22 if kappa == 0
23   kappa = 4;
24 end
25
26 sigma = 1;
27 if Ba == 0
28   Ba = 0.1;
29 end
30 tddlH = 2;
31 gleH = 2;
32
33 % if solform = 1 then a femlab structure is passed as init
34 if solform == 1
35   init = fem;
36 else
37   if vortex == 1
38     %one Vortex at center
39     init = {'x./sqrt(x.^2+y.^2)';'y./sqrt(x.^2+y.^2)';0;0;0;0;0;0;0};
40   else
41     % No Vortex, Meissner phase
42     init = {'sqrt(0.5)';'sqrt(0.5)';0;0;0;0;0;0;0};
43   end

```

```

44 end
45
46 clear geom
47 switch usergeom
48     case 1
49         % A square
50         g1=rect2(10,10,'base','corner','pos',[-5,-5]);
51         geom.objs={g1};
52         bndind = [1,1,1,1];
53         diradd = 'square';
54         plotgeom = [-5,5,-5,5];
55     case 2
56         % Rect with defects as link.
57         % Geometry
58         g1=rect2(6,10,'base','corner','pos',[-3,-5]);
59         g2=ellip2(2,2,'base','center','pos',[-3,0]);
60         g3=ellip2(2,2,'base','center','pos',[3,0]);
61         g4=geomcomp({g1,g2,g3},'ns',{g1','g2','g3'],'sf','g1-g2-g3',
62                     'edge','none');
63         bndind = [1,1,1,1,1,1,1,1];
64         geom.objs={g4};
65         diradd = 'squarelink';
66         plotgeom = [-2.5,2.5,-5,5];
67     case 3
68         % Circle with r=5 and x and y direction, with center at 0,0
69         g1=ellip2(5,5,'base','center','pos',[0,0]);
70         geom.objs={g1};
71         bndind = [1,1,1,1];
72         diradd = 'circle';
73         plotgeom = [-5,5,-5,5];
74     case 4
75         % A circle with a defect
76         % Circle with r=5 and x and y direction, with center at 0,0
77         g1=ellip2(5,5,'base','center','pos',[0,0]);
78         carr={curve2([-5,-4],[1,0],[1,1]), ... %Line from (-5,1)->(-4,0)
79               curve2([-4,-5],[0,-1],[1,1]), ...%Line from (-4,0)->(-5,-1)
80               curve2([-5,-5],[-1,1],[1,1])};%Line from (-5,1)->(-5,1)
81         g2=geomcoerce('solid',carr);%Make the geom solid
82         g3=geomcomp({g1,g2},'ns',{g1','g2'],'sf','g1-g2','edge','none');
83         geom.objs={g3};
84         bndind = [1,1,1,1,1,1];
85         diradd = 'circledef';
86         plotgeom = [-5,5,-5,5];
87     case 5
88         % Triangle
89         carr={curve2([-5,0],[-4,6],[1,1]), ...
90               curve2([0,5],[6,-4],[1,1]), ...
91               curve2([6,-6],[-4,-4],[1,1])};
92         g1=geomcoerce('solid',carr);
93         bndind = [1,1,1];
94         geom.objs={g1};
95         diradd = 'triangle';
96         plotgeom = [-5,5,-4,6];
97     otherwise
98         error('Unknown geometry!')
99 end
100
101 geom.name={'R1'};
102 geom.tags={'g1'};
103
104 sprintf('TDGL for BA = %d',Ba)
105

```

```

106 [tdglfem] = TDGL(geom, bndind, init, solform, time, mode, kappa,
107                Ba, sigma, usergeom, tdglH);
108
109 % Plot solution
110 dir = strcat('./data/',mode, '/',diradd, '/tdgl_');
111 plotter(tdglfem,time,mode,Ba,kappa,201,201,51,21,plotgeom,dir);
112 if glerun == 1
113     sprintf('GLE for BA = %d',Ba)
114     [glefem] = GLE(geom, bndind, tdglfem, 1, mode, kappa, Ba, usergeom, gleH);
115     dir = strcat('./data/',mode, '/',diradd, '/gle_');
116     plotter(glefem,0,mode,Ba,kappa,201,201,51,31,plotgeom,dir);
117 else
118     glefem = 0;
119 end
120
121 varargout{1} = tdglfem;
122 varargout{2} = glefem;

```

C.5 plotter.m

```

1 % function [vargout] = plotter(fem,t,mode,Ba,kappa,pPsi,pB,pJ,
2                               pLine,plotgeom,dir)
3 function [vargout] = plotter(fem,t,mode,Ba,kappa,pPsi,pB,pJ
4                               ,pLine,plotgeom,dir)
5
6 if t == 0
7     time = 1;
8 else
9     time = t; %[t1 t2 t3];
10 end
11 % Create points matrix
12
13 points = zeros(2,pPsi^2);
14 x = linspace(plotgeom(1),plotgeom(2),pPsi);
15 y = linspace(plotgeom(3),plotgeom(4),pPsi);
16 for i = 1:pPsi
17     points(1,(i-1)*pPsi+1:i*pPsi) = x;
18     points(2,(i-1)*pPsi+1:i*pPsi) = y(i);
19 end
20
21 % Extract sol psi^2
22 if t == 0
23     [u1 u2] = postinterp(fem,'u1','u2',points);
24 else
25     [u1 u2] = postinterp(fem,'u1','u2',points,'T',time);
26 end
27
28 Psi = u1.^2+u2.^2;
29
30 clear solpoints;
31 % Construct plot matrix
32 for j = 1:size(time,2)
33     for i = 1:pPsi
34         solpoints(i,:) = Psi(j,(i-1)*pPsi+1:i*pPsi);
35     end
36     % Write matrix
37     dlmwrite(sprintf('%sPsi_Ba_%1.4f_Kappa_%d_p%d_t%05d.txt',
38                     dir,Ba,kappa,pPsi,time(j)),transpose(solpoints),'\t');
39 end
40

```

```

41 % Create points matrix
42 points = zeros(2,pB^2);
43 x = linspace(plotgeom(1),plotgeom(2),pB);
44 y = linspace(plotgeom(3),plotgeom(4),pB);
45 for i = 1:pB
46     points(1,(i-1)*pB+1:i*pB) = x;
47     points(2,(i-1)*pB+1:i*pB) = y(i);
48 end
49
50 % Extract sol Bz
51 if t == 0
52     [ayx axy] = postinterp(fem,'u4x','u3y',points);
53 else
54     [ayx axy] = postinterp(fem,'u4x','u3y',points,'T',time);
55 end
56 B = ayx - axy;
57
58 clear solpoints;
59 % Construct plot matrix
60 for j = 1:size(time,2)
61     for i = 1:pB
62         solpoints(i,:) = B(j,(i-1)*pB+1:i*pB);
63     end
64     % Write matrix
65     dlmwrite(sprintf('%sB_Ba_%1.4f_Kappa_%d_p_%d_t%05d.txt',
66                     dir,Ba,kappa,pB,time(j)),transpose(solpoints),'t');
67 end
68
69 % dump current
70 points = zeros(2,pJ^2);
71 x = linspace(plotgeom(1),plotgeom(2),pJ);
72 y = linspace(plotgeom(3),plotgeom(4),pJ);
73 for i = 1:pJ
74     points(1,(i-1)*pJ+1:i*pJ) = x;
75     points(2,(i-1)*pJ+1:i*pJ) = y(i);
76 end
77
78 % Extract sol Bz
79 if t == 0
80     [u1 u2 ax ay u1x u1y u2x u2y] = ...
81         postinterp(fem,'u1','u2','u3','u4','u1x','u1y','u2x','u2y',points);
82 else
83     [u1 u2 ax ay u1x u1y u2x u2y] = ...
84         postinterp(fem,'u1','u2','u3','u4','u1x','u1y','u2x','u2y',
85                     points,'T',time);
86 end
87 % Current with r -> Xi * r
88 if strcmp(mode,'xi') == 1
89     Jx = 1./(kappa.^2).*(u1.*u2x-u2.*u1x)-(u1.^2+u2.^2).*ax;
90     Jy = 1./(kappa.^2).*(u1.*u2y-u2.*u1y)-(u1.^2+u2.^2).*ay;
91 elseif strcmp(mode,'lambda') == 1
92     % Current with r -> Lambda * r
93     Jx = (1./kappa).*(u1.*u2x-u2.*u1x)-(u1.^2+u2.^2).*ax;
94     Jy = (1./kappa).*(u1.*u2y-u2.*u1y)-(u1.^2+u2.^2).*ay;
95 else
96     error('Unknown mode!')
97 end
98 % Construct plot matrix
99 for j = 1:size(time,2)
100     % Write matrix
101     points(3,:) = Jx(j,:);
102     points(4,:) = Jy(j,:);

```

```
103     dlmwrite(sprintf('%sJ_Ba_%1.4f_Kappa_%d_p%d_t%05d.txt',
104                     dir,Ba,kappa,pJ,time(j)),transpose(points),'\t');
105 end
106
107 clear points
108 % dump for lines
109 if pLine >= 0
110
111     points = zeros(2,pLine*2-1);
112     points(1,:) = linspace(-5,5,pLine*2-1);
113     points(2,:) = 0;
114     [u1 u2 axy ayx] = postinterp(fem,'u1','u2','u3y','u4x',points);
115     Psi = u1.^2+u2.^2;
116     B = ayx-axy;
117     points(2,:) = Psi;
118     dlmwrite(sprintf('%sPsi_Ba_%1.2f_Kappa_%d_line.txt',
119                     dir,Ba,kappa),transpose(points),'\t');
120     points(2,:) = B;
121     dlmwrite(sprintf('%sB_Ba_%1.2f_Kappa_%d_line.txt',
122                     dir,Ba,kappa),transpose(points),'\t');
123 end
```

Appendix D

CD content

The attached CD contains three directories

- **matlab** contains the five matlab scripts written in appendix C.
- **gnuplots** contains a few Gnuplot scripts used to create the figures. It also contains a few bash scripts, which have made the working process a lot easier.
- **movies** has various movies of vortex dynamics.

All the movies recorded should be playable in Windows Media Player without any additional components required. Mplayer, which is available for a vast amount of *nix system, should also be able to play the movies. However, a free version of a movie player, which is found on the website divx.com, can be found in the root of the CD.

There are movies of three geometries which follow the principle

`<geometry>_Ba<applied magnetic field value>_k<kappa>.avi`

Note that all movies changes speed at certain points, so if the vortices suddenly moves a lot faster, then keep an eye on the time above the image.

Bibliography

- [1] V. Z. Kresin and S. A. Wolf. *Fundamentals of Superconductivity*. Plenum Press, 1990.
- [2] M. Tinkham. *Introduction to Superconductivity*. McGraw-Hill, 1996.
- [3] H. K. Onnes. The superconductivity of mercury. *Phys. Lab. Univ. Leiden*, 120b, 1911.
- [4] W. Meissner and R. Ochsenfeld. Ein neuer effekt bei eintritt der supraleitfähigkeit. *Naturwissenschaften*, 21:787, 1933.
- [5] F. London and H. London. Supraleitung und diamagnetismus. *Physica*, 2:341, 1935.
- [6] L. N. Cooper J. Bardeen and J. R. Schrieffer. Theory of superconductivity. *Phys. Rev.*, 108:1175, 1957.
- [7] J. G. Bednorz and K. A. Müller. Possible high t_c superconductivity in the ba-la-cu-o system. *Z. Physik B (Condensed Matter)*, 64:189, 1986.
- [8] W. Buckel and R. Kleiner. *Superconductivity: Fundamentals and Applications*. Wiley-VCH, 2004.
- [9] V. L. Ginzburg and L. D. Landau. On the theory of superconductivity. *Zh. Eksp. Teor. Fiz.*, 20:1064, 1950.
- [10] L. P. Gor'kov. Microscopic derivation of the ginzburg-landau equations in the theory of superconductivity. *Zh. Eksp. Teor. Fiz.*, 36:1916, 1959.
- [11] D. K. Cheng. *Field and Wave electromagnetics*. Addison–Wesley, 1989.
- [12] B. H. Bransden and C. J. Joachain. *Quantum Mechanics Second edition*. Pearson Education Limited, 2000.
- [13] M. D. Gunzburger Q. Du and J. S. Peterson. Analysis and approximation of the ginzburg–landau model of superconductivity. *SIAM Review*, 34:54, 1992.
- [14] T. Schneider and J. M. Singer. *Phase Transition Approach To High Temperature Superconductivity*. Imperial College Press, 2000.
- [15] L. E. Ballentine. *Quantum Mechanics A Modern Development*. World Scientific, 1998.

-
- [16] A. A. Abrikosov. On the magnetic properties of superconductors of the second type. *Zh. Eksp. Teor. Fiz.*, 32:1442, 1957.
- [17] COMSOL AB. *FEMLAB 3.1 Modelling guide*. COMSOL AB, 2004.
- [18] A. Iserles. *A First Course in the Numerical Analysis of Differential Equations*. Cambridge University Press, 1996.
- [19] *Private conversation with Per Grove Thomsen, professor of numerical analysis at the Institute for Informatics and Mathematical Modelling, DTU.*
- [20] H. G. Kaper et al. Numerical simulation of vortex dynamics in type-II superconductors. *Journal of Computational Physics*, 123:254, 1996.
- [21] Q. Du. Global existence and uniqueness of solutions of the time-dependent ginzburg-landau model for superconductivity. *Applicable Analysis*, 53:1, 1994.
- [22] A. Barone and G. Paterno. *Physics and Applications of the Josephson Effect*. Wiley, 1982.